

High voltage Engineering

Module 1

I

Objectives

In this course you will learn the following

- Levels of voltages
- Electrical Insulation and Dielectrics

Levels of high voltage:

World over the levels are classified as:

- LOW
 - MEDIUM
 - HIGH
 - EXTRA and
 - ULTRA HIGH Voltages
- However , the exact magnitude of these levels vary from country to country. Hence this system of technical terms for the voltage levels is inappropriate .
 - In most part of the world even 440 V is considered to be high voltage since it is dangerous for the living being.
 - Hence it would be more appropriate to always mention the level of voltage being referred without any set nomenclature .

VOLTAGE LEVELS

Consumer

- ac power frequency :
 - 110V, 220V-single phase
 - 440 V, 3.3 kV ,6.6 kV, 11 kV-three phase (3.3 & 6.6 kV are being phased out)
- Besides these levels ,the Railway Traction at 25 kV , single phase is one of the biggest consumer of power spread at any particular stretch to 40 km of track length .

Generation : Three phase synchronous generators

440V, 3.3kV, 6.6kV (small generators), 11kV (110 & 220 MW)
21.5kV (500 MW), 33kV (1000 MW)
[limitation due to machine insulation requirement]

Distribution :

Three phase

440V, 3.3kV, 6.6kV, 11kV, 33kV, 66kV

With the increase in power consumption density, the power distribution voltage levels are at rise because the power handling capacity is proportional to the square of the voltage level. (In Germany 440 V , 3.0 kV 6.0 kV, 10 kV, 30 kV, 60 kV)

Ac Transmission : 110 kV, 132 kV, 220 kV, 380-400kV, 500kV, 765-80kV, 1000kV and 1150kV exist.

Work on 1500 kV is complete.

In three phase power system, the rated voltage is always given as line to line, rms voltage .

d.c. transmission : dc single pole and bipolar lines :
 $\pm 100 \text{ kV to } \pm 500 \text{ kV}$

Advance countries like US, Canada and Japan have their single phase ac power consumption level at 110 V .

Rest of the whole world consumes single phase ac power at 220 V .

The only advantage of 110 V single phase consumer voltage is that it is safer over 220 V. However, the disadvantages are many.

Disadvantages :

- It requires double the magnitude of current to deliver the same amount of power as at 220 V
- Hence for the same magnitude of I^2R losses to limit the conductor or the insulation temperature to 70° C (for PVC) , the resistance of the distribution cable should be 4 times lower. Therefore, the cable cross-section area has to be increased four folds.
- Four times more copper requirement, dumped in the building walls is an expensive venture.
- Due to higher magnitude of current, higher magnetic field in the buildings . Not good for health.
- With the installation of modern inexpensive protective devices (earth fault relays), 220 V is equally safe as 110 V

Rated maximum temperature of cables:

- It is important to understand the current and voltage carrying capacities of a conductor separately. While the current carrying capability is determined by the conductivity of the conductors, directly proportional to the area of conductor cross-section, the voltage bearing capacity depends upon the level of insulation provided to the conductor .
- The current carrying capability in turn is determined by maximum permissible temperature of the insulation or that of the conductor.
- The real power loss, I^2R and the rate of cooling determine the temperature rise of the conductor which should not be more than the maximum permissible temperature of the type of insulation provided on the conductor .
- Hence, not only electrical but thermal and mechanical properties of insulation are important in power system .

Electrical Insulation and Dielectrics

Gaseous Dielectrics:

- Atmospheric air is the cheapest and most widely used dielectric . Other gaseous dielectrics, used as compressed gas at higher pressures than atmospheric in power system, are Nitrogen , Sulphurhexafluoride SF₆(an electro-negative gas) and it's mixtures with CO₂ and N₂ . SF₆ is very widely applied for Gas Insulated Systems (GIS), Circuit Breakers and gas filled installations i.e. sub-stations and cables. It is being now applied for power transformers

also.

Vacuum as Dielectric :

- Vacuum of the order of 10^{-5} Torr and lower provides an excellent electrical insulation. Vacuum technology developed and applied for circuit breakers in the last three decades is phenomenon .

Liquid Dielectrics:

- Organic liquids, the mineral insulating oils and impregnating compounds, natural and synthetic, of required physical, chemical and electrical properties are used very widely in transformers, capacitors, cables and circuit breakers.

Solid Dielectrics:

- Very large in number .
- Most widely used are : XLPE, PVC, ceramics, glass, rubber, resins, reinforced plastics, polypropylene, impregnated paper, wood, cotton, mica, pressboards, Bakelite, Perspex, Ebonite, Teflon, etc.
- Introduction of nano materials are in offing.

II

Objectives

In this module you will learn the following

Importance of Electric Field Intensity in the Dielectrics
Types of Electric Fields
Degree of Uniformity of Fields (Schwaiger Factor)
Utilization of Dielectric Properties
Stress Control

ELECTRIC FIELDS:

Faraday described the space around a magnet to be filled with 'lines of magnetic force'. Similarly, the region around an electrified object may be considered to be filled with 'lines of electric force'. To Faraday, these lines existed as mechanical structures in the surrounding medium (the dielectric) and could exert force on an object placed therein. Two typical electrostatic field structures are shown in Fig. 2.1. In figure (a), the field between a sphere or a cylinder and plane is sketched, and in figure(b), the field pattern on a bundle of four conductors used for transmission lines is shown, neglecting the effect of ground.

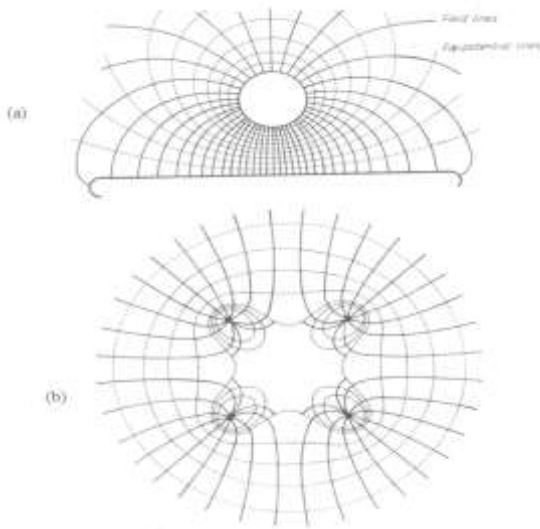


Fig 2.1 Typical electrostatic field configurations.
(a) Field between sphere or cylinder and plane,
(b) Field on a bundle of four conductors.

- The 'electric field intensity', also known as the 'electric field strength', is defined as the electrostatic force F exerted by the field on a unit positive test charge q , placed at a particular point P in a dielectric. It is denoted by E , and expressed in unit 'Newtons per Coulomb', that is, the force per unit charge.
- The electric field intensity is measured in its practical units of 'Volts per meter' (V/m or kV/mm).
- The electric field intensity is often more specifically mentioned as 'electric stress' experienced by a dielectric or an electrical insulating material.
- The potential difference between two points a and b , having scalar potential ϕ_a, ϕ_b in a space charge free electric field \vec{E} , is defined as the work done by an external source in moving a unit positive charge from b to a ,

$$U_{ab} = -\int_b^a \vec{E} \cdot d\vec{x} = (\phi_a - \phi_b)$$

(2.1)

- U_{ab} is positive if the work is done in carrying the positive charge from b to a. The maximum magnitude of electric field intensity is therefore, given by the maximum value of the rate of change of potential with distance. It is obtained when the direction of the increment of distance is opposite to the direction of \vec{E} , in other words, the maximum value of the rate of change of potential is obtained when the direction of \vec{E} is opposite to the direction in which the potential is increasing most rapidly,

$$\frac{dU_{ab}}{dx} \Big|_{\max} = -|\vec{E}|_{\max}$$

(2.2)

The operator on ϕ by which \vec{E} is obtained, is thus known as the 'gradient'. The relationship between ϕ and \vec{E} may be written as,

$$\vec{E} = -\text{grad}\phi$$

(2.3)

- The electric field intensity is, therefore, numerically equal to the 'potential gradient'.

Electric Strength of Dielectrics

- The qualitative definition of 'electric strength' of a dielectric is 'the maximum electric stress a dielectric can withstand'.
- A large number of factors affect the electric breakdown of a dielectric, these include pressure, humidity, temperature, electric field configuration (electrode shape and size) electrode material, applied voltage waveform, its duration and magnitude, presence of impurities and imperfections in the dielectric, the composition of dielectric material. Hence a quantitative definition is complicated.
- In a time varying ac power frequency field (quasi stationary field), the maximum electric stress occur at the peak value of the applied voltage.
- Intrinsic strength of a dielectric: It is defined for gaseous and other than gaseous dielectric differently.
 - Gaseous dielectric: It is the magnitude of breakdown voltage measured across a gap distance of one cm in uniform field ($\eta = 1$) at normal temperature and pressure.
 - Liquid and Solid dielectrics: It is the highest value of breakdown strength obtained after eliminating all known secondary effects which may influence the breakdown adversely. It is measured for the ideal conditions of the dielectric in uniform field. Since it is very very high for solid and liquid dielectrics compared to gaseous dielectrics, it is measured for mm and μm thin films of the liquid and solid dielectrics respectively instead of 1 cm gap distance in case of gaseous dielectrics.

III

Objectives

In this lecture you will learn the following

- Classification of Electric Field configurations
- Degree of Uniformity of Electric Fields, Schwaiger Factor

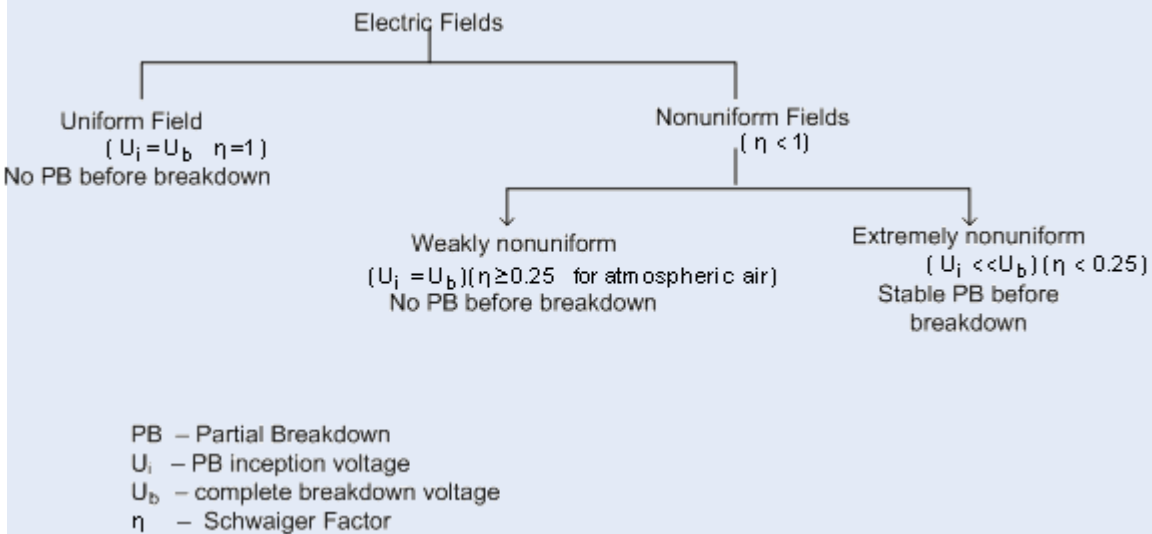
Classification of Electric Fields

Electric field configurations can be classified into two forms of fields;

1. Uniform field.
2. Non-Uniform field.

Non-uniform fields can be further distinguished between two types;

1. Weakly nonuniform fields.
2. Extremely nonuniform fields.



- The two extreme forms of fields, the 'uniform' and the 'extremely nonuniform' fields, are shown in Fig. 3.1. The electric field between two electrodes is plotted beginning with the equipotential lines. An electrode is always at equi-potential. Hence, the electrode surface is the first equipotential line to be plotted. The field lines intersect the equipotential lines at right

angle. Smaller are the squares formed, higher the field intensity.

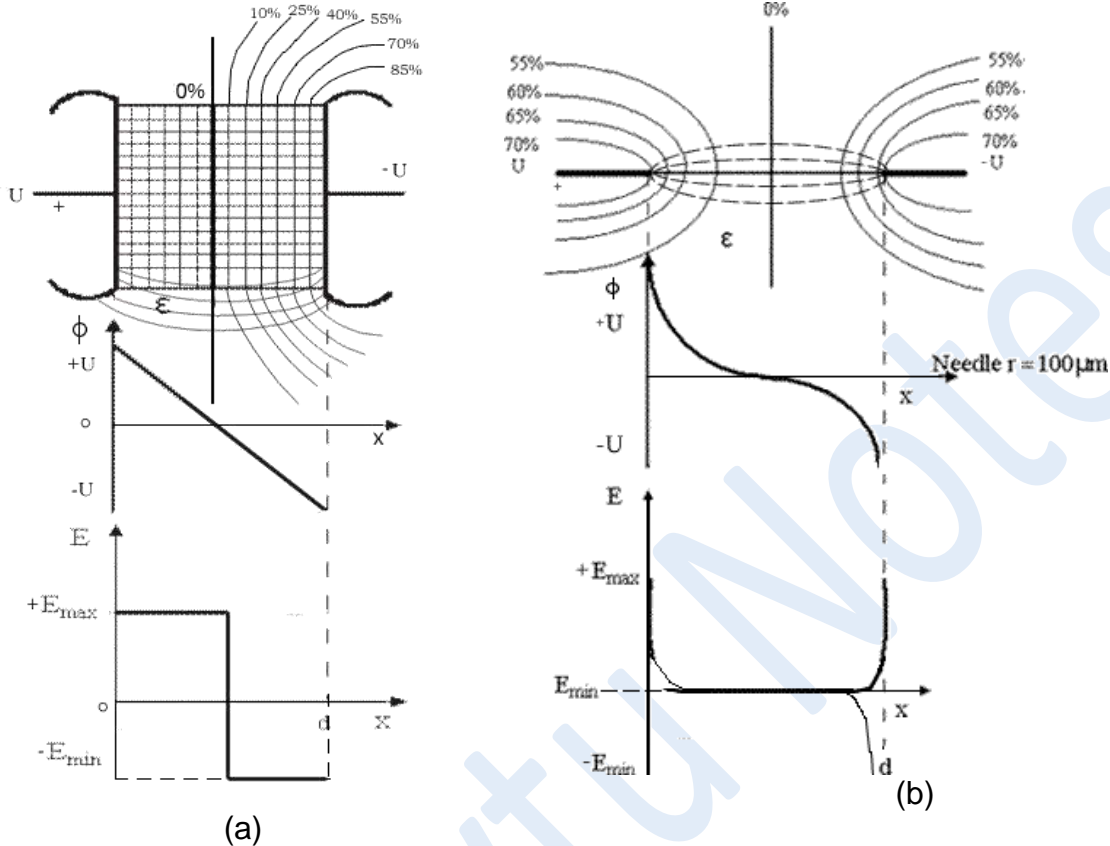


Fig 3.1 The extreme field configurations (a)Uniform field between two parallel plates. (b) Extremely nonuniform field between needle-needle electrodes. (Effect of grounding is neglected in these plots)

- In a 'uniform field', the potential is linearly distributed and the electric field intensity is constant throughout the space in the main field region between the two electrodes, as shown in Fig. 3.1 (a). An important characteristic of this type of field is that the insulation breakdown takes place without any partial discharge preceding the breakdown ($U_i=U_b$)
- There is an extreme nonlinear distribution of potential in the space between two needle electrodes, leading to strong nonuniformity in electric field intensity as in Fig. 3.1 (b). This is a typical case of an 'extremely nonuniform field'. Unlike in uniform fields, the insulation breakdown in extremely nonuniform fields takes place after stable partial breakdown are set ($U_i < U_b$). The partial breakdown are rendered to be unstable only just before the complete breakdown. This field configuration is of great technical importance, as it is the most unfavourable condition of electric field faced by a dielectric. At the tip of the electrodes the dielectric is subjected to a very high electric stress, but elsewhere between the electrodes it is stressed moderately.
- For a given electrode gap distance in uniform field a dielectric has the highest breakdown strength. However, it is very difficult to realize a uniform field in practice. It

is accomplished only for experimental purposes in research laboratories with tremendous effort and utmost care. The size of the electrodes may have to be increased extraordinarily large, whereas the slightest irregularity on the electrode surface may change the field characteristics in case of small gap distance.

- Between the two extreme field configurations explained above, another important type of field is classified as 'weakly nonuniform field'. Like in uniform field, in weakly nonuniform fields also no stable partial breakdown occur before the breakdown ($U_i=U_b$). Electrodes like concentric spheres and coaxial cylinders having a 'radial field' are typical examples of weakly nonuniform fields, if the concentric electrode dimensions are suitably designed. The exact value of η , defining weakly nonuniform field, depends upon the particular dielectric and its physical conditions. Nevertheless, the main criterion must be fulfilled that no stable partial breakdown occur before the breakdown.

Degree of Uniformity of Electric Fields

- The degree of uniformity η introduced by Schwaiger in 1922 as a measure of the uniformity of a field, is defined as follows

$$\eta = \frac{\hat{E}_{\text{mean}}}{\hat{E}_{\text{max}}} = \frac{\hat{U}}{d} \cdot \frac{1}{\hat{E}_{\text{max}}}$$

or

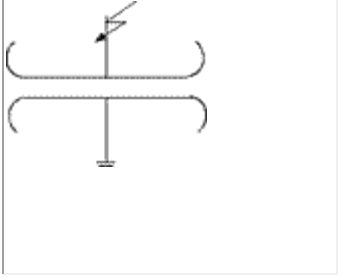
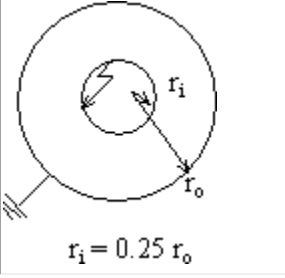
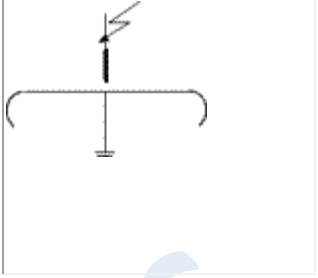
$$\hat{U} = \hat{E}_{\text{max}} \cdot \eta \cdot d$$

\hat{E}_{mean} and \hat{E}_{max} are the peak values of the Mean and the Maximum field Intensities in a dielectric respectively. \hat{U} is the peak value of potential difference applied between the two electrodes at distance 'd' apart.

- The value of η also represents the degree of utilization of the dielectric in between electrodes. A higher value of η represents better utilization of the insulating properties of dielectric. Thus η , a dimensionless quantity enables a comparison of the uniformity of field configuration formed between different electrodes. Table 3.1 gives the values of η for typical fields. The value of η lies between, $0 \leq \eta \leq 1$

Table 3.1

Field Classification	Uniform	Weakly non-uniform	Extremely non-uniform
Electrode Configuration	Parallel plates	Concentric cylinders	Needle-plane

			
η	1	≤ 0.25	$\ll 0.01$

- Knowledge of the value for η serves as a ready reference, an important information for insulation design in equipment. For determining the exact magnitude of maximum electric stress, numerical estimation techniques have to be applied for the shapes of electrodes used in the equipment.
- Schwaiger also introduced 'p', a geometrical characteristics for an electrode configuration and established that it is possible to represent η as a function of 'p',

$$p = \frac{r+d}{r} \quad (1.5)$$

$$(1 \leq p < \infty) \quad (1.6)$$

and $\eta = f(p)$

where r is the radius of curvature of the sharpest electrode and d the shortest gap distance between the two electrodes under consideration.

For some common and practical electrode configurations, the equation (1.6) is represented graphically in Figure 2.2 in double logarithmic scale. These are known as 'Schwaiger curves'.

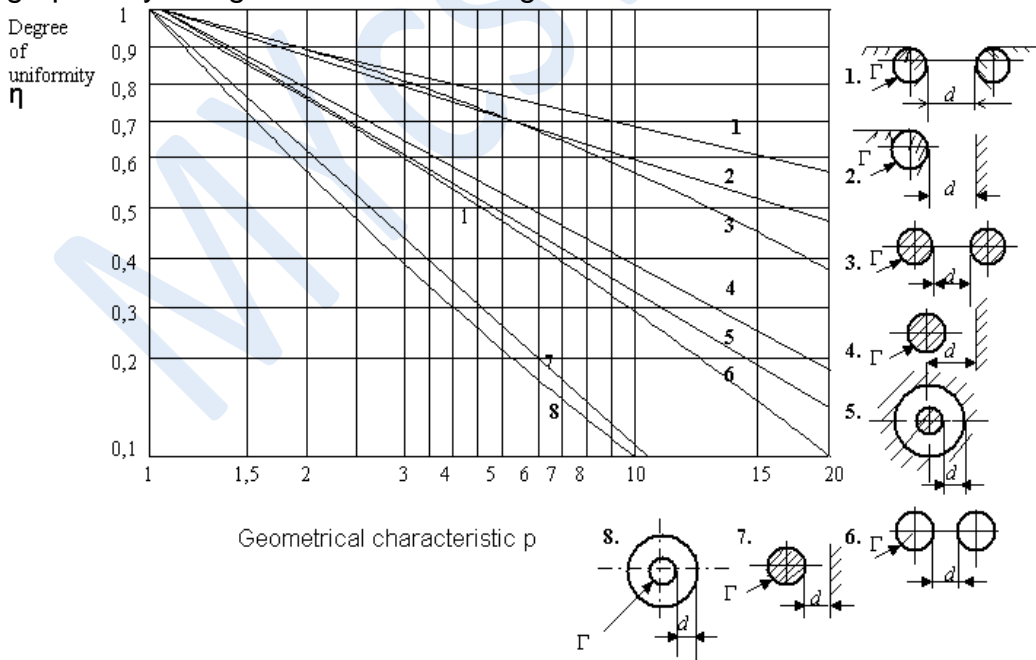


Fig 2.2 Schwaiger curves for spherical, cylindrical and curved electrode field configurations.

For a fixed value of 'p', the following important basic relations of dependency of η are observed from these curves,

- fields between cylindrical electrode systems; cylinder-cylinder (3) , cylinder - plane (4) , concentric cylinders (5) etc., have a higher value of η , that is , they are more uniform than the fields in spherical electrode systems; sphere - sphere (6) , sphere - plane (7) , concentric spheres (8) , etc.,
- a symmetrical electrode system, for example, sphere - sphere or cylinder - cylinder, has a higher value of η than the corresponding unsymmetrical system, that is sphere - plane or cylinder - plane systems.
- the field between two similar electrodes, cylinders or spheres, placed adjacent to each other is more uniform or has a higher value of η than when the electrodes are placed coaxial or concentric.

IV

Objectives

In this lecture you will learn the following

Utilization of Dielectric Properties
Stress Control

Utilization of Dielectric Properties

The value of η also represents the degree of utilization of the dielectric in between two electrodes. A higher value of η represents better utilization of the insulating properties of a dielectric. It compares the ideal condition of electric field intensity (uniform field between electrodes at the same distance d apart) with the existing actual maximum field intensity. Thus η , a dimensionless quantity enables a comparison of the degree of uniformity of field configurations formed between different electrodes. Table 2.1 gives the values of η for typical fields. The value of η lies between, $0 \leq \eta \leq 1$

With the knowledge of the value of η for a particular field configuration, the maximum electric field intensity or the maximum electric stress on a dielectric can easily be estimated. η serves as a ready reference which is an important information for insulation design in equipment. However, for determining the exact magnitude of maximum electric stress, at different shapes of electrodes used in the equipment, numerical estimation techniques have to be applied .

Utilization of Dielectric Properties

The value of η also represents the degree of utilization of the dielectric in between two elec

A higher value of η represents better utilization of the insulating properties of a dielectric. It compares the ideal condition of electric field intensity (uniform field between electrodes at the same distance d apart) with the existing actual maximum field intensity. Thus η , a dimensionless quantity enables a comparison of the degree of uniformity of field configurations formed between different electrodes. Table 2.1 gives the values of η for typical fields. The value of η lies between, $0 \leq \eta \leq 1$

With the knowledge of the value of η for a particular field configuration, the maximum electric field intensity or the maximum electric stress on a dielectric can easily be estimated. η serves as a ready reference which is an important information for insulation design in equipment. However, for determining the exact magnitude of maximum electric stress, at different shapes of electrodes used in the equipment, numerical estimation techniques have to be applied .

Stress Control

- More the uniformity in field, better is the utilisation of the dielectric.
- An ideal utilisation is accomplished only where η is equal to one, which is not possible in practice.
- More nonuniform field represents higher electric stress in the dielectric. It could be at only a particular location. Insulation design in an equipment is made with due consideration to the value of estimated maximum electric field intensity.
- It is possible to achieve a higher degree of uniformity of fields by giving suitable shapes and sizes to various electrodes in an equipment. For example, abrupt interruption of electrodes, both anode or cathode, in high voltage equipment leads to concentration of electric field at the brim, resulting in a tremendous enhancement of electric stress on the dielectric. The dielectric in the vicinity thus becomes highly vulnerable to breakdown.
- The electrodes must be given a suitable shape at the brim to control the stress.
- For stress control, in principle the electrodes are extended and formed in such a way that higher field intensity than in the main field region does not appear anywhere in the dielectric.
- Rogowski suggested in 1923, a shape by which the electrodes could be extended, known as 'Rogowski Profile', Fig. 4.1(a).
- One can see in this figure that the field intensity continuously reduces beyond the main field region.
- Another shape of the electrode credited to Borda known as 'Borda Profile' , Fig 4.1(b), was actually worked out by him in as early as 1766 in France, more than 200 years ago.

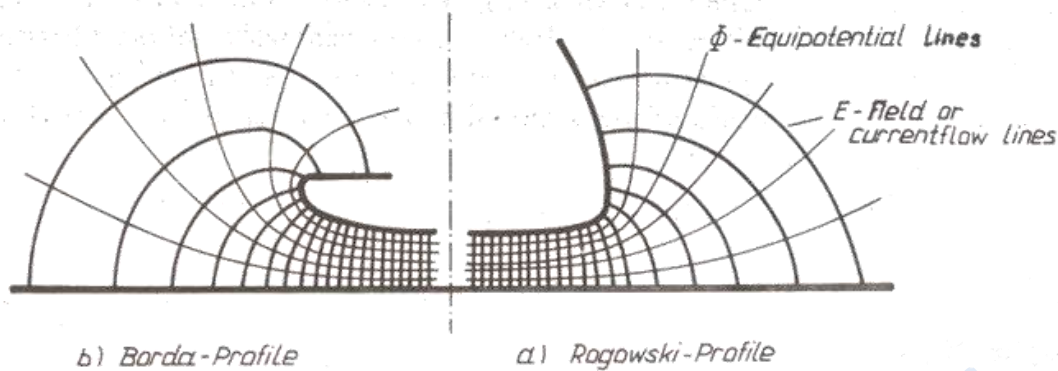


Fig 4.1 Equipotential and Field (current flow) lines between plane

and brim field

- Electrodes at high potentials in the laboratory are given large, smooth shaped dome like bodies or shapes like toroids to bring down electric stress on the atmospheric air (dielectric). The modern trend in such electrode design includes 'segmented electrodes' constituting a number of small, identical, smooth discs given a large desired continuous shape as per requirement. The curvatures of the individual segment discs are worked out by optimisation of the suggested profiles. Fig 4.2 shows both, single metallic body and segmented electrodes used in HV test apparatus for stress control.
- Extended shapes of electrodes, also known as 'shields', are suitably provided on high voltage apparatus for electric stress control as shown in Fig 4.3. Sharp contacts are often enveloped by a large diameter hemispherical electrode having an aperture, or provided with concentric toroidal rings (doughnut shaped ring). Spheres with smooth holes are provided at bends for the connections of circular and tubular electrodes. Instead of wires, tubular electrodes of large diameters are used for connections in high voltage laboratories which bring down the field intensity at higher voltages considerably. These measures are necessary not only to prevent any partial breakdown (corona occurring in the laboratory) but also to check radio interference.
- It is a common practice to use bundles of two or more number of conductors at the same potential instead of a single conductor, to bring down the electric stress, i.e., for stress control, (Fig. 2.1 b). As the transmission voltages are increasing, bundles with eight or even more number of conductors are being used at higher voltages.
- Capacitive grading is provided in high voltage bushings, potential transformers and cable terminations in order to achieve a better potential distribution leading to a more uniform field distribution in the dielectric. It is achieved by inserting concentric conductive layers at appropriate positions, known as 'floating screens', to control the electric stress as shown in Fig. 4.4. This enables an economic utilisation of the insulating material by evenly distributing the equipotential surfaces in the complete

dielectric.

- Use of screen (also known as concentric conductor at ground potential) over the insulation in coaxial high voltage cables is made to control the electric stress. The field achieved in these screened cables is radial and generally a weakly nonuniform field. For making cable joints and terminations, the screen is extended in the form of a cone, known as 'stress cone'. This helps in achieving a more uniform distribution of electric stress in the dielectric at cable end termination as shown in Fig. 4.3 (d).
- A modest thumb rule to control electric stress in high voltage apparatus is to avoid sharp points and edges. Symmetrical, smooth shaped and large electrodes are preferable. It must be borne in mind that even the roughness on metallic surfaces can lead to distortions in the field at higher voltages. Furthermore, microprotrusions may grow and penetrate deeper in the dielectric leading to excessive field enhancement. These must be prevented from developing, firstly during manufacturing stage and subsequently during service and maintenance.



Segmented electrodes(Complete HV lab (600 kV AC))



Single metallic body (DC Generator 900 kV)

Fig 4.2 (Click on images to have an enlarged view)

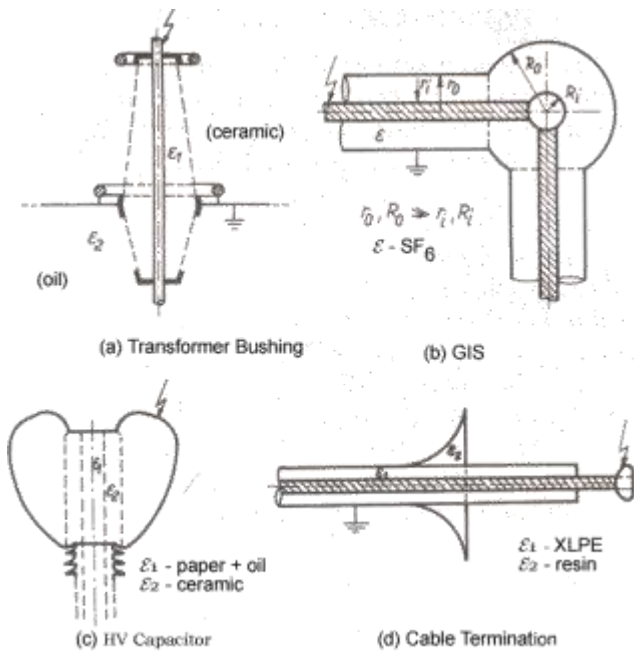


Fig 4.3 Extended shapes of electrodes for stress control (a) A bushing with toroids (b) Right angle bend of a bus bar in gas insulated switchgear (GIS), (c) HV electrode on a condenser, (d) stress cone at a screened cable end.

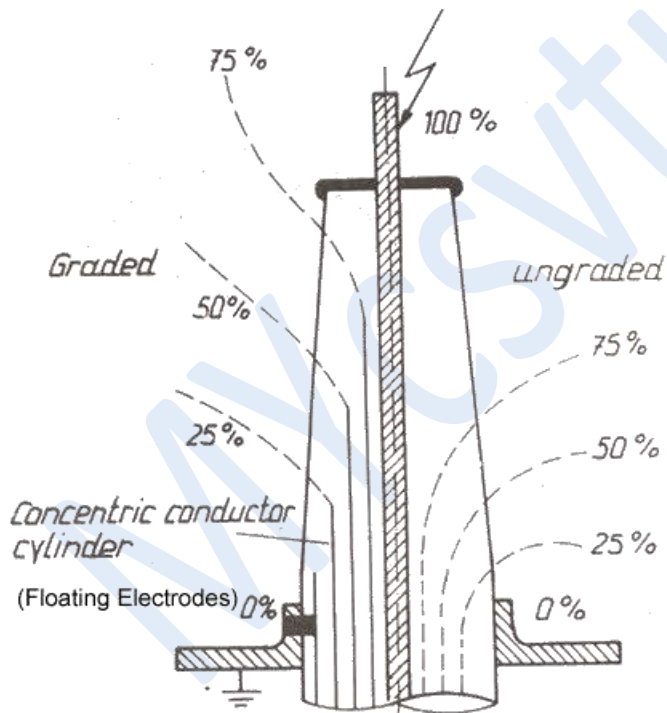


Fig 4.4 Potential distribution in a bushing with and without capacitive grading [1.1, 1.2]

MYCSVTU Notes

Objectives

In this lecture you will learn the following

- Properties of atmospheric air (N_2)
- Properties of Sulphurhexafluoride SF_6 Gas
- Electrical Properties of Vacuum as High Voltage Insulation

Properties of atmospheric air (N_2)

The most important, freely available and the cheapest gaseous dielectric is air. The atmospheric air is in fact a mixture of a number of gases. The detailed composition of earth's atmosphere is given in Table 5.1 as given by Goody and Walker in their book Atmospheres.

Table 5.1 Composition of the earth's atmosphere

Constituent	Percent by volume or by number of molecules of dry air
Nitrogen (N_2)	78.084
Oxygen (O_2)	20.946
Argon (A)	0.934
Carbon dioxide (CO_2)	0.031
Neon (Ne)	1.82×10^{-3}
Helium (He)	5.24×10^{-4}
Methane (CH_4)	1.5×10^{-4}
Krypton (Kr)	1.14×10^{-4}
Hydrogen (H_2)	5×10^{-5}
Nitrous oxide (N_2O)	3×10^{-5}
Xenon (Xe)	8.7×10^{-6}
Carbon monoxide (CO)	1×10^{-5}
Ozone (O_3)	upto 10^{-5}
Water (average)	upto 1

The largest percentage content of atmospheric air is nitrogen (about 78%), which is an electropositive gas. The second largest constituent is oxygen (about 20%), which is a very weak electronegative gas. The content of hydrogen, an electronegative gas too, is so low ($5 \times 10^{-5}\%$) that for all practical purposes the air can be considered as an electropositive gas. Majority of the

theoretical as well as experimental research work available in literature to study the complicated discharge processes in gaseous dielectrics have been performed on air.

Properties of Sulphurhexafluoride, SF₆ Gas

Sulphurhexafluoride was first produced in 1900 by French scientists Moissan and Lebeau by direct fluoronisation of sulphur. In the beginning it was mainly used as a dielectric in atomic physics. During late 1950s, it found application in high voltage circuit breakers. Ever since, its application in power systems has been continuously increasing.

Physical Properties

- In a SF₆ molecule, six fluorine atoms arrange themselves uniformly like an octahedron on a central sulphur atom. An excited sulphur atom can therefore form six stable covalence bonds with the strongly electronegative fluorine atoms by sharing the pair of electrons.
- Amongst halogens, the fluorine element and the sulphur atom both have very high coefficients of electronegativity, of the order of 4 and 2.5, respectively. This coefficient is a measure of the tendency to attract electrons of other atoms to form dipole bondage.
- The rigid symmetrical structure, small binding distance and high binding energy between atoms of a SF₆ molecule provide it high stability.
- Thermal dissociation in highly purified SF₆ gas begins at extremely high temperatures (above 1000 K). Such high temperatures in power systems occur only in electrical arcs. Even at continuous temperatures upto about 500 K, neither thermal decomposition of SF₆ nor its chemical reaction with other materials have been reported.
- Further, SF₆ is a nontoxic, colourless and odourless gas.
- Some important physical properties of SF₆, other than molecular properties, are brought together in Table 5.2.

Table 5.2 Physical properties of SF₆ [2.1]

Property	Physical conditions	Symbol	Unit	Value
Relative Permittivity	0.1 MPa, 25°C - 51°C (liquid)	ϵ_r	--	1.002 1.81 ± 0.02
Dielectric loss tangent	0.1 MPa, - 51°C (liquid)	$\tan \delta$	--	$< 5 \cdot 10^{-6}$ $< 5 \cdot 10^{-6}$
Critical temperature	--	θ_{cr}	°C	45.5
Tripple point	p=0.22 MPa	θ_T	°C	-50.8
Sublimation point	.	θ_s	°C	-63.8
Specific heat	at 10 ⁰ C and	C_p	$\frac{J}{molK}$	5.13

capacity	constant p=0.1 MPa			
	at 10 ⁰ C and const. volume	C _v	$\frac{\text{J}}{\text{molK}}$	4.06
Heat conductivity	30 ⁰ C	--	$\frac{\text{J}}{\text{cmsK}}$	0.82.10 ⁻⁵
Heat transition No.	--	--	$\frac{\text{J}}{\text{cmsK}}$	0.44.10 ⁻⁵

- The molecular mass of SF₆ is quite high (146), it has a high density. Because of high density the charge carriers have short mean free path. This property, along with the properties of electron attachment, that is, electronegativity and high ionization energy result in high dielectric strength of SF₆.

In Fig. 5.1 the two states of SF₆, liquid or gaseous, are shown at varying pressures and temperatures for different constant densities of the gas. This diagram is important from the point of view of practical application of SF₆ in GIS. Within the range of working pressure and temperature of the gas, it should not liquefy as its electrical insulation properties are affected.

Electrical Properties of Vacuum as High Voltage Insulation

The idea of vacuum as insulation is quite old. Tracing the historical development, it goes back to 1897 when R.W. Wood first gave description of discharges in vacuum while investigating the production of X-ray tubes. The desire to produce X-ray tubes operating at high voltages, impelled the investigators to study the dielectric properties of vacuum. Ever since, the vacuum as an insulation has gradually found its application in electronic valves, microwave tubes, Klystrons, photocells, particle accelerators and separators, controlled nuclear fusion devices, etc. On the other hand vacuum insulation is applied in high voltage apparatuses such as electrostatic generators, low-loss capacitors, circuit breakers and also for outer space applications.

- At extremely low gas pressures, electron ionization process becomes inadequate to cause a breakdown because the 'mean free path' of an electron (defined as the distance an electron can travel without colliding with another particle) is very long.
- In a vacuum better than 10⁻⁴ Torr (1.333 x 10⁻² Pa), less than 3 x 10¹² molecules per cm³ are estimated to be present and the length of the mean free path is of the order of meters. In such vacuum, an electron may cross a gap of a few cm between two electrodes without any collision.
- Therefore, unlike in gases, in vacuum the initial stage of breakdown cannot be due to the formation of electron avalanche.
- The process of multiplication of charged particles by collision in the space between the electrodes is far too insufficient to create avalanches. However, if a gas cloud forms in the vacuum, the usual kind of breakdown process can take place. Thus investigations of the

breakdown mechanism in vacuum have been oriented to establish the way gas clouds could be created in a vacuum. Mechanism, suggests that the prebreakdown currents that flow between vacuum insulated high voltage electrodes, frequently originate from nonmetallic emission mechanisms. These are associated with some kind of insulating/semiconducting surface oxides or impurity concentrations. From the technological point of view, the microscopic conditions of electrode surfaces continue to play an important role. Breakdown in vacuum is rather a complicated phenomenon involving a large number of processes with high electric field intensities. The 'field emission' process, that is, the electron emission from metallic surfaces in presence of strong electric fields, established itself through a considerable amount of work performed in the 20th century. After this a new process, a form of complex nonmetallic emission mechanism has made its break through to explain the prebreakdown conduction.

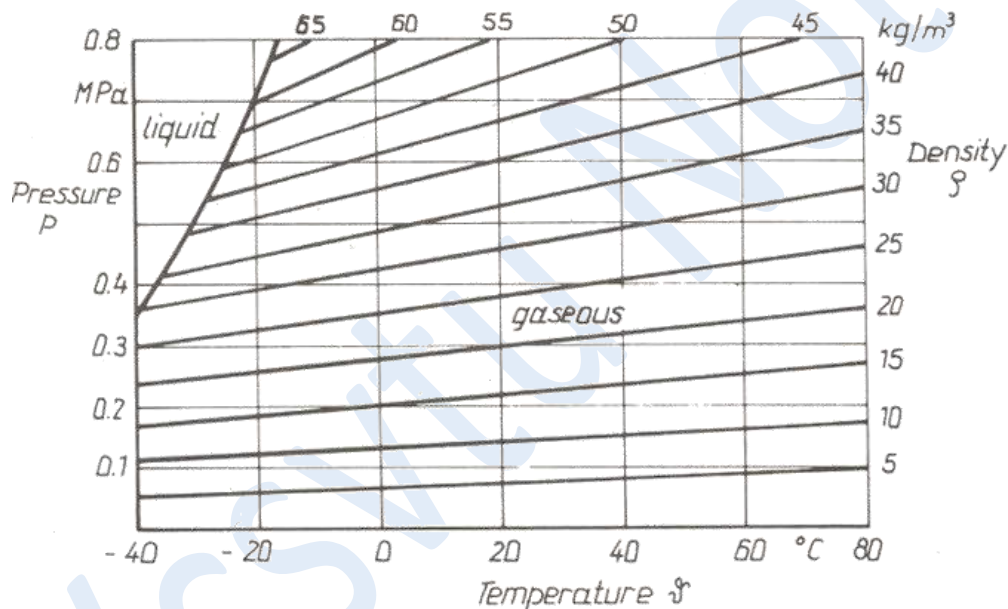


Fig 5.1 States of SF₆ for different constant gas densities and varying temperature and pressure within practical application range

VI

Objectives

In this lecture you will learn the following

- Prebreakdown of electron emission in vacuum
- Generation of Charge Carriers
- Impact Ionization
- Photoionization and Interaction of Metastables with Molecules

PREBREAKDOWN ELECTRON EMISSION IN VACUUM

- When the voltage across a very small gap (a few mm) is sufficiently increased, a relatively steady current

- A general observation made for small gaps is, that the prebreakdown current flow has been found to con
- For longer gap spacings ($> 1\text{ cm}$), small pulse currents of millisecond durations and charges of the order of microcoulombs (microdischarges) are measured.
- On raising the voltage further, the micro-discharge eventually give rise to a steady current .

Mechanisms of Electron Emission from Metallic Surfaces

There are a large number of mechanisms described in the literature that can produce electron emission from metallic surfaces under various conditions, for example, thermionic emission, field assisted thermionic, also known as Schottky or T-F emission, photoelectric emission, secondary emission caused by electron bombardment of an electrode and emission of ions under ion bombardment and metastable atoms [2.2]. Out of these, the most important mechanisms of electron emission in the prebreakdown regime are field assisted thermionic and thermionic emission.

Non-Metallic Electron Emission Mechanisms

Prebreakdown conduction currents between vacuum insulated high voltage electrodes frequently originate from microscopic field enhancement. These are associated with some form of insulating/semiconducting oxide layer on the surfaces or insulating microinclusions present on electrode surfaces can stimulate strong electron emission and significantly reduce the gap.

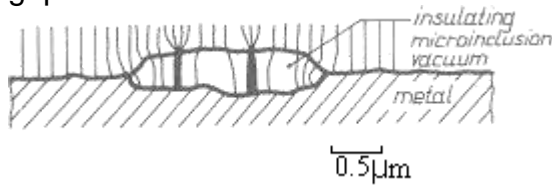


Fig 6.1 A schematic representation of insulating microinclusion emission regime with conducting microscopic field enhancement, Latham, [2.3, 2.4]

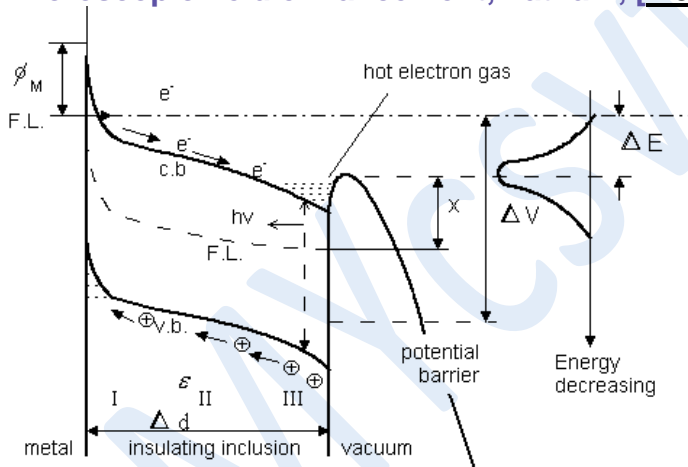


Fig 6.2 A band structure representation of an insulating microparticle in 'switched on state' of a vacuum electron emission. F.L.-Fermi level, c.b.-conduction band, v.b.-valence band, Latham generation of Charge Carriers

In a gas, the electrons and ions are the electric charge carriers. Ions are produced from neutral molecules by the attachment of an electron. Ejection of an electron from a neutral molecule leaves behind a positive ion. The attachment of an electron by a molecule produces negative ion. The mass of an electron compared to that of a molecule is very small ($1/1840$), therefore the mass of an ion can be considered to be equal to the corresponding molecule. Because of the small mass of an electron, its drift velocity in atmospheric air is $\sim 10^7\text{ cm/sec}$, whereas a heavy ion moves with a drift velocity of $\sim 10^3\text{ cm/sec}$. For a small gap distance between electrodes, ions can therefore be assumed not to have moved from the cathode to the anode.

generated.

During an electrical breakdown, the insulating gas between the electrodes is bridged by a conducting discharge canal. In a small gap distance the charge carriers required in order to build this discharge canal are not only produced by ionization of the dielectric across the gap (primary or α - process), but are also released from the electrode surfaces (secondary process). The production of charge carriers from the neutral gas molecules is known as ionization process. The ionization energy in long gap distances is the deciding factor leading to breakdown. One of the most significant features of an atom is the electron energy in different shells of a molecule. The total energy of an electron while still attached to the atom is divided into two types of energies. First the kinetic energy W_{KE} , which depends upon its mass and velocity, and the potential energy W_{pot} depending upon its charge in the Coulomb field of the nucleus of a molecule. These energies are given by the following equations:

$$W_{KE} = \frac{1}{2} m_e v_e^2 = \frac{1}{8\pi\epsilon} \cdot \frac{e^2 z}{r_e}$$

$$W_{pot} = -\frac{1}{4\pi\epsilon} \cdot \frac{e^2 z}{r_e} = -2W_{KE}$$

and

where m_e is the electron mass, v_e its velocity and ϵ the permittivity of the dielectric. z is the atomic number of the nucleus with negative elementary charge $e = -1.6 \times 10^{-19}$ As, lying in the discrete circular orbits r_e of an atom. When an electron gets ejected out of an atom shell, that is, $r_e \rightarrow \infty$, the potential energy of the electron becomes zero and the only energy it has, is the kinetic energy acquired externally. The total energy with which an electron is ejected from the molecule is given from Equations 6.1 and 6.2 as follows:

$$\begin{aligned} W_{total} &= W_{KE} + W_{pot} = \frac{1}{2} W_{pot} \\ &= -\frac{1}{8\pi\epsilon_0} \cdot \frac{e^2 z}{r_e} \end{aligned}$$

The binding energy of an electron in the n th shell to its nucleus is given as,

$$W_{total} = -13.61 \text{ eV} \cdot \frac{z^2}{n^2} = -W_1$$

This is the amount of energy required for releasing an electron from its molecule and, therefore, it is known as 'W1' of an electron. If a free electron is absorbed by a molecule forming a negative ion, the energy of ionization is known as 'energy of recombination'. The ionization energy W_1 in eV for different gases are given in Table 6.1

Table 6.1 Ionization energies for the first electron in gas

Gas	First Ionization energy W_1 (eV)
N₂	15.6
SF₆	15.6
H₂	15.9
O₂	12.1
H₂O (vapour)	12.7

CO ₂	14.4
He	24.0

Impact Ionization

- Impact or collision of particles amongst each other, accelerated under electrical field, leads to the formation of ion pairs from neutral gas molecules.
- The multiplication of charge carriers in gas takes place mainly by impact of electrons with neutral molecules (primary process).
- The positive ions make a moderate contribution to ionization only at solid insulation surfaces, which is a secondary process (secondary process) shown in Fig. 6.3.

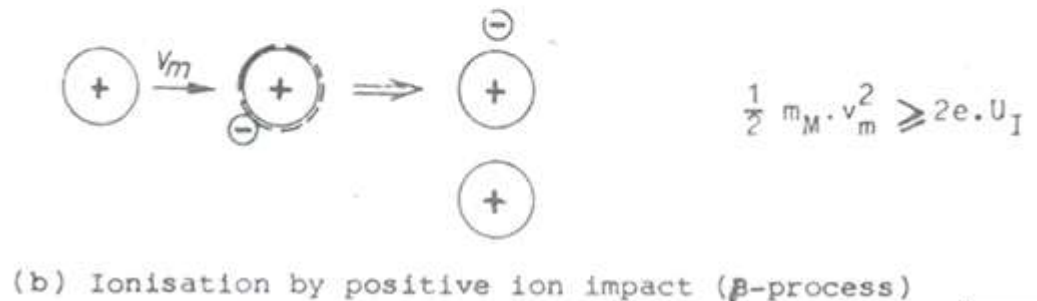
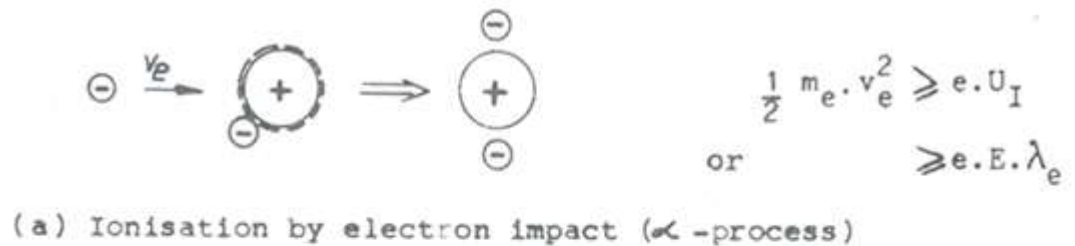


Fig 6.3 Impact ionization by electron and ion

where λ_e - The mean free path of the electron

U_I - The ionization potential

- The β - process does not play any significant role in gaseous dielectrics during the discharge leading to breakdown.
- It is the α -process alone which plays the major role.
- When an electron gains more kinetic energy than the required ionization energy W_1 of the gas molecule, it causes ionization by impact, that is, ejecting an electron from a neutral molecule and thus leaving behind a positive ion.
- To cause ionization, the incoming electron must have a kinetic energy greater than or equal to the ionization energy (eU_I).
- However, not all electrons having gained energy $\geq (eU_I)$ cause ionization on collision with neutral molecules. It is actually a probability process.
- The mean number of ionizing collisions made by a single electron per centimeter drift across the gap in a discharge is known as the Townsend's first or primary 'ionization coefficient', which represents basically a probability. It is a very important coefficient strongly dependent upon the electric field intensity,

$$\alpha = f(E)$$

Thermal Ionization

- If a gas is heated to sufficiently high temperature, to the order of 10,000 K and above, many of them acquire high velocity to cause ionization on collision with other atoms or molecules.
- The molecules excited by photon radiation also affect the ionization process.
- Thermal ionization is the principal source of ionization in flames and arcs.
- Saha derived an expression for the degree of ionization θ in terms of gas pressure p and absolute temperature T . Under the assumption that under thermodynamic equilibrium conditions, the rate of new ion formation must equal the rate of recombination. This expression is given as follows:

$$\frac{\theta^2}{1-\theta^2} = \frac{2.4 \times 10^{-4}}{p} T^{5/2} e^{-W_1/kT}$$

where p is the pressure in Torr, W_1 the ionization energy of the gas, k Boltzmann's constant ($k = 1.38 \times 10^{-23}$ J/K), θ that is, the number of ionized to total particles, and T the absolute temperature in Kelvin.

- Thermal ionization becomes significant only at temperatures above 10,000 K, as shown in Fig. 6.4

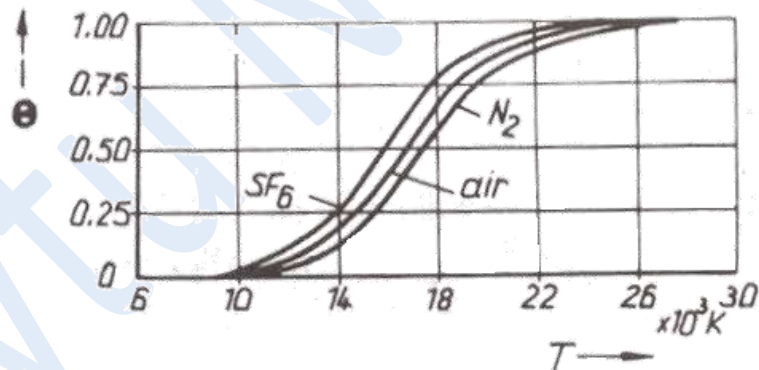


Fig 6.4 Degree of ionization of thermally ionized gases at 1 bar

- During electrical breakdown in gases, thermal ionization has its significance only towards the final stage of breakdown. Because of the transformation of large amount of energy in the electrically conductive channel into heat, the final stage of breakdown, an exceptionally high temperature rise in this channel core is possible.

Photoionization and Interaction of Metastables with Molecules

- The impact ionization process is possible only when the energy exchanged in collision is more than the ionization energy (eUI). The electrons having energy lower than the ionization energy may excite the gas molecules to excited states on collision. Under this condition, an electron is raised from a lower energy level to a higher energy level.
- On recovering from the excited state of electron in 10^{-7} to 10^{-10} sec, a molecule radiates a quantum of energy ($h\nu$).
- This energy in turn may ionize another molecule whose ionization potential energy is equal to or less than the energy.
- This process is known as photoionization and may be represented as $A+h\nu \longrightarrow A^+ + e^-$, where A is a molecule in the gas and $h\nu$ the photon energy.
- For the photoionization to occur,

$$h\nu \geq e.U_I$$

or the photon wavelength λ is,

$$\lambda \leq \frac{c_0 h}{e.U_I}$$

$$\frac{c_0}{\lambda} = \nu$$

as

where c_0 is the velocity of light ($c_0 = 2.998 \times 10^8$ m/s), h is Planck's constant ($h = 6.63 \times 10^{-34}$ J.s) and

- Only a very strong radiation of light quantum (photon) having a short wave-length of less than the photoionization energy of a gas.
- The basic requirement for photoionization to occur is that the quantum energy of electromagnetic radiation must be greater than the ionization energy of the gas.
- If the photon energy is less than (eU_I), it may still be absorbed by the molecule and raise it to an excited state. This process is known as photoexcitation.
- For certain gas molecules, the lifetime in the excited state may extend to a few tens of milliseconds. This state is called 'Metastable state' and the molecules under this state are referred as 'Metastables'.
- Metastables have a relatively higher potential energy and, therefore, ionize neutral particles on collision.
- However, the photons released by this reaction have too low energy to cause ionization in pure gas. The ionization is caused by electrons on striking the cathode. This process is known as the cathode emission or secondary emission. It is described by the secondary emission coefficient δ . Since the ionization caused by metastable interaction is accompanied with a time delay, it has a significant effect on the discharge reactions are responsible for longer time-lags than usual in some gases.

VII

Objectives

In this lecture you will learn the following

- Development of Electron Avalanche in uniform field
- Townsends primary ionization coefficient

Development of Electron Avalanche

- Initially the electrons are originated in a gaseous dielectric gap space between two electrodes either by ionization of gas molecules by photons from cosmic rays, or by ultraviolet illumination of cathode, or at a later stage the discharge itself when electric field is applied.
- The electrons thus generated accelerate towards the anode, gaining kinetic energy of movement from the electric field between the electrodes.
- The kinetic energy thus acquired by the electrons can be so high that on collision with neutral molecules they can ionize them (elastic collision) or render them to a higher excited or vibrational state (inelastic collision).
- When an electron gains more energy than required for ionization of the gas molecules (Table 6.1), it ionizes the molecule, that is, ejecting an electron from the neutral molecule, and leaving behind a positive ion.

- The new electron thus ejected along with the primary one repeat the process of ionization.
- Since a molecule is much heavier compared to an electron, it can be considered relatively stationary during the ionization process.
- On the contrary, the electrons move very fast under the influence of applied electric field and collect electrons from the gas molecules.
- An 'avalanche' of electrons finally reaches the anode as shown in Fig. 7.1

VIII

Objectives

In this lecture you will learn the following

Breakdown with Avalanche Discharge (Townsend Mechanism)
Growth of conduction current in gaseous dielectrics

Breakdown by Avalanche Discharge (Townsend Mechanism)

- When the distance d between two electrodes in a uniform field is very small, α the Townsend's first ionization coefficient which is a function of field intensity E , may still have quite a low value even at the breakdown field intensity.
 - Under these conditions, the avalanche space charge concentration is not able to acquire its critical value for amplification (the total number of electrons $\approx 10^8$).
 - Production of sufficient number of charge carriers in the gap under such conditions is possible only through secondary ionization process, also known as γ - process.
 - These secondary processes are ionization of the gas 'by positive ions and photons from the excited molecules, and ejection of electrons from the cathode by following effects:
1. Positive ion effect ' γ_{ion} ': While the positive ions, produced in the primary avalanche, cannot gain enough kinetic energy in the electric field to ionize molecules, they may have sufficient potential energy to cause ejection of electrons upon striking the cathode.
 2. Photon effect ' γ_p ': Excited molecules in the avalanche may emit photons on returning to their ground state. This radiation falling on cathode may produce photo-emission of electrons.
 3. Metastable effect ' γ_m ': Metastable molecules may diffuse back to the cathode and cause electron emission on striking it.
- The three processes of cathode effect are described quantitatively by a coefficient ' γ ' as follows,

$$\gamma = \gamma_{ion} + \gamma_p + \gamma_m$$

- ' γ ' is known as Townsend's secondary ionization coefficient. It is defined as the number of secondary electrons on an average produced at the cathode per electron generated by the primary process, that is, per ionizing collision in the gap. ' γ ' strongly depends upon the cathode material and is a function of field intensity and pressure of the gas."

$$\gamma = f\left(\frac{E}{p}\right)$$

- Like α , γ also represents a probability process. If the mean number of secondary electrons per avalanche produced are μ , then considering Equation 7.4,

$$\mu = \gamma(e^{\alpha d} - 1) \quad (8.1)$$

If the primary electron generation process begins with n_0 number of electrons, the second generation begins with μn_0 number of electrons.

- Average current growth with respect to the applied voltage and time are shown in Figs. 8.1 - 8.3

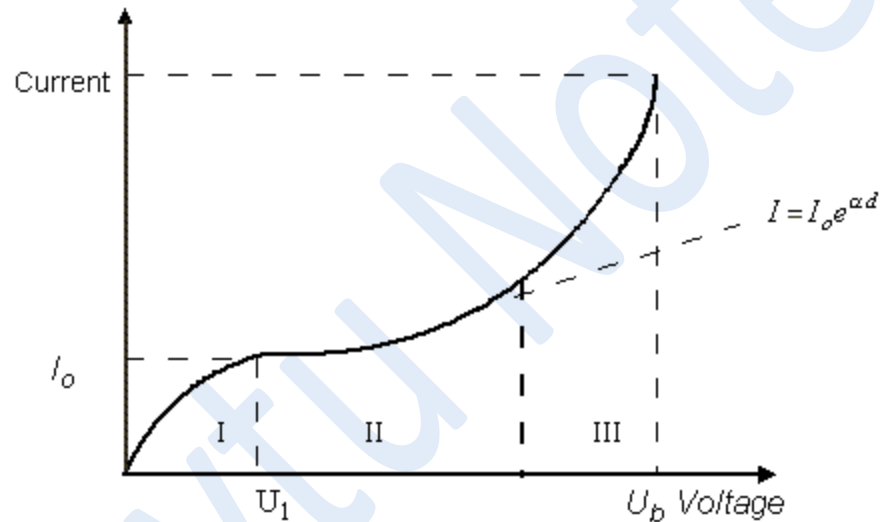


Fig 8.1 General conduction current-voltage characteristics before breakdown.

- In order to measure the U-I characteristic, Townsend's original experimental arrangement had uniform field electrodes enclosed in a glass vessel. This vessel was provided with a quartz window irradiating the cathode with ultra violet light to emit photo electrons [2.9].
- As the voltage applied is raised, the initial current through the gap increases slowly to a value I_0 .
- The magnitude of this current depends upon the ultra violet illumination level of the cathode, region shown in Fig. 8.1.
- The electrons emitted from the cathode move through the gas with an average velocity determined by their mobility at the field intensity in the gap.
- The initial increase in current is followed by an approach to saturation because some of the electrons emitted from the cathode return to it by diffusion.
- The proportion of electrons which diffuse back decreases as the voltage is increased, but not all the electrons emitted reach the anode, even at the voltages at which ionization in the gas begins to occur.
- Thus, in general, there is no well defined plateau in the U-I characteristic, and the current eventually increases rapidly through the regions II and III with increasing voltage until a breakdown occurs at some well defined voltage $U = U_b$ [2.10].
- Whatever may be the level of initial illumination of cathode, the voltage U_b at which the breakdown occurs remains unaltered.
- The increase in current in region II is derived from the process of field intensified ionization by primary electrons.

or α - process.

- The secondary or γ -process accounts for the sharper increase in current in region III and for eventual spark breakdown of the gap. Figure. 8.2 shows the U-I characteristic in helium at a pressure of 488 Torr, measured by Rees [2.11]. It is evident from the Fig. 8.1 and 8.2 that the characteristics measured by Townsend and Rees are very similar.

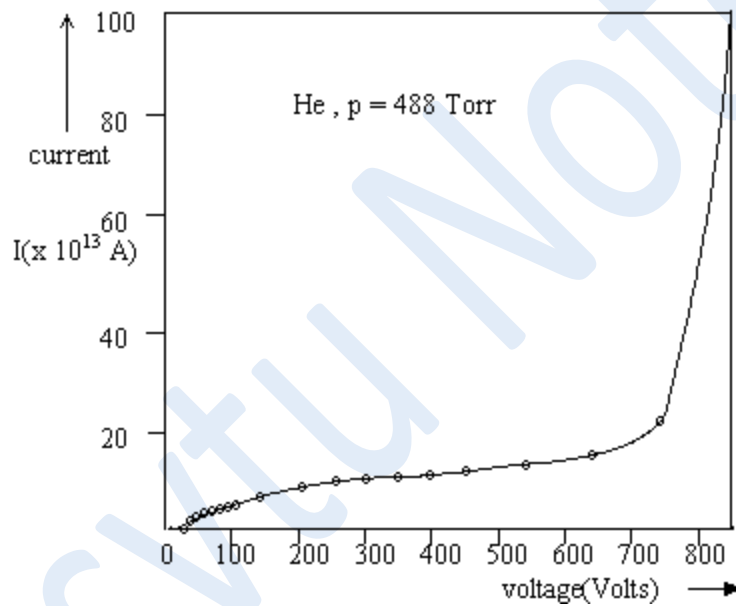


Fig 8.2 Voltage-current (U-I) characteristics in helium measured by Rees [2.11] in 1963.

- It is a distinguishing feature of breakdown that the voltage across the gap drops in the process which produces a high conductivity between the electrodes. This takes place in a very short time (in μ secs).
- If α is the primary ionization coefficient for the applied uniform field E_0 , the amplification of ionization collisions of the electrons is given by $e^{\alpha x}$.
- In the event of positive ion space charge distorting the field, the amplification of α which increases with distance and time is given as,

$$\exp \left[\int_0^d \alpha(x,t) dx \right]$$

For this case, $\mu(t)$ can be written as,

$$\mu(t) = \gamma \left\{ \exp \left[\int_0^d \alpha(x,t) dx \right] - 1 \right\}$$

which grows continuously above 1, till breakdown occurs.

- Experiments have been performed to study the current growth in uniform fields in air and other gases initiated by a single electron ($n_0 = 1$) with the help of a light flash. The process with higher number of electrons ($n_0 \gg 1$) is achieved by illuminating the cathode with constant intense light [2.12-2.14].
- Heger [2.13] developed one such method of measurement in nitrogen.
- With the help of theoretical considerations confirmed with experimental results, he computed the current growth started by a single and more number of electrons as in Fig. 8.3. The measured values are indicated by the vertical lines.
- At lower values of current, the statistical distribution scatters more compared to the distribution at higher current values.

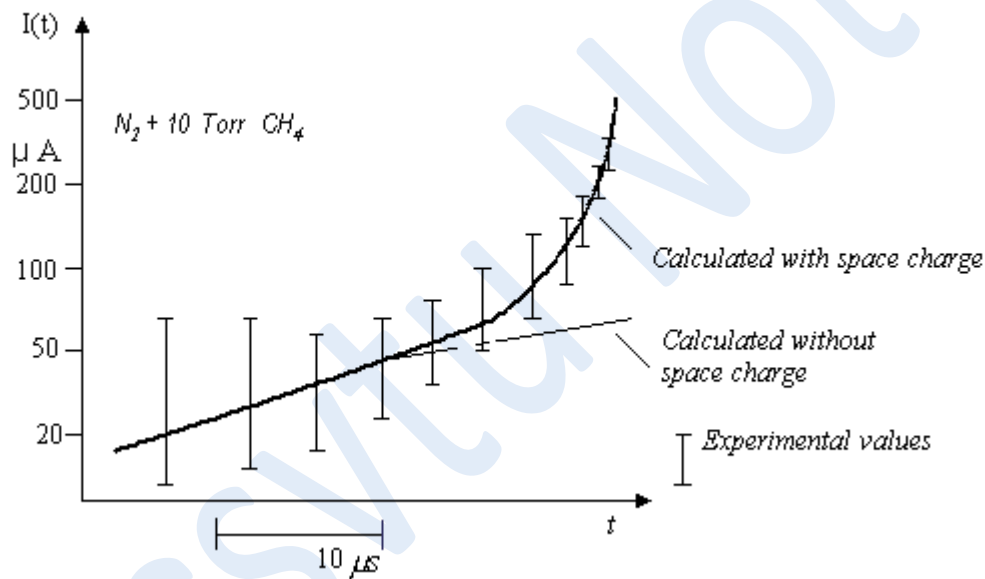


Fig 8.3 Current growth initiated by a single electron, ($E/p_{20} = 44.8$ V/cm. Torr, $d = 2$ cm, $\alpha d = 12.3$, $\mu = 1$) on semilogarithmic plot by Heger [2.13] 1963.

- The movement of charge carriers (electrons and positive ions) in the gap is responsible for the growth of circuit current.
- The saturation level of the curve in Fig 8.1 (region II) is also called the steady state region.
- If it is assumed that the number of positive ions diffusing per second at the cathode are just equal to the number of newly formed electrons arriving at the anode, the growth of current in this region can be given by,

$$I = I_0 e^{\alpha d}$$

(8.2)

where I_0 is the initial photo-electric current at the cathode.

- Although this expression represents the averaged effect of a number of avalanches, it fails to signify the breakdown.
- The current in region III has a much steeper rise till a breakdown occurs which is rendered to the γ secondary ionization process.
- The Townsend's current growth equation in this region is derived in [2.9] as follows:

Let

n_0 = the number of primary electrons (photo electrons) emitted from the cathode (at $x = 0$) per second. In other words, an avalanche in uniform field develops at the cathode with n_0 initial electrons.
 n_0' = the number of secondary electrons produced at the cathode per second. and
 n_0'' = the total number of electrons leaving the cathode per second.

Thus

$$n_0'' = n_0 + n_0' \quad (8.3)$$

- Since each electron leaving the cathode makes on an average $(e^{\alpha d} - 1)$ collisions in the gap d , therefore, the total number of ionizing collisions per second in the gap will be $n_0'' (e^{\alpha d} - 1)$.
- By definition, γ is the number of secondary electrons produced on an average at the cathode per ionizing collision in the gap, then,

$$n_0' = \gamma n_0'' (e^{\alpha d} - 1) \quad (8.4)$$

Substituting Equation 5.9 in 5.8, we have

$$n_0'' = n_0 + \gamma n_0'' (e^{\alpha d} - 1)$$

or

$$n_0'' = \frac{n_0}{1 - \gamma(e^{\alpha d} - 1)} \quad (8.5)$$

- From Equation 7.4, the number of electrons arriving at the anode is given by,

$$n_d = n_0'' e^{\alpha d}$$

By putting the value of n_0'' in the above equation, we have

$$n_d = \frac{n_0 e^{\alpha d}}{1 - \gamma(e^{\alpha d} - 1)} \quad (8.6)$$

- Under the steady state conditions, the current in the gap can therefore be given by,

$$I = \frac{I_0 e^{\alpha d}}{1 - \gamma(e^{\alpha d} - 1)}$$

(8.7)

This equation describes the growth of average current in the gap before the breakdown.

- According to Equation 8.1, $\gamma(e^{\alpha d} - 1)$ in the denominator of Equation 8.7 represents μ , the mean

number of secondary electrons produced per avalanche. For $\mu \ll 1$, the secondary ionization, or process is insignificant. Then equation 8.7 reduces to $I \approx I_0 e^{\alpha d}$, which represents the region II in Fig. 8.1. The applied voltage and hence the field intensity is low in this region. This condition is described as 'non-self-sustaining discharge', or ionization process, under which a breakdown would not be able to develop by itself.

- As the applied voltage, and thus the field intensity E is increased, the value of μ approaches 1. The denominator of this equation approaches zero and, therefore, the current I tends to rise unlimitedly. At this stage, the current is however limited by the impedance offered by the power supply and by the gas itself. Under these conditions, the discharge or ionization process becomes self-sustained and maintains the level of required charge carriers, described as a 'self-sustaining discharge'.
- The quantitative condition for breakdown can be expressed as,

$$\mu = \gamma(e^{\alpha d} - 1) = 1 \tag{8.8}$$

This equation is known as the 'Townsend Criterion' for spark breakdown in uniform field.

- At the final stage of breakdown, the electron amplification is normally much greater than one ($e^{\alpha d} \gg 1$), so the criterion reduces to

$$\gamma e^{\alpha d} = 1 \tag{8.9}$$

- Under the condition when $\mu > 1$, a strong concentration of charge carriers grows in the subsequent 'generations' of electron production.
- These equations and conclusions are also valid for weakly nonuniform fields where the μ is defined in a slightly different way as follows:

$$\mu = \gamma \left[\exp\left(\int_0^d \alpha dx\right) - 1 \right] \tag{8.10}$$

- The Townsend's mechanism of spark breakdown can, therefore, be explained on the basis of the observation that the ionization process begins with a number of 'series of avalanches'.
- It extends over the whole gap and ultimately constricts into a spark or breakdown channel. A conceptual schematic of the breakdown mechanism is shown in Fig. 8.4.

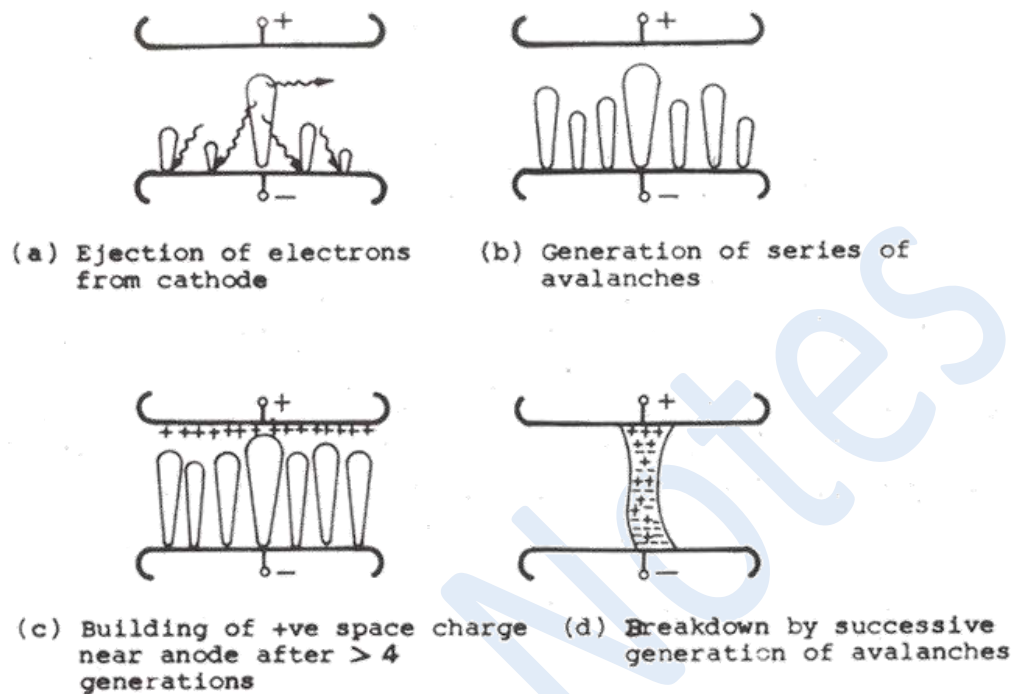


Fig 8.4 Townsend breakdown mechanism schematic.

IX

Objectives

In this lecture you will learn the following

- Breakdown with Streamer Discharge (Streamer or Kanal Mechanism)
- Critical amplification of avalanche

Breakdown by Streamer Discharge (Streamer or Kanal Mechanism)

According to Townsend's generation mechanism, the time required for breakdown by normal avalanche propagation is determined by the drift velocity of electrons in a few generations. The estimated time required for breakdown in comparatively longer gap distances by this theory was too long, contrary to the actual time measured experimentally. With the development of electrical and optical measurement methods, this was confirmed by Raether as early as 1939 [2.6]. This necessitated a novel approach for breakdown mechanism suitable for longer gap distances than as explained by Townsend in uniform fields.

- The streamer breakdown mechanism describes the development of spark breakdown directly from a single avalanche.
- The space charge developed by the avalanche itself due to rapid growth of charge carriers transforms it into a conducting channel. As described by Raether, it is the 'eigen space charge' which produces the instability of the avalanche.
- The word streamer literally means a ribbon attached at one end and floating or waving at the other which appears to be a set of waves or ripples moving forward. Streamer also means a column of light shooting up in aurora.

- This kind of visual display results during a discharge due to the movement of pockets of ionized particles.
- The term 'Kanal' is taken from German language which means a canal or a channel.
- The approximate calculations of the conditions required for the space charge field of avalanche E_a to be able to acquire the magnitude of the order of the externally applied field E_0 , confirmed that the transformation from avalanche to streamer began to develop from the head of an electron avalanche when the number of charge carriers increased to a critical value,

$$n_0 e^{\alpha x_c} \approx 10^8$$

- For an avalanche initiated by a single electron ($n_0 = 1$) in a uniform field, this corresponds to a value,

$$\alpha x_c = \alpha d_c = \ln 10^8 \approx 20$$

where x_c is the length of avalanche in the field direction when it amplifies to its critical size.

In other words, x_c is the critical length of the electrode gap d_c . This means that the streamer mechanism is possible only when $d \geq x_c$. If x_c is longer than the gap length d ($x_c > d$) then the initiation of streamer is unlikely as shown in Fig.9.1

- On the basis of experimental results and some simple assumptions, Raether developed the following empirical formula for the 'streamer breakdown criterion'.

$$\alpha x_c = 17.7 + \ln x_c + \ln \frac{E_a}{E_0}$$

- The interaction between the space charges and the polarities of the electrodes results in distortion of the uniform field.
- Field intensities towards the head and the tail of avalanche acquire a magnitude $(E_a + E_0)$, while above the positive ion region, just behind the head, the field is reduced to a value $(E_0 - E_a)$, (see Fig. 9.1).

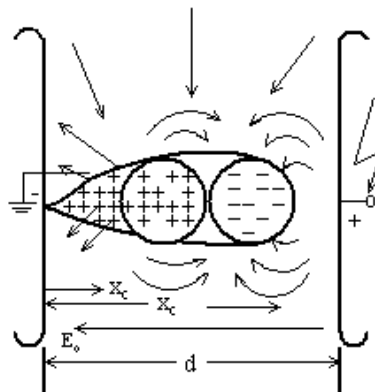


Fig 9.1 Effect of space charge field E_a of an avalanche of critical amplification on the applied uniform field.

- If the charge lies nearly in a spherical shape of radius r_a then the field at the surface of this space charge in the form of a sphere is,

$$E_a = \frac{e \exp(\alpha x)}{4\pi\epsilon_0 r_a^2}$$

where e is the elementary charge of an electron and ϵ_0 the absolute permittivity constant.

- The condition for transition from avalanche to streamer breakdown assumes that this eigen space charge field approaches near the externally applied field ($E_a \approx E_0$). Hence the above breakdown criterion becomes,

$$\alpha x_c = 17.7 + \ln x_c$$

- The minimum value of αx_c required for breakdown in a uniform field gap by streamer mechanism is obtained on the assumption that the transition from avalanche to streamer occurs when an avalanche of critical size just extends across the gap d . By incorporating this condition, the breakdown criterion takes the form,

$$\begin{aligned} \alpha d_c &= 17.7 + \ln x_c \\ &\approx 20 \end{aligned}$$

- Thus the condition $x_c = d_c$ gives the smallest value of α to produce streamer breakdown, where d_c is given in cm. For $\alpha x_c = \ln 10^8$, x_c works out to be equal to 2cm which can be considered to be critical gap distance, d_c , for streamer phenomenon to take place in atmospheric air in uniform field.
- The 'streamer breakdown criterion' can be therefore interpreted as a condition for the development of significant field distortion caused by stark space charge within a single avalanche so that its field intensity is comparable to the externally applied field.

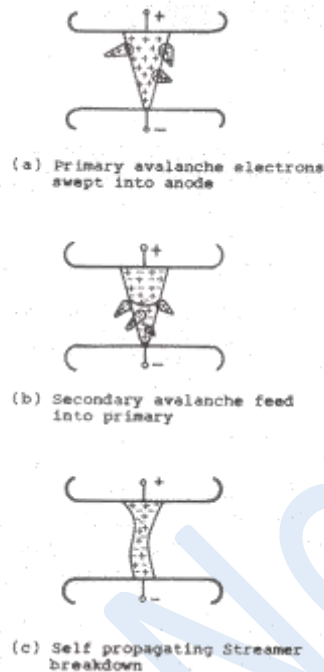


Fig 9.2 Schematic of a cathode directed streamer breakdown showing development stages.

- In sufficiently long air gap in uniform field when the avalanche extends across the gap, the electrons are swept into the anode, and the positive ions in the tail of the avalanche stretch out across the gap as shown in Fig. 9.2.
- A highly localized space charge field due to positive ions is produced near the anode but since the ion density elsewhere is low, it does not constitute a breakdown in the gap.
- In the gas surrounding the avalanche, secondary electrons are produced by photons and photoelectric effect from the cathode.
- The secondary electrons initiate the secondary avalanches, which are directed towards the stem of the main avalanche, if the space charge field developed by the main avalanche is of the order of the applied field. Thus the secondary avalanches feed into the primary avalanche as shown in Fig. 9.2 (a), (b).
- The positive ions left behind by the secondary avalanches effectively lengthen and intensify the space charge of the main avalanche in the direction of the cathode and the process develops a self propagating streamer breakdown shown in Fig. 9.2 (c).
- Significant development in high-speed photographic techniques, strengthened by the incorporation of image converters and image intensifiers have made it possible to record the progress of the discharge light output at earlier stages than hitherto.
- Figure 9.3 shows the photograph of an avalanche where secondary avalanches are feeding into the primary avalanche, taken in a gap of 3.6 cm in air at 270 Torr and a field intensity of about 12,200 V/cm by Raether [2.6.]

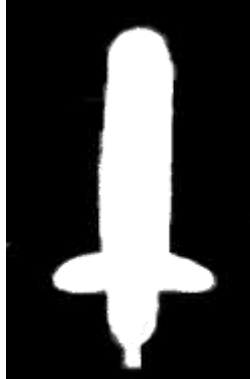


Fig. 9.3 Photograph of a cathode directed streamer developed from an avalanche, Raether [2.7]

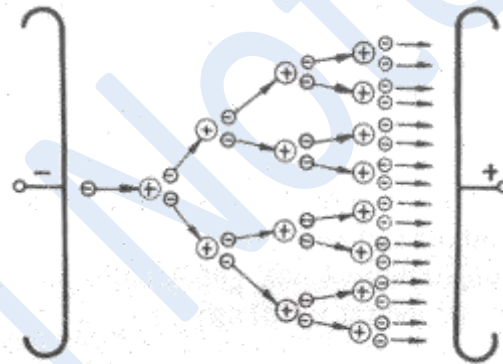


Fig 7.1 Development of an electron avalanche in uniform field

- At the field intensities at which impact ionization occurs, the value of drift velocity of electrons in air of positive ions it is about 150 times lower $\sim 10^5$ cm/s. Accordingly, the transit time required by electrons differ about 150 times.
- The process of avalanche form of charge carrier multiplication was first described by Townsend(19 mathematical formulation.
- If only the process of electron multiplication by electron collision is considered in uniform field between neglecting other processes (recombination and diffusion), the number of electrons produced by col distance x from the cathode is,

$$dn_x = n_x \alpha dx$$

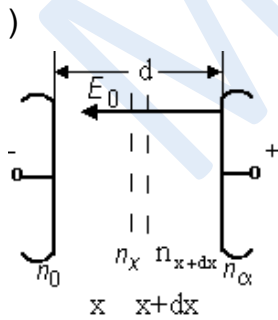


Fig. 7.2 Electrons in a uniform field

where x is the distance from the cathode, α the Townsend's primary ionization coefficient, and n_x the number of electrons at distance x from the cathode.

- In a uniform field where the field intensity E is constant, the ionization coefficient α can be considered constant. From Equation 7.1 and applying the initial condition $n_x = n_0$ at $x = 0$, the following equation is derived for a uniform field:

$$n_x = n_0 e^{\alpha x} \quad (7.2)$$

- For weakly nonuniform fields, where α is not constant, the above equation is written as,

$$n_x = n_0 \exp \left[\int_0^x \alpha dx \right] \quad (7.3)$$

where n_0 is the number of electrons emitted per second from the cathode, also known as the initial number of electrons.

- Therefore, in case of very small gap distances, the number of electrons striking the anode per second is given by

$$n_d = n_0 e^{\alpha d} \quad (7.4)$$

- This means that on an average each electron leaving the cathode produces $(e^{\alpha d} - 1)$ new electrons and $(e^{\alpha d} - 1)$ positive ions in traversing the distance d .
- The expressions 7.2 - 7.4 show distinctly the exponential or avalanche form of growth of the number of electrons in the primary or α process.
- The Townsend's first ionization coefficient α is a function of the electric field intensity E , and at a given field intensity it is dependent upon the gas pressure p . It can be proved that,

$$\frac{\alpha}{p} = f\left(\frac{E}{p}\right)$$

- The coefficient α can be calculated with the help of molecular parameters. However, α is usually obtained by measuring the multiplication of electrons in high electric fields. For air, the following equation is approximately valid:

$$\frac{\alpha}{p} \approx 1.11 \times 10^{-4} \left(\frac{E}{p} - 25.1 \right)^2$$

where E is in V/cm, p in Torr and α in cm^{-1} .

- Equation 7.5 is plotted for α/p and E/p in Fig. 7.3 at constant temperature.
- Raether was able to take first photographs of the trace of an electron avalanche in 1939 [2.6]. He called it 'Cloud Chamber', which caused condensation of water vapour droplets on the charge carriers of an

gas pressure.

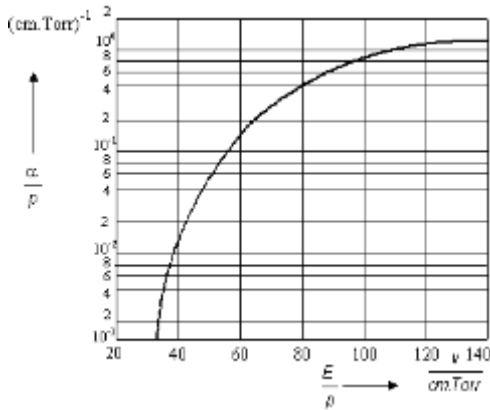


Fig 7.3 Apparent ionization coefficient α / p as function of E/p for air.

- In his experiment, a short duration voltage pulse was applied on the electrode system shown in Fig 7.4 (a).
- When the voltage applied reached its desired peak value, just sufficient to develop an avalanche magnitude, but was not allowed to lead to a breakdown.
- Just at this stage, primary electrons were produced in the electrode system with the help of an external source, as shown in Fig. 7.4 (b).
- This gave rise to the development of an electron avalanche.
- In order to avoid a breakdown, the process was controlled by a steep reduction in the applied voltage of a few tens of nanoseconds.

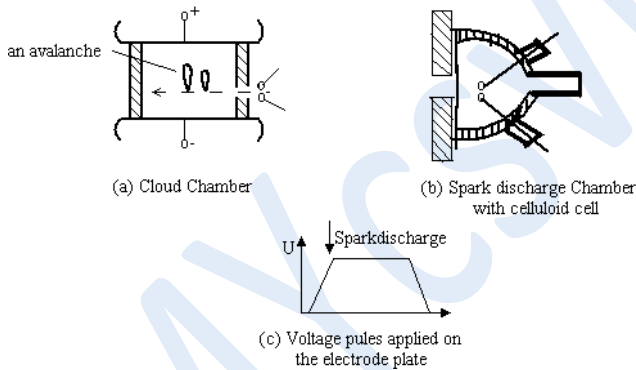


Fig 7.4 Experimental arrangement to produce an avalanche.

- Since the drift velocity of electrons is about 150 times more than that of the ions, hence as soon as a positive ions remain practically stationary where they are produced, i.e, at the tail of the avalanche.
- The head of the avalanche is consequently built-up by electrons.
- The form of the track is wedge shaped, apparently due to the thermal diffusion of the drifting electrons and the acceleration in the direction of electric field.
- The head of the avalanche is rounded since the diffusion of electrons takes place in all directions.
- Fig 7.5 shows the distribution of charge carriers and actual photographs of avalanche [2.7, 2.8].

Objectives

In this lecture you will learn the following

Paschen's Law

Breakdown in gaseous dielectrics in Uniform Fields

Breakdown Voltage Characteristics in Uniform Fields (Paschen's Law)

- In uniform fields, the Townsend's criterion for breakdown in electropositive gases is given by the following equation,

$$\gamma (e^{\alpha d} - 1) = 1$$

or

$$\alpha d = \ln (1/\gamma + 1)$$

where the coefficients α and γ are functions of E/p and are given as follows:

$$\alpha = p f_1 \left(\frac{E_0}{p} \right)$$

$$\gamma = f_2 \left(\frac{E_0}{p} \right)$$

and

where E_0 is the applied electric field, and p the gas pressure. In a uniform field electrode system of gap distance d ,

$$E_b = \frac{U_b}{d}$$

where U_b is the breakdown voltage and E_b the corresponding field intensity. E_b is equal to the electric strength of the dielectric under given conditions. When the applied field intensity $E_0 = E_b$, the Townsend's criterion for breakdown in electropositive gases in uniform field can be represented in terms of the product of the gas pressure and the electrode gap distance ' pd ' as,

$$f_2 \left(\frac{U_b}{pd} \right) \left\{ \exp \left[pd f_1 \left(\frac{U_b}{pd} \right) \right] - 1 \right\} = 1$$

(10.1)

or

$$U_b = f(pd)$$

(10.2)

This is known as Paschen's law. The scientist, Paschen, established it experimentally in 1889 from the measurement of breakdown voltage in air, carbon dioxide and hydrogen. It can be shown that this law is also applicable to electronegative gases. The values of α depend upon the particular gas and of γ upon the electrode material. The breakdown voltage of a gas in uniform field is, therefore, a unique function of the product of gas pressure, ' p ' and the gap distance between electrodes ' d ' for a given electrode material and its condition.

- At low value of E/p , that is at high pressures, where a steady state can be achieved, experiments have been performed on the spatial growth of ionization in a large number of both, electropositive and electronegative gases. In these experiments the conduction gap currents were maintained below $0.1 \mu\text{A}$, so that the field distortions due to space charge remained at a minimum. The results have shown that this generalised Townsend's theory of breakdown is applicable over a wide range of physical conditions. The values of the breakdown voltages U_b estimated theoretically have been found in good agreement with those

observed experimentally.

- A schematic of the variation of U_b with respect to ' pd ' is shown in Fig. 10.1. Equation 10.1 does not imply that the breakdown voltage varies linearly with ' pd ', although in practice it is found to be nearly linear over certain regions. The breakdown voltage attains a minimum value $U_{b\ min}$ around a particular value of the product $(pd)_{\min}$.

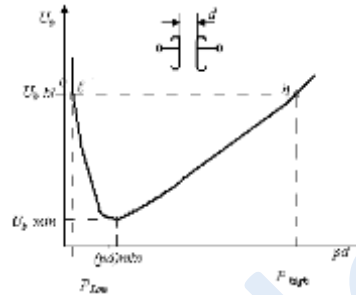


Fig 10.1 Breakdown voltage vs pd characteristics in uniform field (Paschen's curve)

Breakdown Voltage Characteristics in Uniform Fields (Paschen's Law) (contd.)

- To explain the shape of the curve in last slide, it is convenient to consider a gap with fixed space (constant), and let the pressure decrease from a point P_{high} on the curve at the right of the minimum. As pressure is decreased, the density of the gas decreases, consequently the probability of an electron collisions with the molecules goes down as it travels towards the anode. Since each collision results in a loss of energy, a lower electric field intensity, hence a lower voltage suffices to provide electrons the energy required for ionization by collision to achieve breakdown.
- When the minimum of the breakdown voltage is reached and the pressure still continues to be decreased, the density of the gas becomes so low that relatively fewer collisions occur. Under such conditions, an electron may not necessarily ionize a molecule on colliding with it, even if the kinetic energy of the electron is more than the energy required for ionization. In other words, an electron has a finite chance of ionizing a molecule which depends upon its energy. The breakdown can occur only if the probability of ionization becomes greater than one by increasing the field intensity. This explains the increase in breakdown voltage to the left of the minimum. At very low pressures, P_{low} , partial vacuum conditions exist, hence this phenomenon is applicable in high vacuum tubes and switchgears. Under these conditions, the effect of electrode material surface roughness plays an important role on the breakdown voltage especially at small gap distances and the Paschen's Law is no more valid to the left of the minimum of this curve.

With the help of many scientists, Schumann, Sohst and Schröder, the following equation for breakdown voltage in air in uniform field was derived.

$$\hat{U}_b = 6.72 \sqrt{pd} + 24.36 (pd) \text{ kV}$$

(10.3)

where p is given in bar and d in cm, therefore pd in bar.cm

- Calculated values of breakdown voltages using Equation 10.3 for uniform field in air have been compared with the available experimental results from different authors by Dakin et al. [2.15] as shown in Fig. 10.2. The peak values of the breakdown voltages in kV and pd in bar. mm are plotted on a double logarithmic scale.

paper. As seen in this figure, the calculated and the measured results agree with each other well, except for the very low values of pd . In this region where the E/p values are quite high due to low pressure, equation 10.3 no longer holds good and the Paschens law is no more valid. In this region or in the pressure range of ≤ 25 Torr till upto 10^{-3} Torr, the phenomenon of Faraday Glow occurs. The air acquires a glow state on applying quite low voltages depending upon the actual pressure.

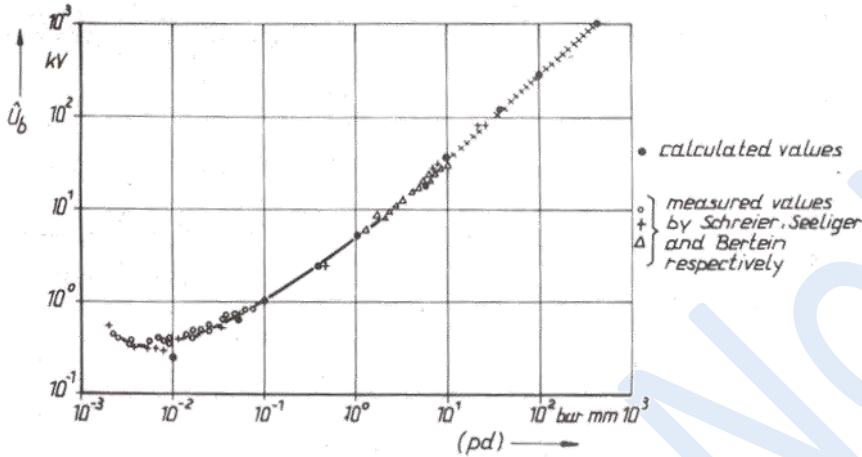


Fig 10.2 Paschen's curve for air at temperature 20°C

Breakdown Voltage Characteristics in Uniform Fields (Paschen's Law) (contd.)

- It is more convenient to introduce the 'relative gas density', δ - a dimensionless quantity, in place of gas pressure p . ' δ ' takes care of the effect of temperature on the mean free path of electrons in the gas at constant pressure. The number of collisions made by an electron in crossing a gap is, therefore, proportional to the product δd and γ . Correction for the variation in ambient conditions of air is made by introducing the 'relative air density', δ , defined as,

$$\delta = \frac{p}{760} \cdot \frac{293}{273+t} = 0.386 \frac{p}{273+t} \tag{10.4}$$

where p is in Torr and t in °C.

At normal temperature ($t= 20^\circ\text{C}$) and pressure ($p = 760$ Torr), δ is equal to one. Equation for normal temperature and pressure will be,

$$\hat{U}_b = 6.72 \sqrt{d} + 24.36 d$$

or

$$\hat{E}_b = 24.36 + \frac{6.72}{\sqrt{d}} \quad \text{kV/cm}$$

(10.5)

It is interesting to note that even in uniform field at constant pressure and temperature, the electric strength of air is not constant. It tends to 24 kV /cm for very long gaps. The value 31 kV/cm is applicable only for $d = 1$, that is for one cm gap at 760 Torr and 20°C. For gaps of a few mm, the electric strength is much higher than 31 kV/cm. It has been measured to rise to about 92 kV/cm for a gap of 0.1 mm. A plot of Equation 10.5

shown in Fig. 6.3. This is representing the breakdown characteristic of atmospheric air at normal temperature and pressure in uniform fields. The electric strength value 31 kV/cm, measured across one cm gap in uniform field at normal temperature and pressure, is known as the 'inherent' or 'intrinsic strength' of air E_{bi} . For long gap lengths in uniform fields, the electric strength of air reduces to about 25 kV/cm, where a breakdown with streamer mechanism is more likely to develop.

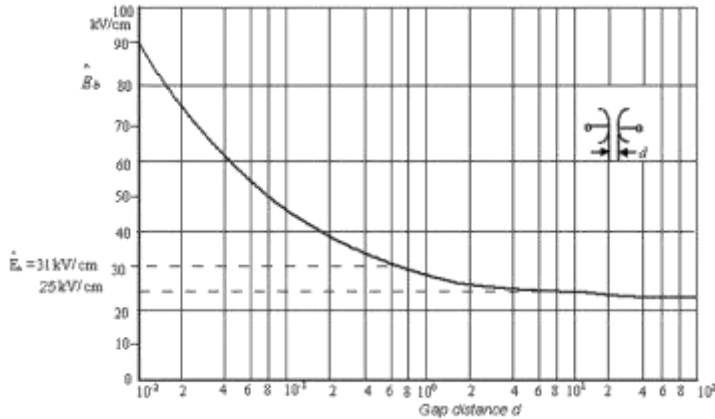


Fig 10.3 Breakdown voltage characteristics of atmospheric air in uniform fields.

XI

Objectives

In this lecture you will learn the following

- Breakdown Voltage Characteristics in Weakly NonUniform Fields
- Limiting value of Schwaiger factor

Breakdown Voltage Characteristics in Weakly Non-Uniform Fields

- The breakdown mechanism in weakly nonuniform fields is similar to uniform fields. Like in uniform fields the PB inception, U_i , and the breakdown voltages in weakly nonuniform fields are equal, the breakdown voltage can be estimated from the following relationship given by Schwaiger,

$$U_i = U_b \approx E_{b_{max}} d \eta$$

(11.1)

- At breakdown the 'maximum breakdown field intensity', $E_{b_{max}}$ in an electrode system or equipment having gaseous dielectric is always higher than the intrinsic 'electric strength', E_b , of the gas in uniform fields. The breakdown characteristics in weakly nonuniform fields mainly depend upon the geometrical factor of uniformity η of the electrode configuration. Breakdown characteristic for different gap lengths between two spheres in air having diameters of 10 cm each is shown in Fig. 11.1 for ac power frequency voltage. Knowing the dimensions, the factor η can be found out. It can be seen that as the gap distance d between the spheres is increased, the Schwaiger factor

decreases, i.e. the field becomes more nonuniform. If the measured values of U_b - d characteristic are known, E_{bmax} - d characteristic can be plotted. From these curves it is evident that E_{bmax} does not change much within a certain range of gap distance d , as also shown by the straight-line part of the U_b - d curve. For this particular electrode configuration, it is limited upto a gap distance nearly equal to the radius of the sphere. For a rough estimation of breakdown voltage, one may take, therefore, a mean value of E_{bmax} from the curve in Fig. 11.1. It works out to be equal to 34.5 kV/cm.

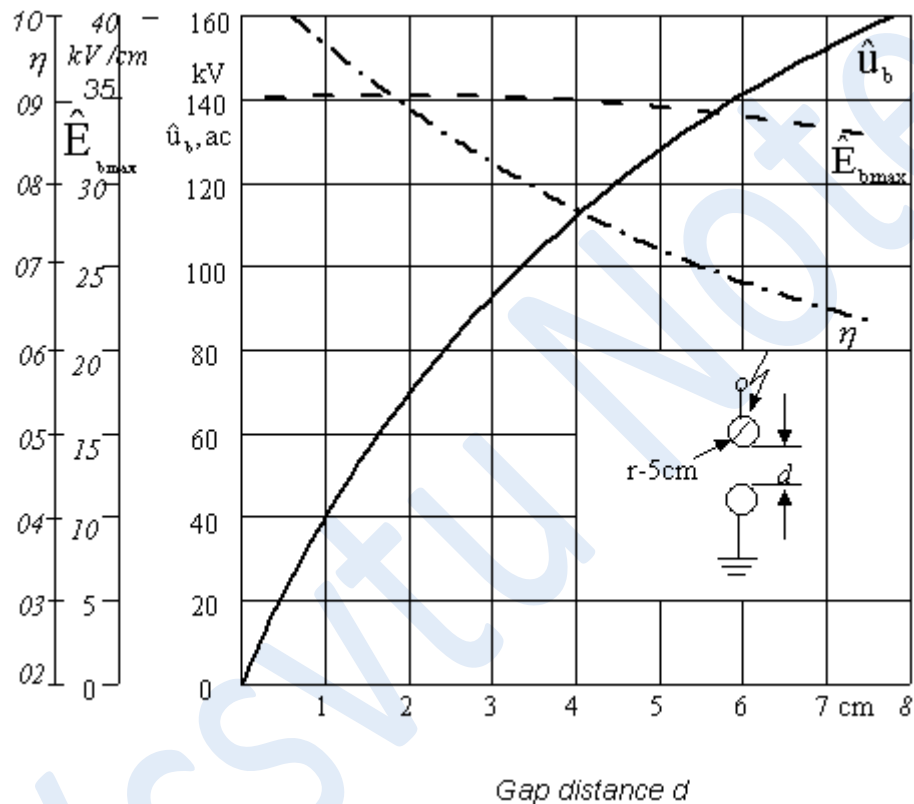


Fig 11.1 ac Breakdown voltage in air, maximum breakdown field intensity at the electrode and factor of uniformity for different gap distances in weakly nonuniform field

Limiting value of η , the η_{lim}

The value of η at which the transition from a weakly nonuniform to extremely nonuniform field configuration takes place is termed as η_{lim} . The exact value of η_{lim} in gaseous dielectrics depends not only upon the field nonuniformity but also upon the gas pressure and the type and polarity of the voltage since it is related with the inception of PB (Lecture 2).

The distinction between breakdown with and without stable PB can be made in terms of the value of degree of uniformity, η of the field. Consider a positive sphere-plane electrode configuration. As the gap distance ' d ' between these two electrodes is increased, the field becomes more nonuniform, resulting in decrease in the value of η .

For small gap distances, a weakly nonuniform field exists in the gap. On applying a sufficient magnitude of the voltage to the sphere, the required maximum field intensity for breakdown

E_{bmax} is achieved. An abrupt breakdown without any stable PB takes place, region A in Fig. 11.2 .

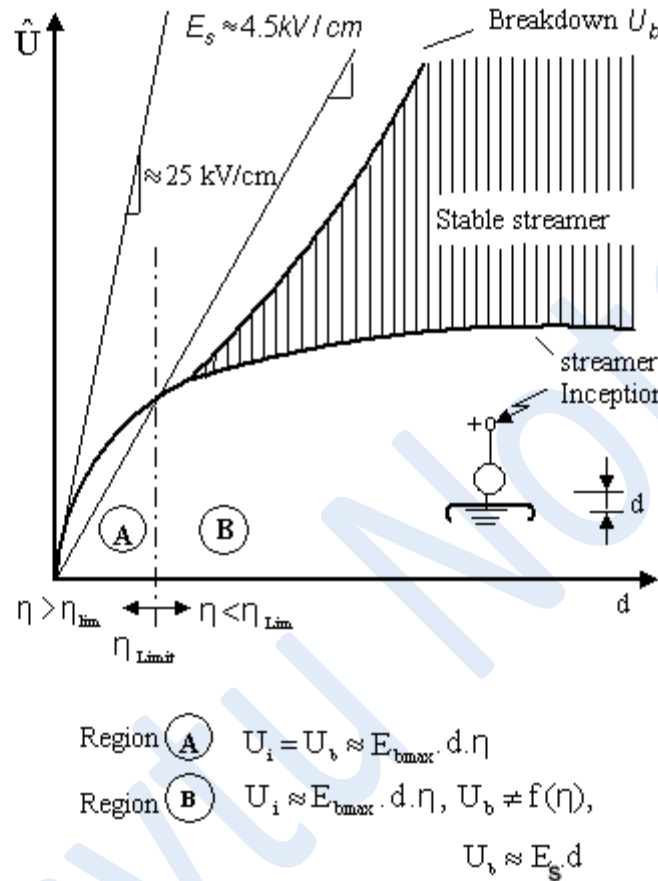


Fig 11.2 Threshold curves showing breakdown with stable streamer for positive sphere-plane electrode configuration.

On increasing the gap distance d , the field becomes more nonuniform. In the region B, in contrast to region A, stable PB takes place below the breakdown voltage. The borderline between these two regions is described in terms of η limit or η_{lim} , the threshold degree of uniformity. As illustrated in this figure, stable PB take place only in the shaded area in region B. As explained, the breakdown voltage in the region A and the PB inception voltage in the region B can be estimated with the knowledge of E_{bmax} and the electrode geometry determining the value of η . The boderline between the two regions A and B, represented by η_{lim} , represents the transition from the weakly to the extremely non uniform fields.

XII

Objectives

In this lecture you will learn the following

- Development of corona in extremely nonuniform fields
- Development of Star Corona
- Development of Streamer or Kanal Discharge (Corona)
- Development of Leader corona

BREAKDOWN IN EXTREMELY NONUNIFORM FIELDS AND CORONA

As the difference between the maximum and the mean field intensities increases leading to smaller η factor, the field becomes more nonuniform. Consequently, a poorer utilization of the insulating properties of the dielectric takes place. In extremely nonuniform fields at voltages much below the breakdown, a stable partial breakdown in the gas, confined locally to the region of extreme field intensity, can be maintained. This phenomenon is known as 'Partial Breakdown' (PB) and when it occurs at free electrodes in a gas, it is called 'corona'. At higher working voltages (above 100 kV), it is often very difficult, and economically not viable, to produce apparatus free of PB at normal working voltages.

Three types of coronas can be distinguished as they appear at different electrode shapes and gap distances in the power system. These are given names Star, Streamer and Leader coronas described in the following lectures.

Development of Star Corona

Consider a point or needle and plane electrode configuration in air, Fig 12.1, with a positive dc voltage greater than required for producing electric field to cause impact ionisation at the tip of the needle electrode. The plane electrode being grounded. The impact ionisation grows in the form of development of avalanche process in the direction shown in the figure. The avalanche process becomes vigorous on increasing the applied voltage. It then leads to Partial or Local Breakdown of the air in the region where the field intensity in the dielectric is higher than the required for PB inception. The local breakdown process leads to the development of production of very large amount of charge particles. Due to the considerable difference in the movement of electrons and positive ions, it leads to space charge formation. Since the resultant electric field in the gap depends upon the interaction between the fields produced by space charge and the applied electric field, it is very much dependent upon the polarity of the electrode. Both, the positive and the negative polarities are therefore, considered separately.

Positive Point - Plane Electrode Configuration (Positive or Anode Star Corona)

The process through which an avalanche is formed at a positive point electrode is analogous to the one in uniform field. However, the applied field intensity E in this case of electrode system falls sharply close to the point electrode. Beyond a short-distance Δx , the field intensity falls below the minimum field required for partial breakdown, E_i (Fig 12.1a). Thus the strong space charge formation process is able to extend itself to a maximum length of Δx in the gap, which is shorter than the critical amplification of length required by the avalanche. This is given again in

Fig. 12.1(b) on a lower scale ratio diagram for x .

At an advance stage of space charge formation the basic ionisation process must be considered once again. When a positive dc voltage is applied to the point (the anode) the direction of the avalanche is as shown in Fig 12.1(a) .

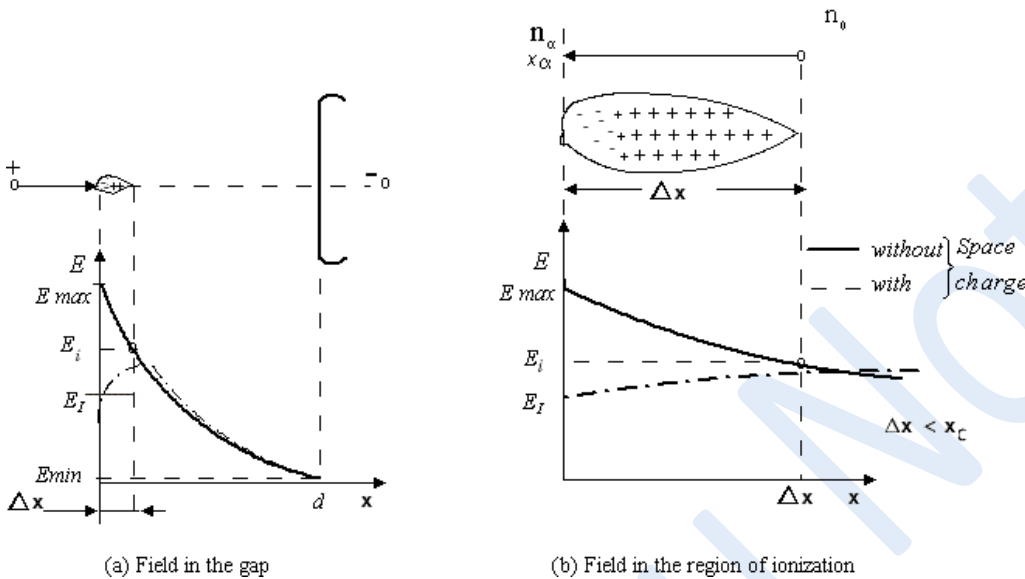


Fig 12.1 An Electron avalanche in front of positive point electrode. (a) Field in the gap, (b) Field in the region of ionization.

The electrons are absorbed fast by the positive electrode. A positive space charge due to the heavy and slow ions remains at the back. It has a very slow movement, especially because of rapidly decreasing applied field at the tip of the anode. This results in weakening of the resultant electric field in the region in front of the tip due to like polarity space charge at the positive electrode, as shown by the dotted lines in Fig 12.1(b) . Inception of further partial breakdown is possible only when there is a drift of space charge away from the anode due to radial diffusion which re-establishes the applied electric field, Fig 12.2(a). This type of a discontinuous process gives rise to an impulse form of discharge current at voltages just above the inception of PB, inspite of applying a dc voltage. The rise time of this PB current is of the order of a few tens of ns, whereas the time required to reach the instant on the tail when it decreases to half of its peak value is about 100ns. The peak value of this current is of the order of 50 μ A and the impulse charge is about 1pC. The frequency of the impulse discharge current may go beyond 400 MHz. Knowledge of this information may be of particular interest to communication engineers who would like to site their radio instruments away from such source of electromagnetic interference (EMI).

On increasing the applied voltage considerably above the PB inception voltage, the PB process becomes intensive. It leads ultimately to a continuous time variant overlapping process, establishing a balance among the ionization, diffusion and recombination processes. The impulse character of PB current is gradually lost and a direct current is observed which however, is accompanied with irregular fluctuations. The PB process becomes more intensive and

concentrated in the region near the point. The magnitude of mean potential gradient, required for complete breakdown between the electrodes with stable positive PB (star corona) process lies between 15-10 kV/cm.

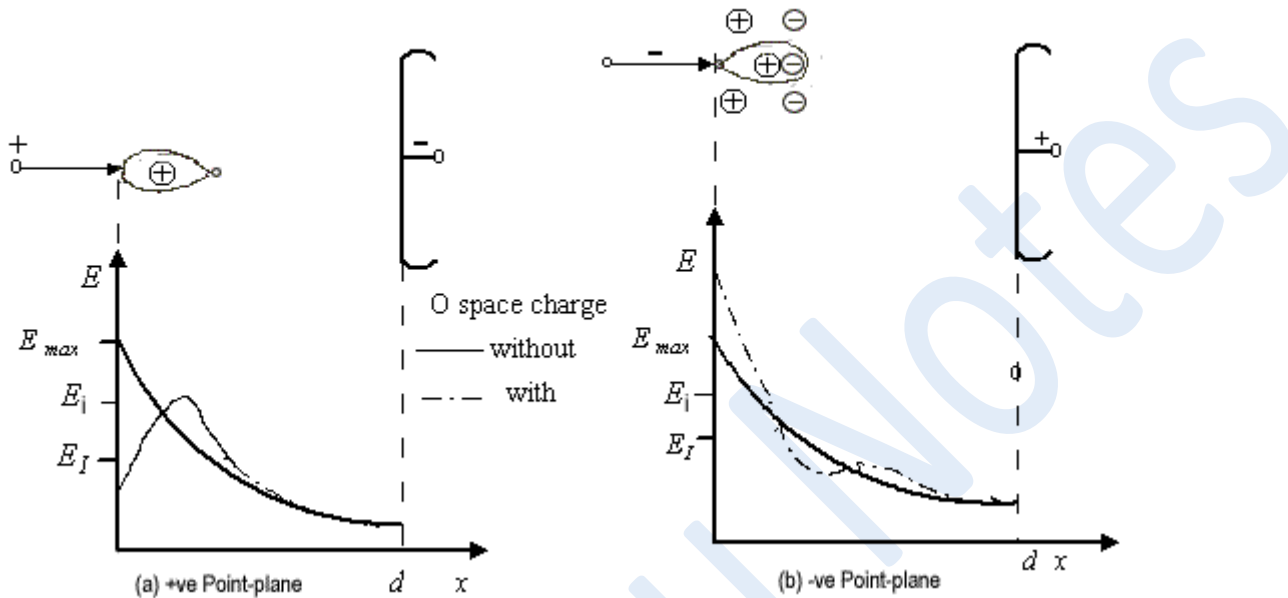


Fig 12.2 Field intensity distribution between point-plane electrodes for when PB occur.

The optical impression of this quasi stationary partial breakdown process is a weak, bluish 'glow' adjacent to the point electrode. This light phenomenon is explained owing to the excited state of gas molecules due to ionization. The electrons at higher energy levels emit a quantum of light and fall back to the original state of lower energy level. This PB process is known as positive (anode) (in German Glimmentladung) or popularly 'corona discharge', also mentioned sometimes as 'continuous discharge'. It appears like a 'star' in the sky when seen in dark. Hence it is proposed to be called 'star corona'. The word 'corona' is taken from Greek where it means the halo of light seen around an heavenly body. In Latin it means a crown. The corona discharge usually takes place at extremely sharp and pointed electrodes, for example, at needles, thin wires and sharp edges etc., on applying a relatively slower changing either dc or power frequency ac voltages. The situation demands on one hand a steep fall in potential gradient so that the avalanches do not achieve their critical length of amplification, and on the other, the charge carriers must get enough time to build the space charge. The audible noise produced by star corona is a continuous 'hissing' sound.

Negative Point-Plane Electrode Configuration (Negative or Cathode Glow Corona)

When a negative dc voltage, just sufficient for the inception of PB, is applied to a point (the cathode), the condition is similar to the one discussed in the previous section. In this case also, the possibility of PB is limited to a short distance Δx because of a steep potential gradient fall

from the point towards the plane. The ionization process adjacent to the point is able to extend the avalanche to a maximum length of Δx only, analogous to the conditions shown in Fig. 12.1. However, in this case the avalanche develops in the opposite direction, that is, the avalanche head is towards the plane (anode), as shown in Fig. 12.2(b). The avalanche does not acquire its critical length of amplification. Hence the PB process limits itself within a short region and it is not able to expand farther. Due to the high field, the electrons first drift very fast nearer to the point electrode but then slow down because of the steep fall in field intensity. Since oxygen in the air is an electronegative gas, the slow electrons in front of the avalanche are absorbed by oxygen molecules forming negative ions. Again, because of these heavy and slow ions, a negative space charge is developed leading to weakening of the field at a short distance away from the negative point electrode, preventing the avalanche hence the PB process from developing further. In the mean time, the positive space charge left behind, shifts towards the negative point electrode, increasing the field intensity there considerably, as shown in Fig. 12.2 (b). After a certain time, even the negative space charge shifts away from the vicinity of point, diminishing the field weakening effect. New avalanche and PB processes are then possible. Under the influence of the +ve and -ve space charges, a less nonuniform field is resulted away from the gap, leading to a higher breakdown voltage.

In short, it can be concluded that like in case of positive polarity point, in case of negative polarity point also a discontinuous process of charge carrier production and their migration takes place. Under static conditions above the inception level, an impulse form of partial breakdown current is conducted in a very regular and repetitive pulse form, as shown in Fig. 12.3. The frequency of these current pulses vary from a few kHz to MHz. This pulse current was first measured and studied in detail by Trichel [2.16] in 1939, and hence are named after him as "TRICHEL pulses". These have been measured by many researchers later on. An oscillogram of measured Trichel pulses by Woboditsch [2.17] is shown in Fig. 12.3.

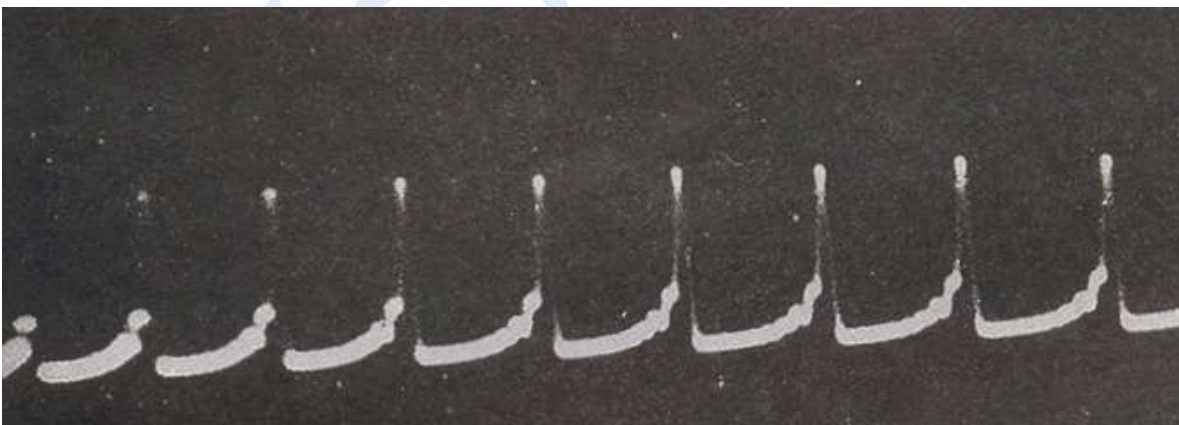


Fig 12.3 Impulse form of PD current measured at negative point electrode. 'Trichel pulses' by Woboditsch [2.17].

The inception voltage of Trichel pulses is practically independent of the gap length. The pulse frequency increases with the voltage and depends upon the geometrical radius of the cathode,

the gap length and the gas pressure. On raising the voltage, the mode of these pulses does not change over a wide range. Eventually, at much higher voltages, the impulse character of the PB current is lost due to overlapping of individual pulses. A direct current is then measured, which is accompanied with certain fluctuations. A steady 'star like' discharge' or 'corona discharge', similar to anode corona is also observed in this case but it is located slightly away from the tip. The cathode corona appears as a reddish glow unlike the bluish glow in case of anode corona. The average breakdown strength of the gap for this case is measured slightly higher, between 20-15 kV/cm.

Development of Streamer or Kanal Discharge (Corona)

Let the field distribution between the point-plane electrode system be modified in such a way that the fall in field intensity (the potential gradient) at the tip of the electrode is no more so steep as in the case of star corona. It can be achieved, for example, by increasing the radius of curvature of the point, taking most suitably a rod in place of a needle electrode. This will increase the depth region of Δx , where the impact ionization and PB is possible at a given voltage application. With the result, the avalanche developed in this region can acquire their critical length of amplification x_c , leading to a transformation from avalanche to streamer discharge. As a consequence of the interaction between field produced by the space charge and the applied basic field, a strong effect of polarity is observed here too as in case of the development of star corona. Both the polarities are, therefore, discussed separately. Practical experience has shown that pure stable streamer discharge may be produced on applying dc, ac as well as switching (si) impulse type of voltages to a hemispherical rod-plane electrode system for gap lengths beginning with a few cm. The magnitude of voltage required is comparatively higher than needed to produce star corona with below critical amplification of avalanche because of a lower intensity of field at a given voltage in this case.

Positive Rod-Plane Electrode (Positive Steamer Corona)

Consider a situation after the inception of an avalanche discharge in the region next to a positive rod. When the avalanche has grown to its critical amplification, the following equation must hold true:

$$\int_0^{x_c} \alpha dx = \ln \frac{n_{xc}}{n_0} \approx 20$$

(12.1)

where x_c is the length of an avalanche when it acquires its critical amplification. The avalanche developed under this condition must, however, remain in the field region above E_1 the minimum field intensity required for impact ionization, as shown in Fig. 12.1.

Electrons at the head of the avalanche are absorbed immediately by the positive rod electrode (anode). The positive space charge left behind can lead to a weakening of the field next to the anode to such an extent that further discharges may not be possible in this region. Since the

avalanche has acquired its critical stage, there is a strong concentration of positive space charge till upto the tail end of the avalanche, shown in a circular form for the sake of explanation in Fig. 12.4. An increase in field intensity towards the tail of this avalanche results due to the presence of a weak negative space charge, produced at the front of the next avalanche which is formed by photon emission from the avalanche head. The resultant enhanced field intensity magnitude may, therefore, be much higher than the minimum intensity required for impact ionization E_i or even for partial breakdown inception E_{i1} at higher voltages (curve 1 in Fig.12.4). In this process, the second avalanche grows to some extent into the first avalanche. Because of similar reasons explained above, an increase in field intensity is caused again due to the positive space charge of the second and the negative of the third avalanche at its head, which has grown to some extent into the second (curve 2 in Fig. 12.4). This process continues so long as a subsequent avalanche started by photoionization falls in the field region above E_i , inspite of the basic field decreasing below this level.

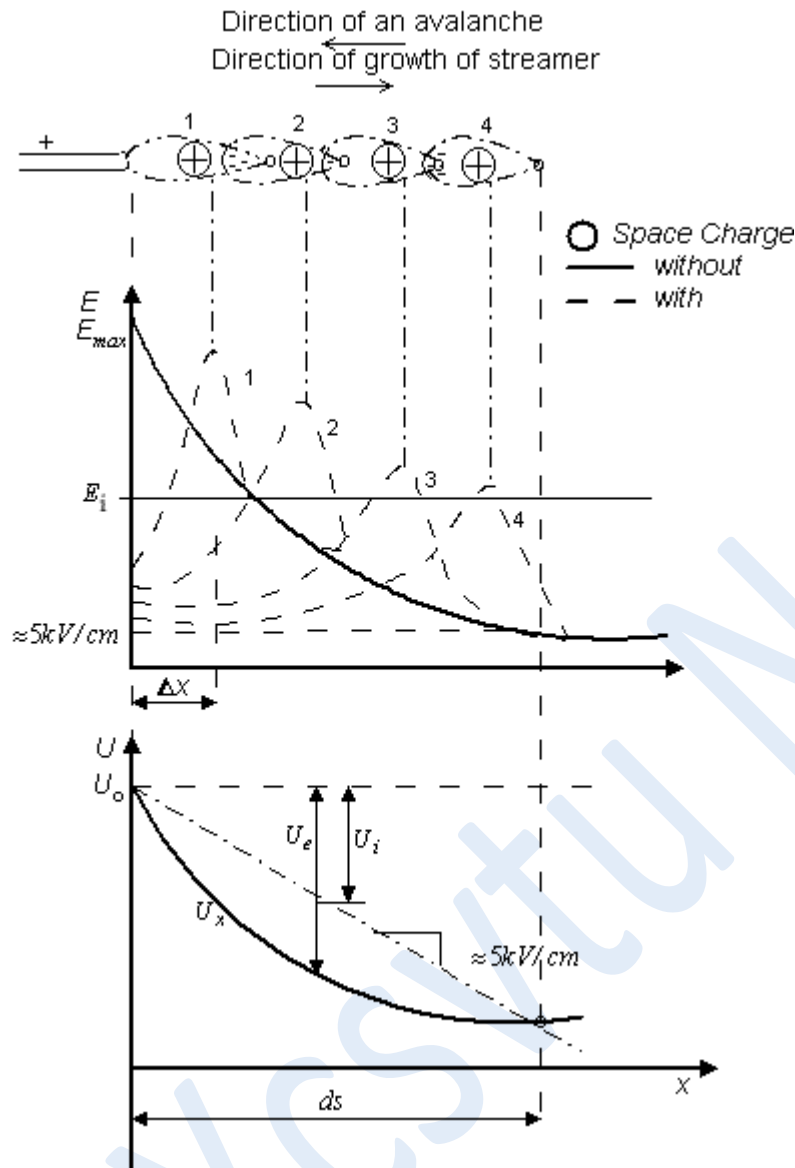


Fig 12.4 Schematic of streamer discharge in front of a positive rod electrode with variation in field and potential as a consequence of space charge

The mechanism of development of streamer described above can be compared to the one explained for uniform fields. The positive and the negative space charges involved in the growth of the streamer string compensate for each other. The conductivity of this nearly neutral charge carrier channel is, therefore, quite low. However, the basic condition for the development of

streamer discharge ($\int_0^{x_i} \alpha x_a \approx 20$) must be accomplished at each point. Since the positive charge carriers, being heavier particles, do not move themselves much, the process is comparable to the movement of a wave. In fact, numerous avalanches begin together and the whole process is a continuous development of a large number of streamer trajectories of partial breakdown in the region where the resultant (enhanced) field intensity is greater than E_i . These spread in space

around the rod electrode in the main field direction as shown in the photograph in Fig. 12.5.

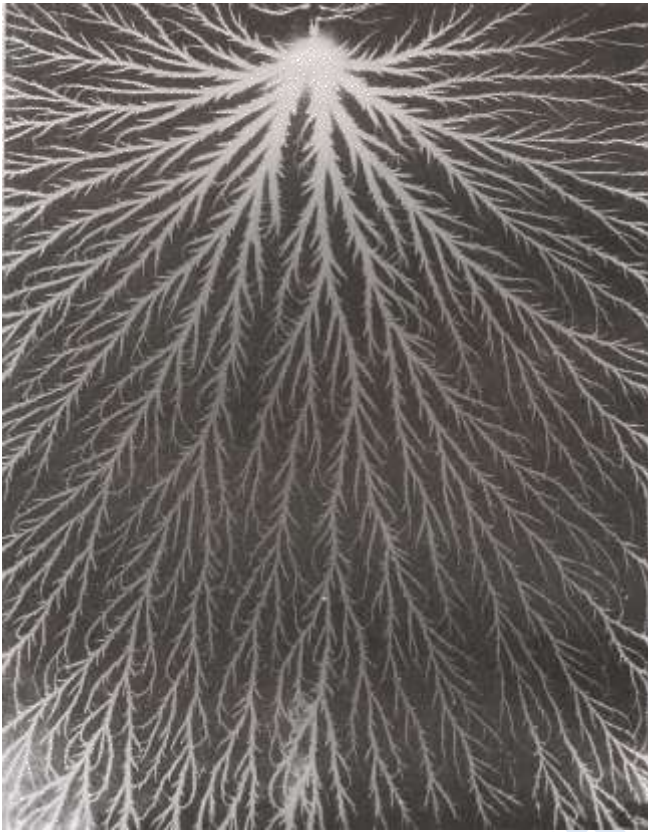


Fig 12.5 Photograph of a positive streamer discharge Lemke [2.18, 2.19].

This photograph was taken by Lemke [2.18] on applying a long duration $1/5000 \mu\text{s}$ 100 kV positive peak impulse voltage on a point-plane electrode system having a gap distance of 20 cm. Similar photographs were also taken by Nasser [2.20]. The experiments conducted by Nasser revealed that, on applying a single impulse voltage, even 200 partial discharge branches may develop in a gap length of only 2.5 cm. The number of these branches grow exponentially with increasing gap length, but it is an interesting characteristic to note that these large number of branches never cross each other.

The streamer corona is also accompanied with an impulse form of current. Depending upon the range of streamer, this current may acquire its maximum magnitude of a few milliamperes to an ampere within nano seconds. The streamer current decays to its 50% value within about 100 ns. The impulse discharge is generally in the range of 100 pC to 100 nC but may be even higher in some cases. The next process of displacement and formation of space charge introduces a time lag. The streamer discharges are, therefore, repetitive having irregular frequency. This is the reason that the audible noise produced by streamer corona is a flutter sound, unlike a hiss in case of star corona.

The integrated optical light appearance of streamer corona is like a weakly illuminated 'bunch' or more appropriately a 'shower' of discharge. Hence, it is also known as 'bunch discharge',

mentioned sometimes as 'illuminated string discharge', (in German 'Büschel' and 'Leuchtfaden' discharge respectively). However, it is popularly known as 'streamer corona'.

Referring to Fig. 12.4, it can be seen that, for a known potential distribution U_x in the gap, the range of growth of streamer discharge can be determined, if the potential gradient requirement for the streamer to grow is known. Let the process be analyzed through the involvement of energy in the space between electrodes. The gain in potential due to space charge U_e is represented by its corresponding energy gain (where $U_e = U_0 - U_x$). Because of continuous production of new charge carriers, some energy is consumed simultaneously. Hence a loss of energy in the gap is caused. Let this loss be represented by a potential U_l . The discharge process ceases to continue when this loss of energy is no more compensated by the gain, that is, when $U_l \approx U_e$. This occurs at $x = d_s$, the extent of streamer as shown in Fig. 12.4.

Measurements by Lemke [2.18] in 1967 revealed that the mean potential drop per centimeter length in a positive streamer is 4.5 kV. In other words, it can be said that, for a positive streamer discharge to grow, a potential gradient above 4.5 kV/cm is required.

Negative Rod-Plane Electrode (Negative Streamer Corona)

Like positive rod-plane electrode, in case of negative rod also, the development of a streamer discharge begins with an avalanche which acquires its critical amplification. The mechanism in principle is comparable to the positive streamer discharge except for the location of space charge formation. The direction of the avalanches is however opposite, that is, their heads are away from the rod. A strong positive space charge is, therefore, built in front of the rod in the dielectric, increasing the field intensity right at the tip of the electrode. The electrons form a negative space charge at the head of the avalanche slightly away from the electrode tip, thereby weakening the field in the vicinity.

When the discharge process develops farther, a sort of 'scattering' of negative space charge takes place by radial diffusion, because of the high mobility of electrons. Consequently, a weakening of the negative space charge results. The field intensity, which is affected by the concentration of the space charge, increases to some extent again. Because of this space charge effect on the field, the negative discharge process does not grow towards the opposite electrode to that extent compared to positive discharge at the same applied potential magnitude, as shown in Fig. 12.6. The radial diffusion of electrons is also responsible for a comparatively lesser number of distinct trajectories of negative streamer corona able to develop at the rod. This phenomenon is very clearly seen in Fig. 12.6. These photographs, commonly known as 'Lichtenberg figures', were originally taken by Toepler in Technische Hochschule, Dresden. Lichtenberg, a German scientist, lived in the eighteenth century and studied this phenomenon in 1777.

While the average potential gradient requirement for the propagation of positive streamer is estimated to be about 5 kV/cm, it is of the order of 10 to 15 kV/cm for negative streamer. This has also been confirmed by Les Renardieres [2.21].

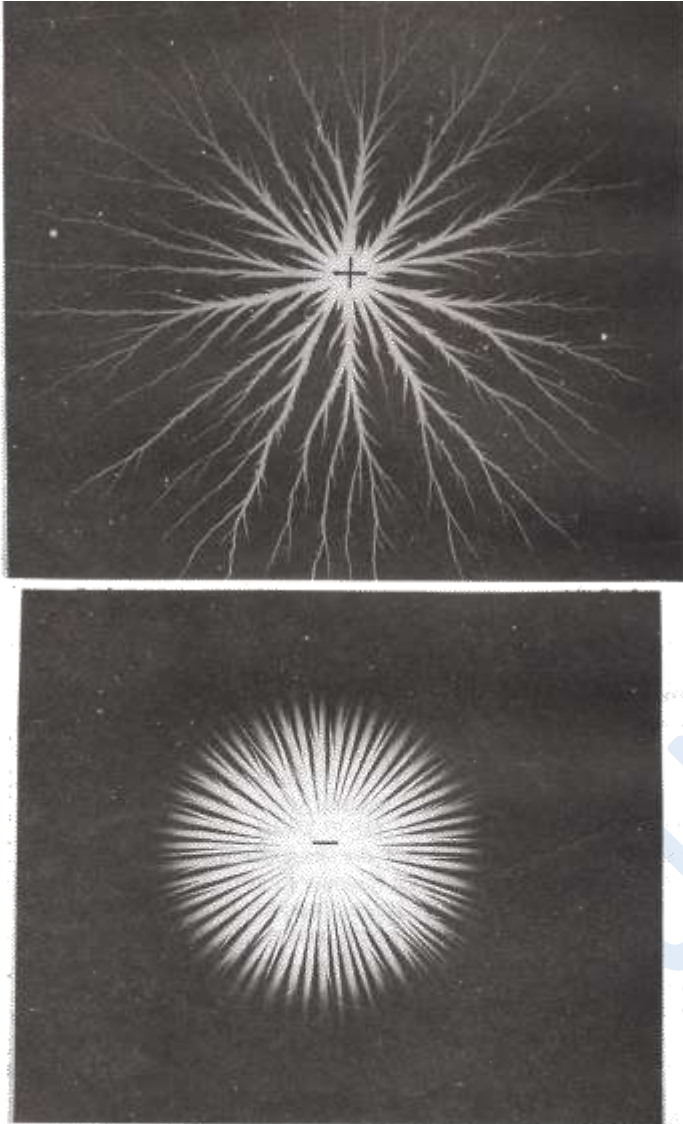


Fig 12.6 Photographs of positive and negative streamer discharge, 'Lichtenberg figures' taken by Toepler, TU Dresden.

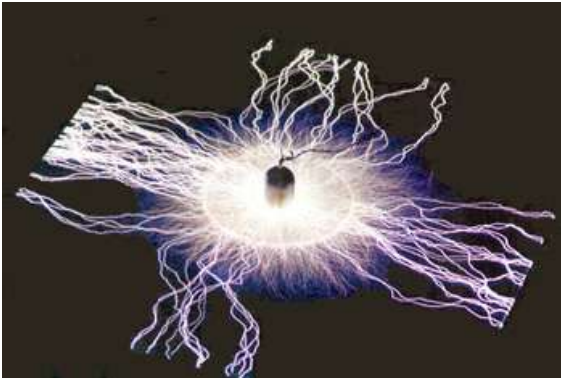
Development of Leader Corona:

If the gap distance between the rod and plane electrodes is increased above one meter and sufficient potential applied to the rod, after vigorous activity of streamer corona at the tip a 'constriction' of streamer trajectories takes place and a stem is formed. On increasing the applied voltage further, the stem of this discharge grows in to a few bright, stepped trajectories in the gap towards the plane. This is described as 'Leader corona'. Much higher magnitude of the voltage is required to be applied on log gap distance as compared to star and streamer coronas. However, Leader corona can easily be produced as 'Surface Discharge' on a glass plate on applying quite low magnitude of voltage. Fig 12.7 shows (a) Leader corona as surface discharge on a glass

plate and (b) Leader corona in free air.

The mean axial potential gradient across stable leader corona channels is quite low due to high charge density or current. For stable positive leader it was estimated by Lemke[2.19] to be about 1 kV/cm and for negative leader it is estimated to be 2-3 kV/cm.

The audible noise produced by Leader corona is a loud cracking sound. The EMI produced by this corona extends to a band width upto 2 GHz. The leader corona can be seen to happen in nature. The cloud to cloud as well as cloud to ground lightning discharge phenomenon is accomplished with leader channels.



(a) AC Discharges over surfaces of a 1m² glass plate



(b) Leader corona in free air

Fig. 12.7 Stable Leader corona in free air gap and as Surface discharge on a glass plate

Summary of the Development of discharges in Extremely Nonuniform Fields

The quasi continuous partial breakdown process in air is basically characterized by three distinguished stages of its development. These essential stages are star, streamer and leader corona. It took a very long time (over two centuries, beginning with Lichtenberg) for the researchers to be able to distinctly separate and understand these partial breakdown phenomena. Thanks to advance electrical measurement and photographic techniques for achieving these results. Beginning with very small gaps,

of the order of a few mm and cm, the production of very high voltages aspired the scientists to study the discharge phenomena in very long gaps, of a few tens of meters.

A fairly large variety of terminology, evolved in different countries with time, is available in the literature. Even the same stage of development of discharge is sometimes described with different technical terms by different authors. Besides, some stages of discharge are so closely intermingled that to find the appropriate term becomes difficult. Hence, it might lead to confusion for some, while going through the part of this chapter describing development of discharge process in extremely nonuniform fields.

XIII

Objectives

In this lecture you will learn the following

- Breakdown with stable Star corona
- Breakdown with Stable Streamer and Leader Coronas

Breakdown with Stable Star corona

- Unlike uniform and weakly nonuniform fields, in case of extremely nonuniform fields, the process of avalanche formation at the tip of a sharp electrode is not able to grow deeper in the gap towards the opposite electrode because of steep fall in potential gradient at the tip.

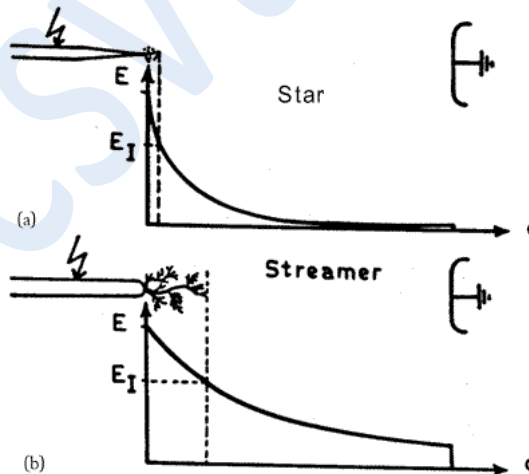


Fig 13.1 Variation of field intensity at needle and rod-plane electrode configurations

- Hence, the partial breakdown process, in this case, begins at the tip of the sharp electrode. Breakdown with stable avalanche discharge is therefore possible in this case only in very small gap length of a few mm to a few cm range, having a high potential gradient at the electrode. Stable avalanche discharges are possible to be produced only with static dc or

slow changing ac power frequency voltages. These provide sufficient time to build a steady space charge field. Under these conditions, the avalanches formed are not able to achieve their critical stage of amplification before the breakdown. With the result, the mean breakdown voltage in the electrode gap acquires comparatively higher value, of the order of 10 to 20 kV/cm (peak) depending upon the polarity of the applied voltage.

- Uhlmann in his dissertation in 1929 [2.22], measured breakdown voltage characteristics between a 30° point and plane electrode configuration for increasing gap distance with positive as well as negative polarity dc voltages, shown in Fig. 13.2. A strong effect of polarity on the breakdown voltage magnitudes is observed in this case of extremely nonuniform field. The ratio is almost 1:2. The ac (peak) breakdown voltage characteristic would fall nearly in between the positive and negative polarity dc.

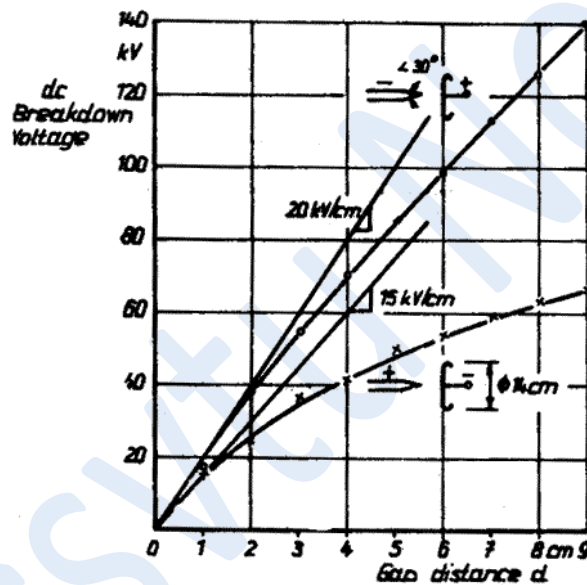


Fig 13.2 dc breakdown voltage characteristics of a 30° point and a plane of 14 cm dia in air, with respect to increasing gap distance, Uhlmann [2.22].

- As seen in Fig. 13.2, the average potential gradient required for breakdown decreases as the electrode gap distance is increased. This is because at larger gap distances breakdown with stable pure avalanche discharge is no more possible. One may conclude that for this electrode configuration, breakdown with stable pure avalanche discharge is possible only upto a gap length of about 2 cm. Under these conditions, the average potential gradient for breakdown in the gap is about 10 kV/cm for positive polarity, and 20 kV/cm for negative polarity voltages, as described earlier. At longer gap lengths, where a lower average breakdown potential gradient is required, streamer discharge may commence.
- Similar characteristics were measured for negative polarity point-plane electrode with dc for different gap lengths by Kuffel and Zaengl. The point electrode (cathode) is reported to

have a radius of 0.06 mm (Fig. 13.3). Below the lowest curve, no conduction current is measurable. The PB and the Trichel pulse inception voltages, U_i , for increasing gap length are given by this curve. As it can be observed, the gap length does not appreciably change the PB inception voltage. On increasing the voltage applied between the two electrodes, the mode of Trichel pulse does not change over a wide range of voltage. The avalanche process is limited within its critical stage, as explained earlier. A steady and stable partial breakdown phenomenon is observed like a 'star' in the dark. On raising the voltage the PB process at the tip of the sharp electrode intensifies, increasing the current density so much that thermal ionization begins. This gives rise to an unstable leader discharge extending instantaneously towards the opposite electrode, accomplishing a spark breakdown with an arc.

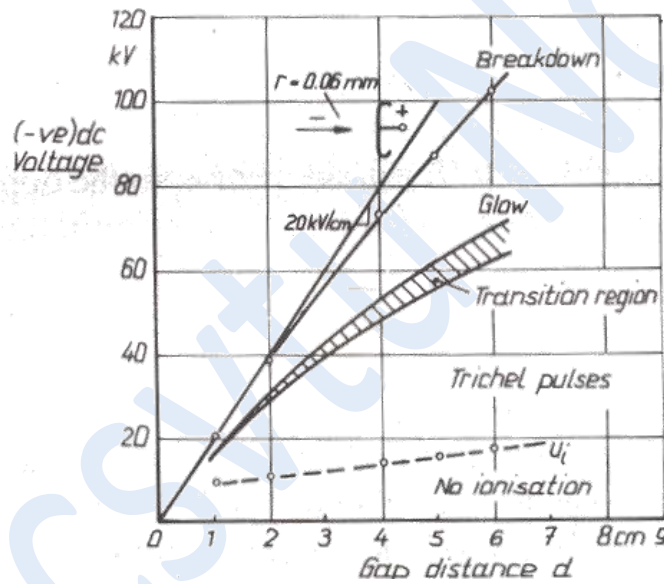


Fig 13.3 dc negative point-plane breakdown and corona discharge characteristics in atmospheric air, Kuffel [2.23].

Breakdown with Stable Streamer Corona

- As described in earlier lecture, when the basic requirement for the field intensity distribution in the gap is met, streamer or Kanal discharge, that is, avalanche with above critical amplification incept. On raising the applied voltage, these streamers propagate in the main field direction towards the opposite electrode, besides spreading in radial direction also as shown in Fig. 13.1(b). If the conditions required for the growth of streamer is met throughout the gap length, the discharge can extend upto the opposite electrode. It is at this stage that a stable streamer discharge is rendered instable. A schematic illustration of the development of breakdown mechanism with stable positive streamer discharge throughout the gap

length is shown in Fig. 13.4.

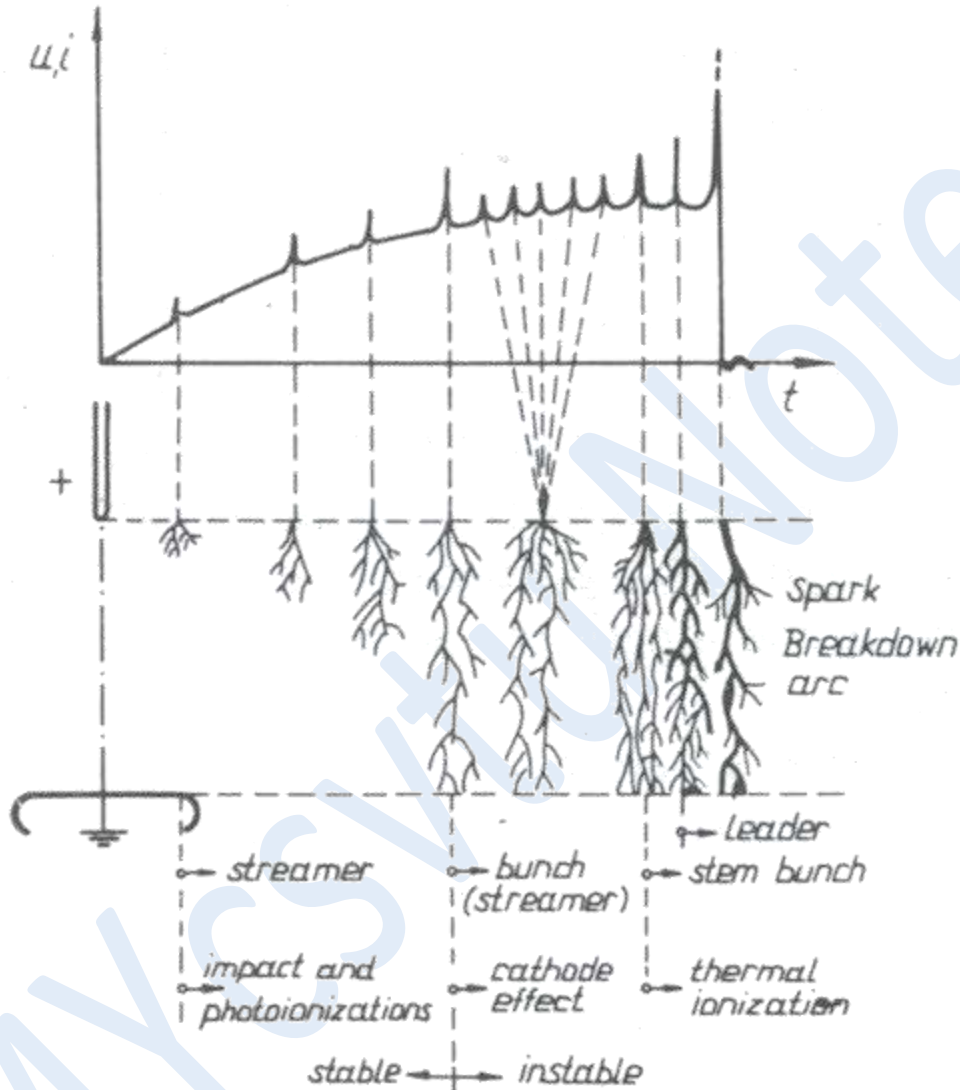


Fig 13.4 Breakdown mechanism development with stable streamer discharge.

- As soon as the streamer is able to extend itself upto the opposite electrode, say the cathode, more dense streamer discharge erupts from the anode because of 'cathode effect', also known as ' γ -effect' or secondary process. The current density at the tip of the rod electrode increases considerably due to the conduction of charge carriers, leading to an excessive temperature rise. This causes thermal ionization in front of the tip of the electrode due to the constriction of streamer channels. Subsequently, first a short bright 'stem' and then a 'stembunch' discharge breaks out, turning into a thriving instable leader as shown in Fig. 13.4. Breakdown is accomplished with a 'final jump' of the leader bridging the two

electrodes. Ultimately an arc is produced which conducts the short circuit current. This type of breakdown mechanism is primarily observed in medium gap lengths, say upto about 1 m, depending upon the electrode configuration and the type of applied voltage. All the three types of voltages, that is, ac, dc and si may produce breakdown with stable streamer. Since the total duration of li is very short , it is unable to produce a stable corona.

- An analytical explanation of the mechanism described above is difficult. However, a distinction between breakdown with stable and instable streamers can be made in terms of the degree of uniformity of the field.

Consider in fig 11.2, a breakdown when η is greater or equal to η_{lim} . The breakdown voltage for the region A can be estimated by Equation 13.1;

$$U_b = E_{bmax} \cdot d \cdot \eta_{lim} \quad (13.1)$$

The breakdown voltage for the region B is given by the equation;

$$U_b = E_s \cdot d \quad (13.2)$$

where E_s is the average potential gradient required for breakdown with stable streamer discharge or across the streamer channels which is about 4.5 kV/cm for positive polarity voltage. A round figure of 5 kV/cm is accepted in this case.

Equating the two equations given above and considering a value of 25 kV/cm for E_{bmax} (the maximum breakdown field intensity for air in weakly nonuniform fields), the value of η_{lim} for atmospheric air can be determined as follows:

$$E_{bmax} \cdot d \cdot \eta_{lim} = E_s \cdot d$$

or

$$\begin{aligned} \eta_{lim} &= \frac{E_s}{E_{bmax}} \\ &= \frac{4.5}{25} \approx 0.2 \end{aligned}$$

- Characteristics of breakdown with dc voltage for air gaps upto 2.5 m are shown in Fig. 13.5 with both positive and negative polarities for sphere-sphere and rod-plane electrode gaps. The curve number 1 for gaps between large size sphere-sphere configuration represents the weakly nonuniform field even upto 50 cm of gap distance. Since no partial breakdown takes place before the break down in this field, no effect of polarity is measured on the breakdown voltage. The curve number 2, measured with negative polarity voltage on a rod-plane gap, a case of extremely nonuniform field, is accompanied with stable negative streamer corona.

The mean potential gradient requirement of about 10 kV/cm for negative streamer is observed to have met for this curve. The last curve, number 3, accompanied with stable positive streamer, represents an average potential gradient requirement of about 5 kV/cm in the gap.

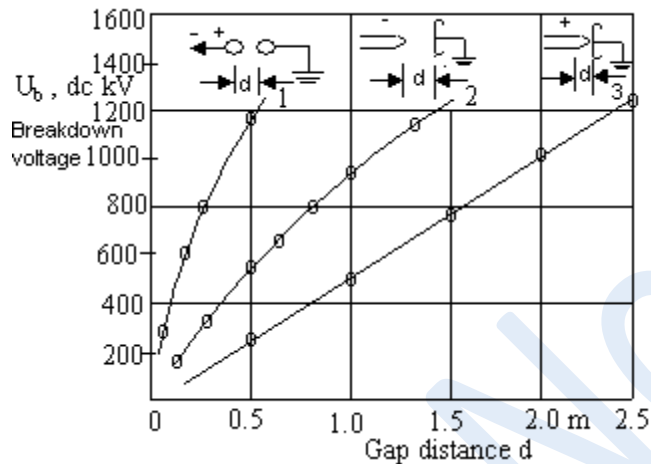


Fig 13.5 dc breakdown voltage characteristic, with both polarities, for 'sphere-sphere' and rod-plane long air gap.

- The development of different breakdown characteristics strongly suggest that the breakdown voltage magnitudes depend upon the type of stable partial breakdown that occur in the gap before the final jump. The breakdown voltage characteristic for a rod-plane gap (Fig. 13.6), on applying positive 60/2500 μ s shape of impulse voltages, represented breakdown with stable streamer corona up to a relatively small gap distance of 1 m. The average potential gradient required for breakdown in this region was 4.5 kV/cm. On increasing the gap distance, a lower average potential gradient requirement for breakdown was measured continuously. Finally, an average potential gradient of 1 kV/cm was required for breakdown of the gaps above 4 m in this case. Stable leader corona could be observed for gap lengths above 2 m for the given electrode system. As illustrated in Fig. 13.6, the breakdown voltage characteristic falls between the two tangents to the curve, representing the potential gradients of circa 4.5 and 1 kV/cm. The region of breakdown with stable streamer corona preceding the breakdown extends to a maximum of 2 m. The breakdown characteristic in the region beyond this length is determined by stable leader corona before the complete breakdown.

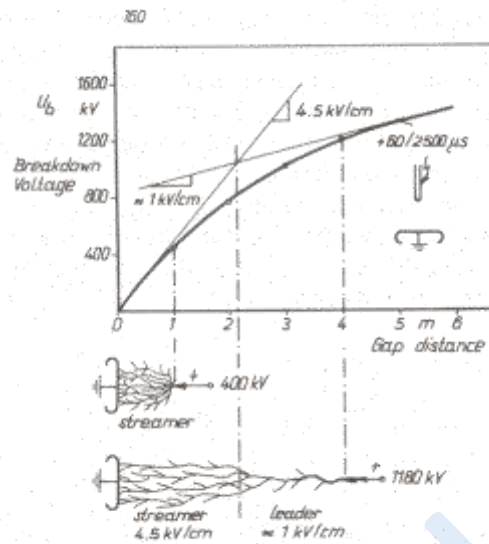


Fig 13.6 Relationship between breakdown voltage characteristics and mean potential gradient requirement for the propagation of stable streamer and leader coronas.

Breakdown with Stable Streamer and Leader Coronas

- Consider a very long gap distance, above 2 m, between positive rod or sphere and plane electrode configuration. On applying preferably a slow changing voltage, that is, ac or si of sufficient large magnitude, at first a very strong and dense filamentary streamer corona appears at the high voltage electrode. This is known as 'first corona' shown in the schematic of breakdown (Fig. 13.7). Unlike in case of shorter gap lengths, in this case the minimum collective current density in discharge channel required to produce a 'leader' (about 200 mA) may be achieved even without the cathode effect. The first corona goes through constriction phenomenon and is then followed by stable stem and leader discharges in the gap. The stepped form of leader is accompanied with streamer coronas at their tips. The leader discharge propagates, traversing the path laid down by streamer corona, as it provides the leader the required current density.
- The stable leader corona prevails in the gap until it extends to the opposite electrode, as illustrated in Fig. 13.7. Breakdown of air between electrodes is accomplished with the 'final jump' of a leader channel bridging the gap, followed by an arc. Photographs of stable leader and breakdown with its final jump on a 7m gap length between rod-plane, applying positive polarity si voltage were taken by Lemke [2.18], shown in Fig. 13.7.

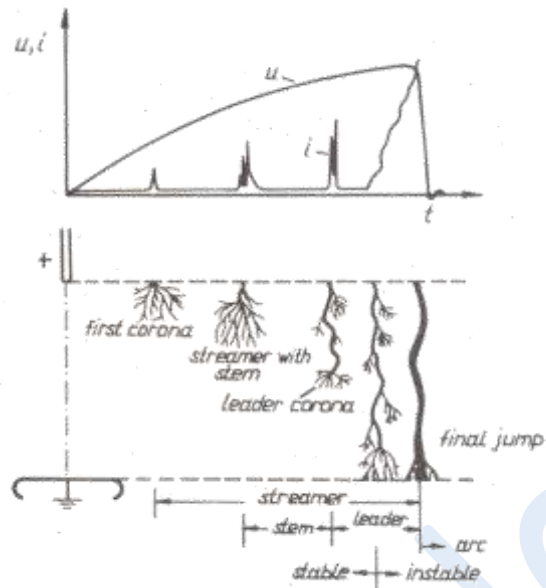


Fig. 13.7 Breakdown mechanism schematic with stable leader and streamer coronas

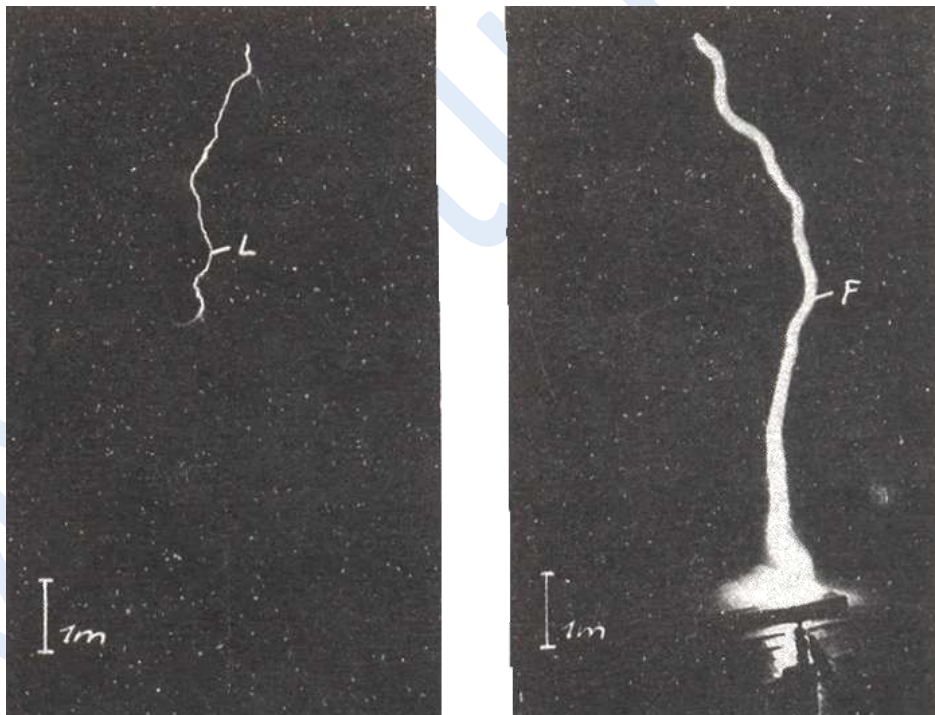


Fig 13.8 Stable leader corona and breakdown with final jump for a 7 m gap with positive polarity si voltage, Lemke [2.18].

XIV

Objectives

In this lecture you will learn the following

Classification of Liquid Dielectrics
Electric Conduction in Insulating Liquids

Liquid Dielectrics and their Classification

From the point of view of molecular arrangements, liquids can be described as 'highly compressed gases' in which the molecules are very closely arranged. This is known as kinetic model of the liquid structure. However, the movement of charged particles, their microscopic streams and interface conditions with other materials cause a distortion in the otherwise undisturbed molecular structure of the liquids. The well known terminology describing the breakdown mechanisms in gaseous dielectrics, such as, impact ionization, mean free path, electron drift etc. is, therefore, also applicable for liquid dielectrics.

Liquid dielectrics are accordingly classified in between the two *states* of matter, that is gaseous and solid insulating materials. This intermediate position of liquid dielectrics is also characterized by its wide range of *application* in power apparatus. Insulating oils are used in power and instrument *transformers*, power cables, circuit breakers, power capacitors etc. Here they perform a number of functions simultaneously, namely:

- insulation between the parts carrying voltage and the grounded container, as in transformers.
- impregnation of insulation provided in thin layers of paper or other materials, as in Transformers, cables and capacitors, where oils or impregnating compounds are used.
- cooling action by convection in transformers and oil filled cables through circulation.
- filling up of the voids to form an electrically stronger integral part of a composite dielectric.
- arc extinction in oil circuit breakers.
- high capacitance provided by liquid dielectrics with high permittivity to power capacitors.

A large number of natural and synthetic liquids are available which can be used as dielectrics. These possess a very high electric strength and their viscosity and permittivity vary in a wide range. The appropriate application of a liquid dielectric in an apparatus is determined by its physical, chemical and electrical properties on one hand, and on the other, it depends upon the requirements of the functions to be performed.

Classification of Liquid Dielectrics

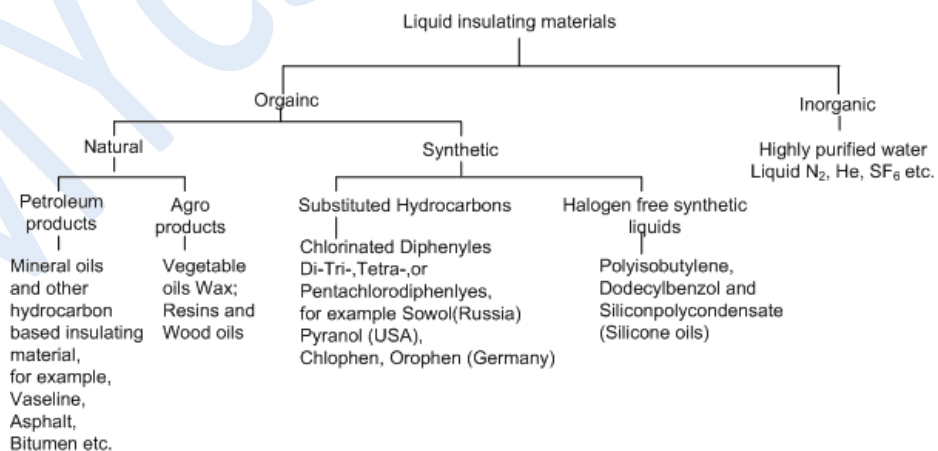
Dielectric materials can be divided into two broad classifications: organic and inorganic. Organic dielectrics are basically chemical compounds containing carbon. Earlier, under organic chemistry only those compounds which were derived from either plant or animal organism were considered. This concept underwent changes with concurrent developments in chemical technology. Carbon compounds, in general, are now called organics. Among the main natural insulating materials of this type are: petroleum products and mineral oils. The most important and widely used organic liquid dielectrics for electrical power equipment are mineral oils. The other natural organic insulating materials are asphalt, vegetable oils, wax, natural resins, wood and fibre plants (fibrins).

A large number of synthetic organic insulating materials are also produced. These are nothing but substituents of hydrocarbons in gaseous or liquid forms. In gaseous forms are fluorinated and chlorinated carbon compounds. Their liquid forms are chlorinated diphenyles, besides some nonchlorinated synthetic hydrocarbons. The chlorodiphenyles, although possessing some special properties, are not widely used because of being unfriendly to human beings and very costly.

Among halogenfree synthetic oils are polymerization products, the polyisobutylenes and the siliconpolycondensates. Polyisobutylene offers, better dielectric and thermal properties than mineral oils for its application in power cables and capacitors, but it is many times more expensive. Silicon oils are top grade, halogenfree synthetic insulating liquids. They have excellent stable properties, but because of being costly, have so far found limited application in power apparatus for special purpose.

Among inorganic liquid insulating materials, highly purified water, liquid nitrogen, oxygen, argon, sulphurhexafluoride, and helium etc. have been investigated for possible use as dielectrics. Liquified gases, having high electric strength, are more frequently used in cryogenic applications, whereas, because of its high relative permittivity, low cost, easy handling and disposal, Water and water mixtures are being actively investigated for use as dielectrics (for example, in pulse power capacitors and pulsed power modulators etc.).

To summarize the classification of liquid dielectrics explained above, a schematic is drawn in the following diagram. The insulating liquids, commonly applied in high voltage apparatus, are classified as illustrated in the following diagram.



Electric Conduction in Insulating Liquids

The conduction mechanism in a dielectric liquid is strongly affected by the degree of its purity. In liquids, which have not been highly purified, when subjected to fields upto about a few kV/cm the conduction is primarily ionic. Ionic conduction is affected by the dissociation process of impurities as well as the injection of charge by the electrodes through electrochemical reactions. The electrons do not take part in the passage of current through such liquids. A typical characteristic of conduction current density J versus the applied dc voltage U in a pure liquid is shown in Fig.14.1. At low voltages, the current varies proportionally to the voltage, region 1, representing the ohmic behavior. On raising the applied voltage, hence the field intensity, the ionic current gets saturated, region 2. At still higher applied voltage the current density increases rapidly until the breakdown occurs, region 3.

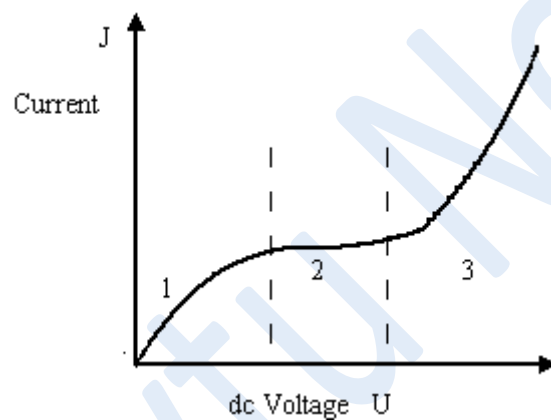


Fig. 14.1 Typical voltage-current (U-J) characteristic in dielectric liquids.

Similar behavior is observed generally in, both, polar and nonpolar liquids. In some cases the saturation region may be completely missing. This characteristic has an analogy to what has also been observed commonly in gases.

In Fig. 14.2 the conduction current characteristics are shown for negative direct voltage applied to a needle-plane electrode configuration in transformer oil and liquid nitrogen, measured by Takashima et al. [3.1] for different radii of curvature ' rt ' of the needle tip. For these experiments, the needle constituted of a polished platinum wire of radius 0.25 mm and the plane of 50 mm diameter Rogowsky profile curved plate of stainless steel. The current was measured through the plane electrode for a constant gap distance of 4 mm. The sharp bend measured on the curve is supposed to represent the development of a strong space charge around the needle.

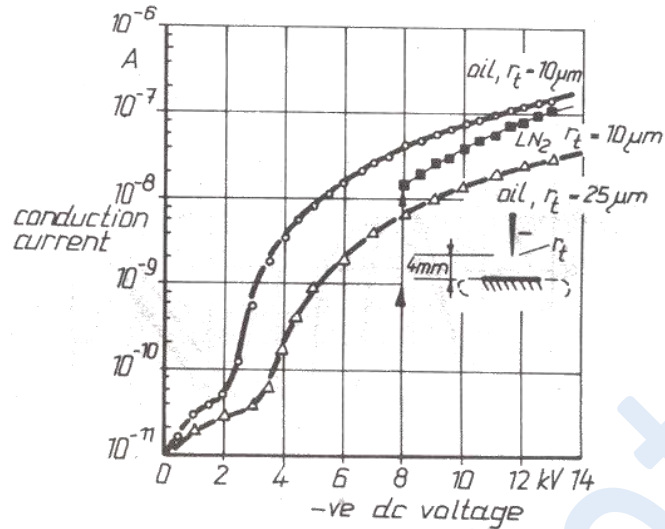


Fig 14.2 Conduction current in oil and liquid nitrogen for negative needle-plane electrode gap of 4mm with increasing voltage. Oil at 20°C and LN₂ at 77.3 K Takashima et al. [3.1].

The concentration of charge carriers and the viscosity of insulating liquids are both strongly affected by the temperature which in turn influences the conductivity of the liquid. According to Van't Hoffsch law, the conductivity 'κ' within a certain range of temperature follows the relation:

$$\kappa = \kappa_0 \exp(-F/kT)$$

where k is Boltzmann constant, T absolute temperature, κ₀ and F are material constants. F is known as 'activation energy' and is expressed as kcal/mole.

However, Van't Hoffsch law is valid only in the region where the conduction current follows the ohmic behavior, that is region 1 in Fig. 14.1. It thus depends upon the particular liquid and its impurity contents (for example, humidity content etc.).

Transformer oil conductivity variation for a wide range of temperature for different moisture contents measured by Holle [3.2] are illustrated in Fig. 14.3. It is evident from this figure that the conductivity of oil increases as the water ppm content rises.

Electric Conduction in Insulating Liquids

The conduction mechanism in a dielectric liquid is strongly affected by the degree of its purity. In liquids, which have not been highly purified, when subjected to fields upto about a few kV/cm the conduction is primarily ionic. Ionic conduction is affected by the dissociation process of impurities as well as the injection of charge by the electrodes through

electrochemical reactions. The electrons do not take part in the passage of current through such liquids. A typical characteristic of conduction current density J versus the applied dc voltage U in a pure liquid is shown in Fig.14.1. At low voltages, the current varies proportionally to the voltage, region 1, representing the ohmic behavior. On raising the applied voltage, hence the field intensity, the ionic current gets saturated, region 2. At still higher applied voltage the current density increases rapidly until the breakdown occurs, region 3.

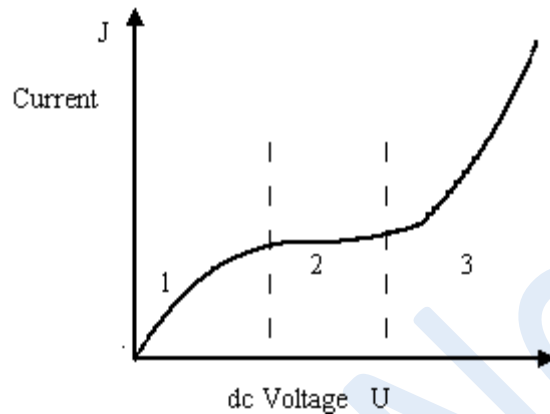


Fig. 14.1 Typical voltage-current (U-J) characteristic in dielectric liquids.

Similar behavior is observed generally in, both, polar and nonpolar liquids. In some cases the saturation region may be completely missing. This characteristic has an analogy to what has also been observed commonly in gases.

In Fig. 14.2 the conduction current characteristics are shown for negative direct voltage applied to a needle-plane electrode configuration in transformer oil and liquid nitrogen, measured by Takashima et al. [3.1] for different radii of curvature ' r_t ' of the needle tip. For these experiments, the needle constituted of a polished platinum wire of radius 0.25 mm and the plane of 50 mm diameter Rogowsky profile curved plate of stainless steel. The current was measured through the plane electrode for a constant gap distance of 4 mm. The sharp bend measured on the curve is supposed to represent the development of a strong space charge around the needle.

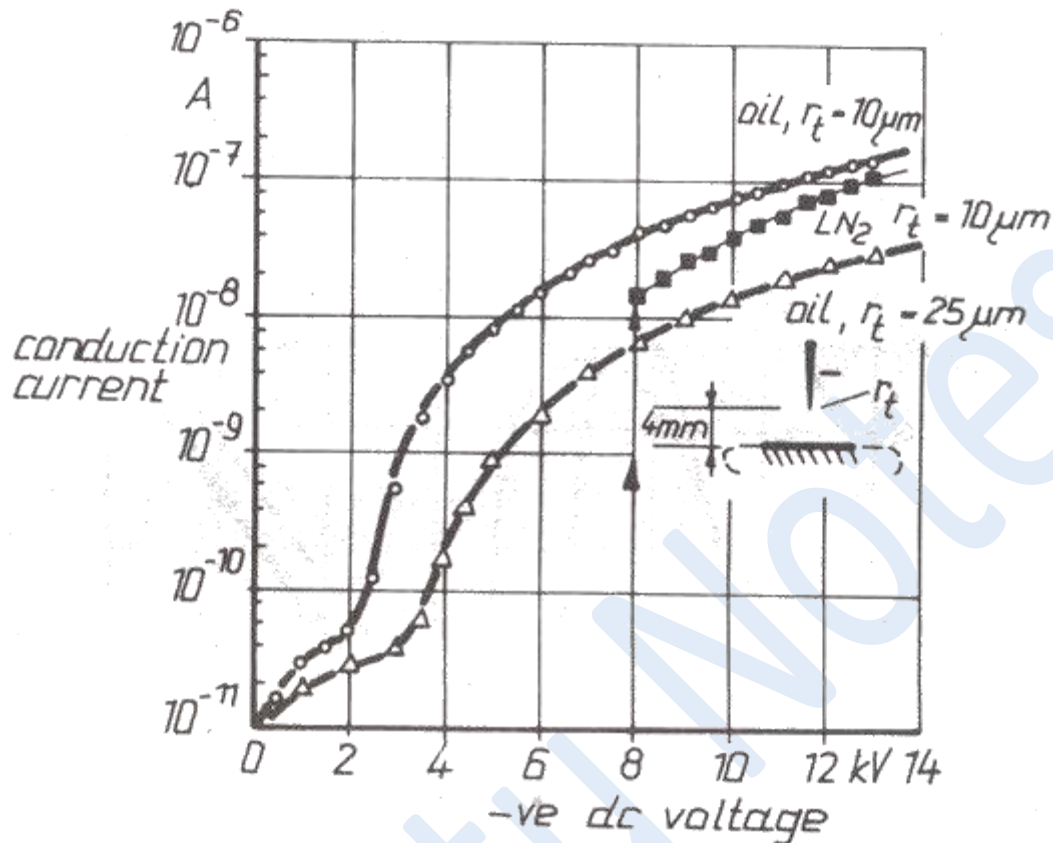


Fig 14.2 Conduction current in oil and liquid nitrogen for negative needle-plane electrode gap of 4mm with increasing voltage. Oil at 20°C and LN₂ at 77.3 K Takashima et al. [3.1].

The concentration of charge carriers and the viscosity of insulating liquids are both strongly affected by the temperature which in turn influences the conductivity of the liquid. According to Van't Hoffsch law, the conductivity ' κ ' within a certain range of temperature follows the relation:

$$\kappa = \kappa_0 \exp (-F/kT)$$

where k is Boltzmann constant, T absolute temperature, κ_0 and F are material constants. F is known as 'activation energy' and is expressed as kcal/mole.

However, Van't Hoffsch law is valid only in the region where the conduction current follows the ohmic behavior, that is region 1 in Fig. 14.1. It thus depends upon the particular liquid and its impurity contents (for example, humidity content etc.).

Transformer oil conductivity variation for a wide range of temperature for different moisture contents measured by Holle [3.2] are illustrated in Fig. 14.3. It is evident from this figure that the conductivity of oil increases as the water ppm content rises.

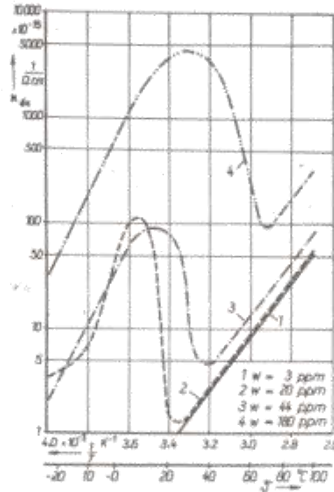


Fig 14.3 Direct current conductivity of transformer oil for different water contents w (ppm) with respect to the reciprocal of absolute temperature, Holle [3.2].

In case of highly purified liquids which are able to withstand high field intensity, the conduction phenomenon is different. By increasing the field intensity to the order of a few hundred kV/cm, the conduction current in both polar and nonpolar liquids is augmented predominantly by charge carriers injected into the liquid from the electrode surfaces. Besides, the field aided dissociation process of molecules is intensified. Under certain given conditions, the presence of an injected space charge, say of density q , gives rise to a Coulomb's force of density qE . Due to the action of this force, hydrodynamic instability is caused, developing convection motion in the liquid. Investigations made by many authors, on both polar and nonpolar liquids, have concluded that whenever conduction in an insulating fluid is accompanied with a significant charge injection, the convection motions occur, which are also known as 'electrohydrodynamic' (EHD) motions. The EHD motions augment the passage of current depending upon the charge injection intensity, which in turn is determined by the applied voltage, the nature of liquid and the electrode material, Zahn [3.3], Takashima [3.1] and Atten [3.4].

Atten [3.4] explained the effect of the phenomenon of EHD motion on the conduction in liquid dielectrics under two extreme conditions: with and without unipolar injection of charge. For his experimentation, an extremely nonuniform field configuration between a knife and a plane was taken, as shown in Fig. 14.4.

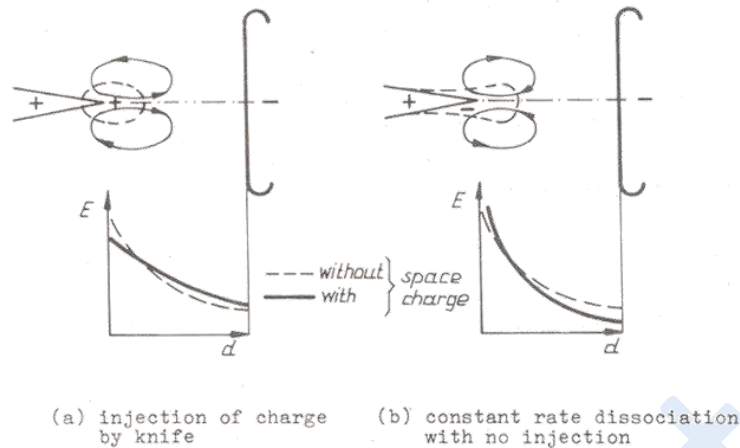


Fig 14.4 Schematic representation of space charge zone and liquid motion streams between knife-plane electrodes and the field distribution along the axis, Atten [3.4].

Consider first the case of injection of unipolar charge (ions) by the knife (Fig. 14.4 a). The field at the tip of the knife electrode is reduced because of the same polarity space charge being injected, whereas an increase in the field intensity is caused over the basic field towards the plane electrode. The space charge zone is of finite extent when a moderate voltage is applied. Under this condition, the liquid relaxation time is lower than the transit time of the ions from the knife to the plane. The total current is, therefore, higher than the ohmic current because of the enhancement of field intensity near the plane. Moreover, due to the action of the electric field on the same polarity charge close to the knife, a 'stream' or 'jet' of liquid towards the plane is induced in this region.

In case of pure conduction with no injection of charge, Fig. 14.4(b), an opposite polarity space charge near the knife extends further. Consequently, the space charge field at the tip increases, and is reduced with respect to the basic field towards the plane. This results in lower total current than the ohmic current (sub-ohmic behavior). The opposite polarity space charge in the vicinity of the knife gives rise to a liquid motion directed towards the knife.

At extremely high field intensities (1000 kV/cm and above) approaching the 'intrinsic strength' of liquid dielectrics, the field emission at the electrode surfaces affects the conduction phenomenon. Under these conditions, the conduction current is dominated by electrons.

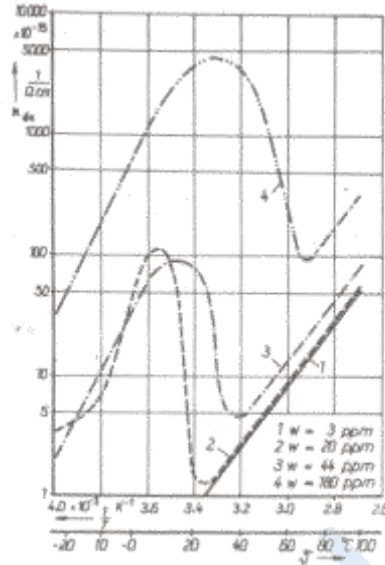


Fig 14.3 Direct current conductivity of transformer oil for different water contents w (ppm) with respect to the reciprocal of absolute temperature, Holle [3.2].

In case of highly purified liquids which are able to withstand high field intensity, the conduction phenomenon is different. By increasing the field intensity to the order of a few hundred kV/cm, the conduction current in both polar and nonpolar liquids is augmented predominantly by charge carriers injected into the liquid from the electrode surfaces. Besides, the field aided dissociation process of molecules is intensified. Under certain given conditions, the presence of an injected space charge, say of density q , gives rise to a Coulomb's force of density qE . Due to the action of this force, hydrodynamic instability is caused, developing convection motion in the liquid. Investigations made by many authors, on both polar and nonpolar liquids, have concluded that whenever conduction in an insulating fluid is accompanied with a significant charge injection, the convection motions occur, which are also known as 'electrohydrodynamic' (EHD) motions. The EHD motions augment the passage of current depending upon the charge injection intensity, which in turn is determined by the applied voltage, the nature of liquid and the electrode material, Zahn [3.3], Takashima [3.1] and Atten [3.4].

Atten [3.4] explained the effect of the phenomenon of EHD motion on the conduction in liquid dielectrics under two extreme conditions: with and without unipolar injection of charge. For his experimentation, an extremely nonuniform field configuration between a knife and a plane was taken, as shown in Fig. 14.4.

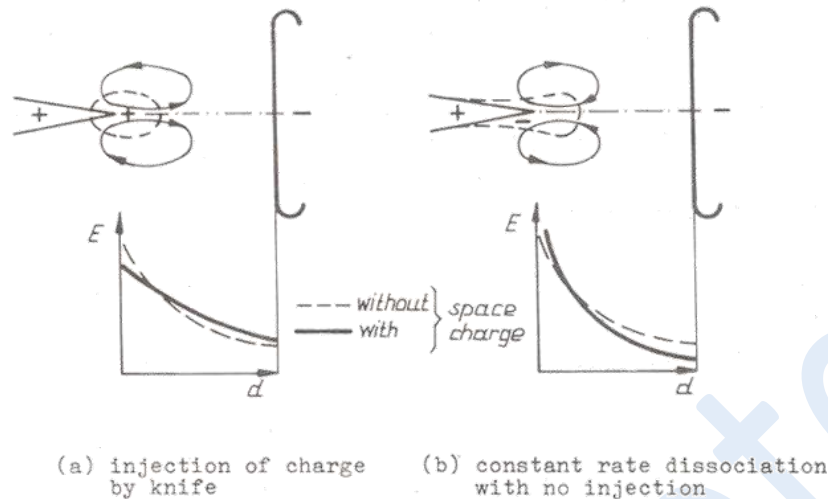


Fig 14.4 Schematic representation of space charge zone and liquid motion streams between knife-plane electrodes and the field distribution along the axis, Atten [3.4].

Consider first the case of injection of unipolar charge (ions) by the knife (Fig. 14.4 a). The field at the tip of the knife electrode is reduced because of the same polarity space charge being injected, whereas an increase in the field intensity is caused over the basic field towards the plane electrode. The space charge zone is of finite extent when a moderate voltage is applied. Under this condition, the liquid relaxation time is lower than the transit time of the ions from the knife to the plane. The total current is, therefore, higher than the ohmic current because of the enhancement of field intensity near the plane. Moreover, due to the action of the electric field on the same polarity charge close to the knife, a 'stream' or 'jet' of liquid towards the plane is induced in this region.

In case of pure conduction with no injection of charge, Fig. 14.4(b), an opposite polarity space charge near the knife extends further. Consequently, the space charge field at the tip increases, and is reduced with respect to the basic field towards the plane. This results in lower total current than the ohmic current (sub-ohmic behavior). The opposite polarity space charge in the vicinity of the knife gives rise to a liquid motion directed towards the knife.

At extremely high field intensities (1000 kV/cm and above) approaching the 'intrinsic strength' of liquid dielectrics, the field emission at the electrode surfaces affects the conduction phenomenon. Under these conditions, the conduction current is dominated by electrons.

Objectives

In this lecture you will learn the following

Classification of solid insulating Materials

Thermoplastic and Thermoset Polymers

Composite Insulating Systems:

CLASSIFICATION OF SOLID INSULATING MATERIALS

A vast number of solid insulating materials are used in electrical power engineering. With the invention of modern insulating materials, many earlier conventional materials have been discarded, especially in case of electrical machines, capacitors and power cables. From the usage point of view, the solid insulating materials can be divided into the following three broad categories:

Moulding materials: These are used for providing mechanically rigid forms of insulation, for example, insulators and bushings etc. Such materials are required to have good electrical insulating properties besides having high mechanical strength. These are usually made out of ceramics, glass (toughened glass), fibre glass reinforced plastics and epoxyresins.

Jacketing materials: Polymers have been found suitable for providing insulating jackets to the conductors. For example, polyethylene (PE), polyvinylchloride (PVC), natural and synthetic rubber and paper used in power cables, capacitors and transformers. Mica and fibre glass based plastic tapes are used in electrical machines.

Filling materials: Beside oils, wax based draining and non draining impregnating compounds of different types are used to impregnate paper in power cables, transformers, capacitors, and instrument transformers.

Insulating mechanical support: In the form of plates, pipes and ledges insulating supports are required in transformers, GIS, circuit breakers and isolators. The products, such as press boards, hard paper (thin paper laminates), wood (yellow teak) are used in transformers. Ebonite, also known as vulcanite, is a form of cross linked rubber containing large proportion of sulphur, bakelite, a hard synthetic material, and acrylic resin plates are used for insulating supports in other equipment.

However, the most common method of classifying the solid insulating materials is based upon their chemical compositions, distinguished mainly between inorganic and organic materials.

Among the inorganic materials; ceramics, glass, fibre glass, enamel, mica and asbestos are important and have found their wide application as dielectrics in the order of the mentioned sequence. They distinguish themselves in their unique ability to withstand high temperatures in addition to their being highly chemical resistant. There is practically negligible sign of ageing in these materials. However, it is difficult to machine or process them. These materials are basically inhomogeneous both microscopically as well as macroscopically.

Solid organic materials used in electrical engineering are: paper, wood, wax, leather, cotton besides a number of natural and synthetic resins, rubbers and plastics, also known as polymers. Wood being so hygroscopic, is rarely used as such, but wooden poles supporting overhead cables and distribution lines are being widely used in North America.

The polymeric organic insulating materials used in electrical engineering have a very high molecular weight and consist of two or more polymeric compounds of several structural units normally bound together by covalent bonds. The individual structural units may consist of single atoms or may be molecular in nature, which repeat in a regular order.

A polymer can be obtained by the reaction of compounds having at least two reactive functional groups which can react under suitable conditions. These chemical compounds are known as 'monomers'. There can be one or a mixture of reacting monomers and in the latter case, the resulting material is called 'copolymer'.

Here are several ways of classifying polymers and one of them is by their response to heat. Accordingly, the polymers are divided into two groups of materials as follows.

Thermoplastic Polymers

Thermoplastic polymers soften and supple on heating and 'solidify' on cooling. The heating and cooling cycle within a certain temperature limit can be applied to these materials several times without affecting their properties. Polymers which generally have a linear structure fall in this category. The synthetic thermoplastic materials used in electrical engineering for insulation purpose are; polyethylene (PE), polyvinylchloride (PVC), polypropylene (PP) and polyamide (PA). The extent of their application in the industry is in the order of their above mentioned sequences. Such materials have relatively poor thermal resistance and their properties deteriorate rapidly at higher temperature.

Thermoset Polymers

The polymers which soften when heated for the first time resulting into cross-linking reaction (network formation), are known as thermoset polymers. This reaction, leading to the formation of network structure, is also known as curing or setting of the polymer. All monomers having functionality equal to two would give rise to linear polymers and, therefore, thermoplastic materials. However, when they have functionality more than two, the resulting polymer has a network structure. The polymers used for electrical insulation purpose are desired to retain their rubbery (flexible) properties. Hence, these are defined as 'lightly cross-linked polymers'.

The chemical reaction leading to cross-linking is achieved with the help of an additive, known as 'agent'. The term 'cross-linking agent' is very general. It refers to (a) molecules which bridge two polymer molecules, for example, vulcanizing agents; such as sulphur, selenium and sulphur monochloride for rubbers; and polyamines in epoxide resins, (b) molecules which initiate a cross-linking reaction, for example, peroxides which initiate a double bond polymerisation in polyesters and dicumyl peroxide in low density polyethylene (LDPE); (c) those which are purely catalytic in their action such as, acids for phenolic resins, amines in epoxides; and (d) active site generators, for example, peroxides which abstract protons from the polymer chains.

The thermal, mechanical and electrical properties of different cross-linked materials vary considerably from each other. However, in general, after cross linking a material does not soften on reheating, instead it becomes thermally more stable compared to thermoplastic materials. Cross-linked polymer resins are, for example; polyester-resin, phenolresin,

silicon resin and the most widely used in electrical engineering are the epoxy resins. Among rubbers, typical examples used for electrical insulation are; natural rubber also known as 'India rubber', and a large number of synthetic rubbers like silicon rubber (SiR), ethylene-propylene rubber (EPR), etc.

The bulk properties of a polymer can be altered suitably by incorporation of a number of additives. Variations in the choice of additives can produce widely differing products. This is true in particular with PVC. In terms of functions, there are a large number of groups of additives, of which the following most important are commonly used in preparing polymer compounds for electrical insulation purpose:

1. Fillers-usually applied to modify physical properties, mainly mechanical, of a polymer.
2. Plasticisers and Softeners-to lower the melt viscosity and also to change physical properties (softness, flexibility).
3. Colorants-normally soluble colorants(dyestuffs) are used.
4. Anti-ageing additives to prevent structural degradation due to chemical reactions like oxidation, ozone attack, dehydrochlorination (especially with PVC) and ultra-violet attack, e.g. sunlight.
5. Flame retarders - to improve the degree of fire resistance of polymers.
6. Cross-linking agents-to achieve intermolecular combination at the chain ends.

Composite Insulating Systems

Some very high quality solid insulating systems have been produced by combining different dielectric materials. Common composites of organic and inorganic materials are; fibre glass reinforced plastics, mica based plastic tapes, quartz, fibre and mica mixed with synthetic resins, such as epoxy resin used in electrical machines, etc. Oil and wax based compound impregnated insulation systems with paper and polymer tapes are commonly applied in power cables, capacitors and transformers. 'Uniaxially oriented polyethylene' (UOPE) tape, developed recently has been found to have very good compatibility with oils besides having good mechanical properties. In such composite insulating systems, the advantages of inherent properties of their constituent materials are made use of. Thus, it is possible to create insulating systems having better thermal, mechanical and electrical properties.

Nano-composite Dielectrics

Research worldwide has been able to document significant improvement in the electrical and other properties of polymer composites through incorporation of nanoparticulates. Research in polymer processing is necessary to study the functionalization of the particulate surfaces to provide preferential coupling to the host polymer in the utilization of the emerging breed of new dielectric material. The nano-composites are intrinsically different in that they appear to be dominated by the characteristics of the internal interfaces. These properties appear to arise when the infilled material has a similar length scale to that of the polymer chain. Attempts to engineer nanodielectrics by changing the conditions at the interface do suggest that indeed some degree of tailoring of dielectric properties and self

assembly may be possible. [3.5]. In table 15., examples of nano-composite insulating materials currently under investigation are given [3.5]

Table 15.1 Examples of nano-composite systems under investigations

Base polymers	Nano-materials
Polyolefins	Clays
Epoxy/phenolics	Inorganic oxides
Elastomers	Carbon nanotubes
Ethylene-vinyl copolymers	Graphite

XVI

Objectives

In this lecture you will learn the following

- Permittivity of Insulating Materials
- Polarization in Insulating Materials

Permittivity of Insulating Materials

The most important electrical parameter of insulating materials is the capacitance offered by them between given electrode systems. The capacitance thus formed is always accompanied with some losses determined by the permittivity ' ϵ ' and the specific insulation resistance ρ_{ins} of the material.

The permittivity of an insulating material ϵ is defined as the product of absolute permittivity of free space (vacuum) ' ϵ_0 ' and the relative permittivity ' ϵ_r ' of the material or the medium:

$$\epsilon = \epsilon_0 \epsilon_r$$

The absolute permittivity of free space, ϵ_0 is constant and has a value,

$$\epsilon_0 = 8.854 \cdot 10^{-12} \text{ F/m}$$

On the contrary, the relative permittivity of a material ϵ_r is not a constant. It depends upon the thermal conditions of the material as well as the frequency and the magnitude of the applied voltage. ϵ_r is often mentioned as dielectric number or permittivity number in the literature. ϵ_r of a dielectric is defined as the quotient of the capacitances C_x to C_0 , where C_x is the capacitance of a condenser constituting the given material as a dielectric and C_0 is the capacitance of the same condenser constituting vacuum as a dielectric in uniform field.

$$\epsilon_r = \frac{C_x}{C_0}$$

(16.1)

For the mathematical analyses taking into account the polarization process in the dielectrics, it was necessary to introduce the complex relative permittivity ' $\bar{\epsilon}_r$.' described as:

$$\bar{\epsilon}_r = \epsilon'_r - j \epsilon''_r \quad (16.2)$$

where ϵ'_r is the real and ϵ''_r the imaginary part of the complex relative permittivity $\bar{\epsilon}_r$, which is also known as 'loss index'.

Polarization in Insulating Materials

Polarization in insulating materials is basically a phenomenon of interaction between the applied external electric field and the inherent charge carriers, the atoms, ions or molecules present in the dielectric. Not only the applied electric field gives rise to the polarization, but in turn, polarization modifies the microscopic field within the dielectric. Thus, it is a process of a reversible displacement between the positions of positive and negative charges in the molecular structure caused by the applied electric field. The interaction takes place by a force, exercised on the basic structural elements (charge carriers) of the dielectric.

The extent of polarization is analytically described by the relative permittivity ϵ_r . Consider a uniform field electrode system in vacuum applied an electric field E . The electric flux density \vec{D}_0 is given by,

$$\vec{D}_0 = \epsilon_0 \cdot \vec{E} \quad (16.3)$$

For the same electrode and the magnitude of the applied electric field, when the vacuum is replaced by an insulating material (solid, liquid or gas), the electric flux density in the dielectric \vec{D}_{ins} , is increased, given by,

$$\vec{D}_{ins} = \epsilon_0 \cdot \epsilon_r \cdot \vec{E} \quad (16.4)$$

The increase in electric flux density, ' \vec{D}_p ' is caused by polarization in the dielectric. \vec{D}_p , therefore, represents the material property and is given as:

$$\vec{D}_p = \vec{D}_{ins} - \vec{D}_0 = \epsilon_0 (\epsilon_r - 1) \vec{E}$$

or

$$\frac{\vec{D}_p}{\vec{D}_0} = (\epsilon_r - 1)$$

(16.5)

The quotient D_p / D_0 is known as dielectric susceptibility or polarization capacity of a dielectric. It is also denoted by χ_e

Most of the gaseous dielectrics have their ϵ_r nearly equal to one. Hence polarization is not an important phenomenon in gases, but in liquid and solid dielectrics it plays an important role determining the conductivity and the losses. Different types of polarization mechanisms are described under the following three main categories.

Displacement Polarization

Within a molecular bond, the positive and negative charges of individual molecule or atom are rendered to oscillate in synchronism under the influence of an applied electric field. Similar oscillations also take place between the nucleus and the electron shell of an atom, building dipoles. The displacement caused by the oscillations is proportional to the applied electric field and on removing the electric field the atoms return back to their original state. Where only this type of polarization mechanism is present, the dielectric materials are described to be 'nonpolar' and these have no dipole moment. Classic examples of such dielectrics are the gases.

Space Charge or Boundary Surface Polarization

Some heterogeneous dielectrics, for example partially crystalline insulating materials, have the positive and negative ions as free charge carriers. Without an external field, the dielectric is in neutral condition and the positive and negative charges neutralise each other. However, under the effect of an external electric field, the charge carriers in the dielectric move towards opposite polarity electrode surfaces, giving rise to a macroscopic dipole. Like the mechanism described in previous case, in this case too on removing the applied electric field, the dielectric returns to its original state, hence it is known as a type of displacement polarization.

Dielectrics having this type of polarization mechanism are also described as nonpolar, that is, these do not build a dipole without an external field. The boundary surface polarization is commonly present in heterogeneous insulating materials, such as, impregnated paper insulations, hard pressed boards, taped insulations used in electrical machines and even at voids in solid homogeneous dielectrics. Such materials normally have a low value of ϵ_r .

Orientation Polarization

Orientation polarization is the main polarization mechanism in liquid dielectrics. Usually, the polarization depends upon the applied electric field intensity. However, in some materials a permanent polarization is 'frozen' due to the permanent dipoles present in the dielectrics even without an external field. Such dielectrics have an asymmetry in their molecular structure and are described as 'polar'.

On applying an external electric field, the dipoles arrange themselves according to the field lines. The effect of applied external field on the dipoles is determined by their dipole moments. Depending upon the bond between the positive and the negative charges in the molecules of a material, the orientation of dipoles takes place. The effective field intensity established in the material is the quantity induced by the external source and the sources within the material itself. The orientation of dipoles may be in the form of an arrangement in an element or they may simply straighten out like a chain, which usually depends upon the local field in which the molecules are situated. The local microscopic field may not be necessarily equal to the macroscopic applied electric field.

In this lecture you will learn the following

Insulation Resistance and conductivity in the Dielectrics
 Dielectric Power Losses in Insulating Materials

Insulation Resistance offered by Dielectrics

The concept of insulation resistance of a dielectric is represented by the dc resistance offered by an insulating material. It is generally described as specific insulation resistance ' ρ_{ins} ', which is reciprocal of the dc conductivity κ_{dc} ,

$$\rho_{ins} = \frac{1}{\kappa_{dc}} \quad \Omega \cdot m$$

(17.1)

Consider a direct voltage U_{dc} applied across two uniform field electrodes separated by a block of insulating material having an area A and length d as shown in Fig. 17.1. From the equivalent circuit diagram constituting a capacitance C and a dc resistance R_{dc} in parallel, following relation can be derived:

$$R_{dc} = \rho_{ins} \frac{d}{A}$$

(17.2)

$$i_{dc} = \frac{U}{R_{dc}} = \frac{U \cdot A}{\rho_{ins} \cdot d}$$

(17.3)

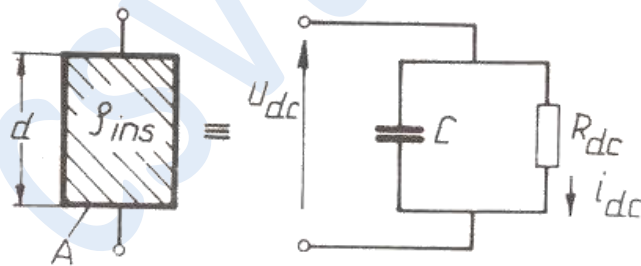


Fig 17.1 An insulating material and its equivalent circuit diagram

for a uniform field where

$$E = \frac{U}{d}$$

$$i_{dc} = \frac{E \cdot A \cdot d}{\rho_{ins} \cdot d} = \frac{E \cdot A}{\rho_{ins}}$$

$$= \kappa_{dc} \cdot A \cdot E$$

(17.4)

Like κ_{dc} , the specific insulation resistance also depends strongly upon the temperature as shown in Fig. 14.3 for transformer oil.

The specific insulation resistance, or the dc conductivity is a function of time for which the voltage is applied. A schematic illustration of the variation of κ_{dc} with respect to the time of application of the direct voltage for an insulating oil is shown in Fig. 17.2. The dc conductivity, which is very

high initially (region A), is determined by the orientation of dipoles.

In region B, the conductivity is determined by the movement of free charge carriers under the influence of applied electric field. The magnitude of conductivity in this region also represents the ac power frequency conductivity ' κ_{ac} '. The region C in the figure represents the development of space charge in front of the electrodes. The steady ion current due to dissociation is depicted by region D.

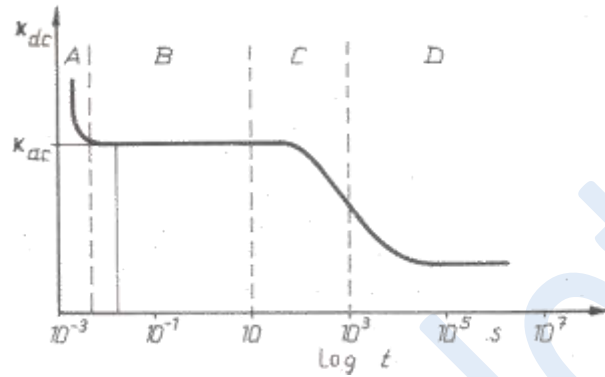


Fig. 17.2 A schematic of dc conductivity of an insulating oil with respect to the time of applied voltage

In every dielectric matter, including those which have a low concentration of free charge carriers, a conductive current through the dielectric is always present on applying a voltage across the volume of the dielectric. Besides, small currents may also flow along the surfaces of the dielectric. Accordingly, two different conductivities, the volume and the surface conductivities of a dielectric, are distinguished. Reciprocal of these are the specific volume and surface insulation resistance's, respectively. The specific insulation resistance ρ_{ins} described above represents the specific volume resistance ' ρ_v ' of the dielectric having a unit of $\Omega \cdot m$. The specific surface resistance ' ρ_s ' has accordingly a unit of Ω only.

Dielectric Power Losses in Insulating Materials

Besides the capacitive charging currents, real or active currents are also present in the dielectrics. These currents are caused due to different types of conductivities and polarizations present in the materials. As shown in the previous sections, these currents not only depend upon the frequency and magnitude of the applied voltage but also upon the thermal conditions of the dielectric. The conductive currents present in an insulating material determine its dielectric power loss property. Each conductive current mechanism causes currents of different characteristics. These currents contribute to the total dielectric current ' i_{ins} ', as depicted schematically for alternating voltage in Fig.17.3.

Conductivity mechanism		
Capacitive charging current	\vec{i}_C	
Partial Discharge impulse currents	\vec{i}_{PD}	
Polarisation	Displacement Boundary surface (multisurface effect) Orientation	\vec{i}_P
Conductive currents	Electron constant ion limited ion	\vec{i}_Σ

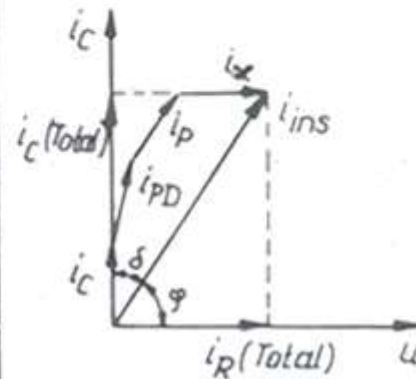
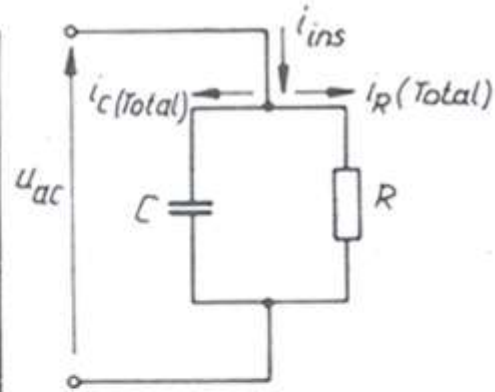


Fig 17.3 Conductive mechanisms in insulating materials for alternating voltage with equivalent circuit and vector diagrams.

The dielectric loss tangent 'tanδ' is defined as the quotient of active to reactive power loss in a capacitor or in a volume of dielectric. It is derived from Fig. 17.3 as follows:

$$\tan \delta = \frac{\text{Active Power}}{\text{Reactive Power}} = \frac{u \cdot i_{ins} \cos \varphi}{u \cdot i_{ins} \sin \varphi} = \frac{i_{R(Total)}}{i_{C(Total)}} \quad (17.5)$$

The dielectric loss tangent (tanδ) represents the complete power loss in a dielectric; hence it is a parameter with which the power losses in a capacitor can be estimated. However, tanδ is a function of frequency and magnitude of the applied voltage as well as the temperature of the dielectric, because these affect the conductivity κ and the polarization processes in the dielectrics.

When alternating voltage of rms magnitude U and frequency ω is applied to a condenser having total effective capacitance C, the total capacitive conductive current I_{c (Total)} is given by

$$I_{c(Total)} = \frac{U}{1/\omega C} = \omega \cdot C \cdot U$$

(17.6)

The active part of the total insulation current is $(\omega CU \cdot \tan\delta)$, hence the active power loss 'Pac' is given by,

$$P_{ac} = \omega \cdot C \cdot U^2 \cdot \tan\delta$$

(17.7)

where $\omega = 2 \pi f$ and if f is in Hz, C in F and U in volts, P is given in Watts. In practice, the capacitance C of the given test object is generally measured. Considering a parallel plate condenser of area A and gap distance d having a dielectric with relative permittivity ϵ_r in a uniform field E , Equation 17.7 can be rewritten as, .

$$P_{ac} = \omega \cdot \epsilon_0 \epsilon_r \frac{A}{d} (E \cdot d)^2 \tan\delta$$

or $P_{ac} = \epsilon_0 \cdot \omega \cdot E^2 \cdot V \cdot \epsilon_r \tan\delta$

(17.8)

where V , the volume of the dielectric, is given by (Ad) in this case. Equation 17.8 shows that the dielectric losses depend upon the applied field intensity and its frequency, volume of the dielectric, its relative permittivity and the loss tangent.

On applying a direct voltage to the dielectric, the losses depend only upon the magnitude of the applied voltage U_{dc} and the dc resistance ' R_{dc} ' offered by the dielectric, determined by Equations 17.3 and 17.4 as follows:

$$P_{dc} = \frac{U_{dc}^2}{R_{dc}}$$

or $P_{dc} = E^2 \cdot V \cdot \kappa_{dc}$

(17.9)

Variation of loss tangent of transformer oil having different moisture contents, measured for a wide range of temperatures by Holle [3.2] is shown in Fig. 17.4. These measurements were conducted on a standard test cell (guard ring capacitor) applying a constant 50 Hz voltage.

Dielectric Power Losses in Insulating Materials

Besides the capacitive charging currents, real or active currents are also present in the dielectrics. These currents are caused due to different types of conductivities and polarizations present in the materials. As shown in the previous sections, these currents not only depend upon the frequency and magnitude of the applied voltage but also upon the thermal conditions of the dielectric. The conductive currents present in an insulating material determine its dielectric power loss property. Each conductive current mechanism causes currents of different characteristics. These currents contribute to the total dielectric current ' i_{ins} ', as depicted schematically for

alternating voltage in Fig.17.3.

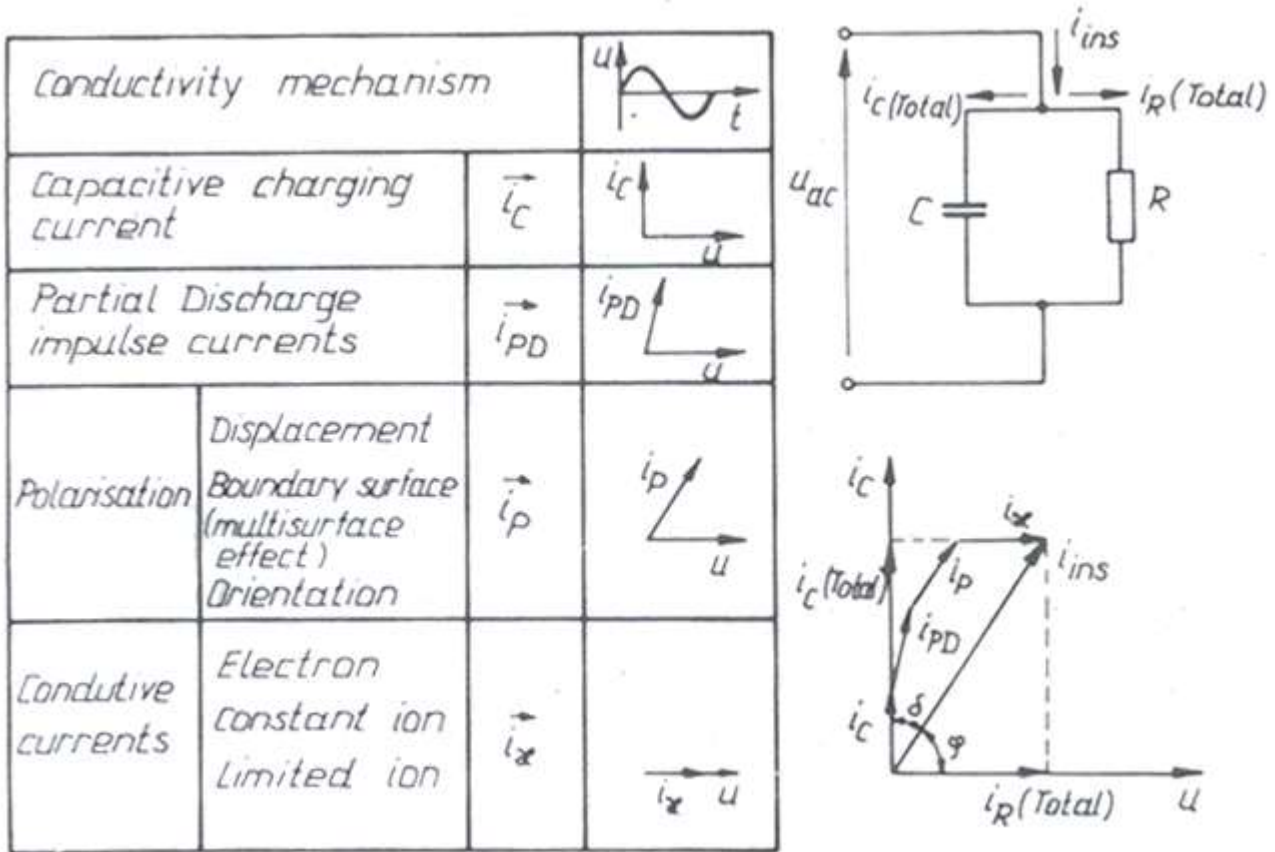


Fig 17.3 Conductive mechanisms in insulating materials for alternating voltage with equivalent circuit and vector diagrams.

The dielectric loss tangent ' $\tan\delta$ ' is defined as the quotient of active to reactive power loss in a capacitor or in a volume of dielectric. It is derived from Fig. 17.3 as follows:

$$\tan \delta = \frac{\text{Active Power}}{\text{Reactive Power}} = \frac{u \cdot i_{ins} \cos \varphi}{u \cdot i_{ins} \sin \varphi} = \frac{i_{R(Total)}}{i_{C(Total)}}$$

(17.5)

The dielectric loss tangent ($\tan\delta$) represents the complete power loss in a dielectric; hence it is a parameter with which the power losses in a capacitor can be estimated. However, $\tan\delta$ is a function of frequency and magnitude of the applied voltage as well as the temperature of the dielectric, because these affect the conductivity κ and the polarization processes in the dielectrics.

When alternating voltage of rms magnitude U and frequency ω is applied to a condenser having total effective capacitance C , the total capacitive conductive current $I_{C(Total)}$ is given by

$$I_{c(\text{Total})} = \frac{U}{1/\omega C} = \omega \cdot C \cdot U$$

(17.6)

The active part of the total insulation current is $(\omega CU \cdot \tan\delta)$, hence the active power loss ' P_{ac} ' is given by,

$$P_{ac} = \omega \cdot C \cdot U^2 \cdot \tan\delta$$

(17.7)

where $\omega = 2 \pi f$ and if f is in Hz, C in F and U in volts, P is given in Watts. In practice, the capacitance C of the given test object is generally measured. Considering a parallel plate condenser of area A and gap distance d having a dielectric with relative permittivity ϵ_r in a uniform field E , Equation 17.7 can be rewritten as, .

$$P_{ac} = \omega \cdot \epsilon_0 \epsilon_r \frac{A}{d} (E \cdot d)^2 \tan\delta$$

or $P_{ac} = \epsilon_0 \cdot \omega \cdot E^2 \cdot V \cdot \epsilon_r \tan\delta$

(17.8)

where V , the volume of the dielectric, is given by (Ad) in this case. Equation 17.8 shows that the dielectric losses depend upon the applied field intensity and its frequency, volume of the dielectric, its relative permittivity and the loss tangent.

On applying a direct voltage to the dielectric, the losses depend only upon the magnitude of the applied voltage U_{dc} and the dc resistance ' R_{dc} ' offered by the dielectric, determined by Equations 17.3 and and 17.4 as follows:

$$P_{dc} = \frac{U_{dc}^2}{R_{dc}}$$

or

$$P_{dc} = E^2 \cdot V \kappa_{dc}$$

(17.9)

Variation of loss tangent of transformer oil having different moisture contents, measured for a wide range of temperatures by Holle [3.2] is shown in Fig. 17.4. These measurements were conducted on a standard test cell (guard ring capacitor) applying a constant 50 Hz voltage.

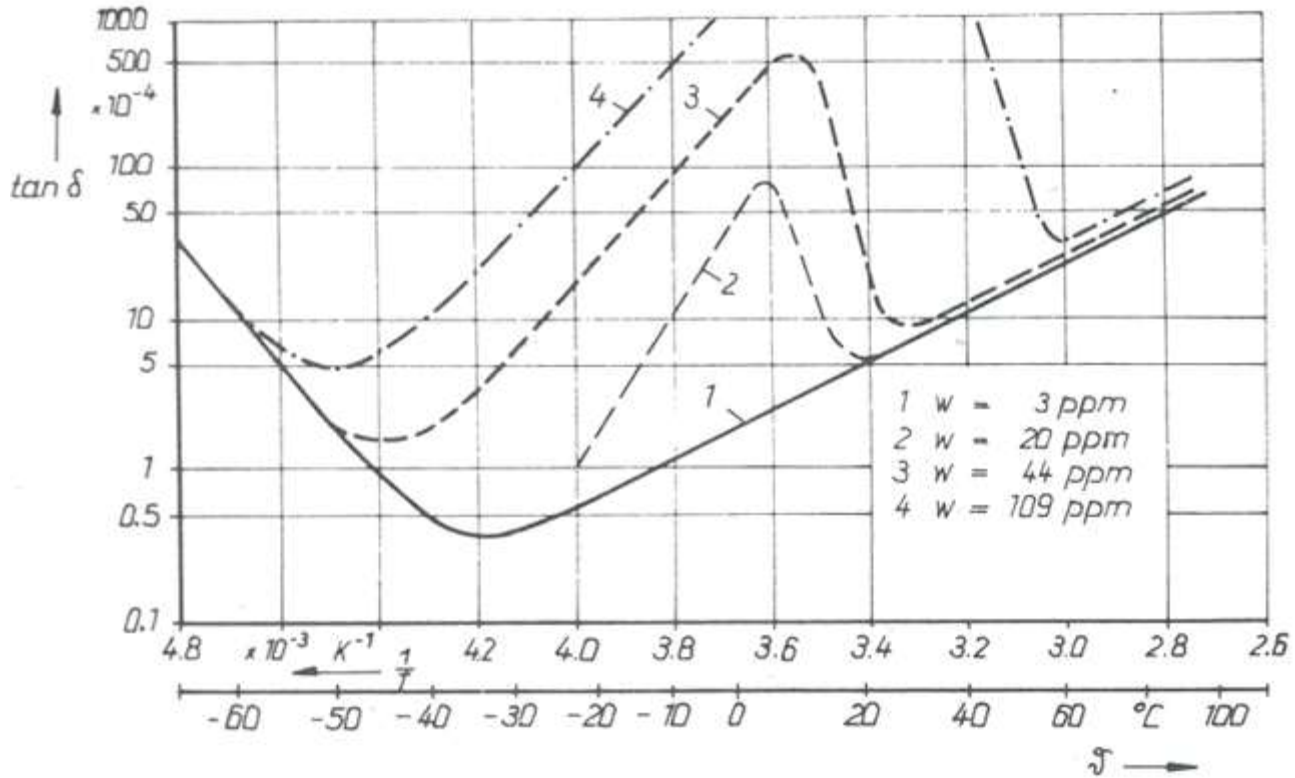


Fig 17.4 Loss tangent ' $\tan \delta$ ' of transformer oil having different ppm moisture contents with varying temperature at 50 Hz constant voltage, Holle [3.2].

The loss tangent is a function of the applied voltage. Increase in $\tan \delta$ of a transformer oil sample, measured at constant temperatures and 50 Hz increasing voltage/field intensity magnitudes is shown in Fig. 17.5 (Beyer et al. [3.6]). These measurements were made at Schering Institute of HV Engineering, University of Hannover. Extra care was taken to design the measuring arrangement which was developed to be PB free for upto 200 kV. As seen from these curves, the increase in temperature as well as moisture content in oil, both result in a premature increase in $\tan \delta$ values with increasing voltage.

Fig. 17.5 shows the variation of $\tan \delta$ and ϵ_r of synthetic insulating liquid 'Clophen A 50', with respect to temperature measured at 50Hz constant voltage.

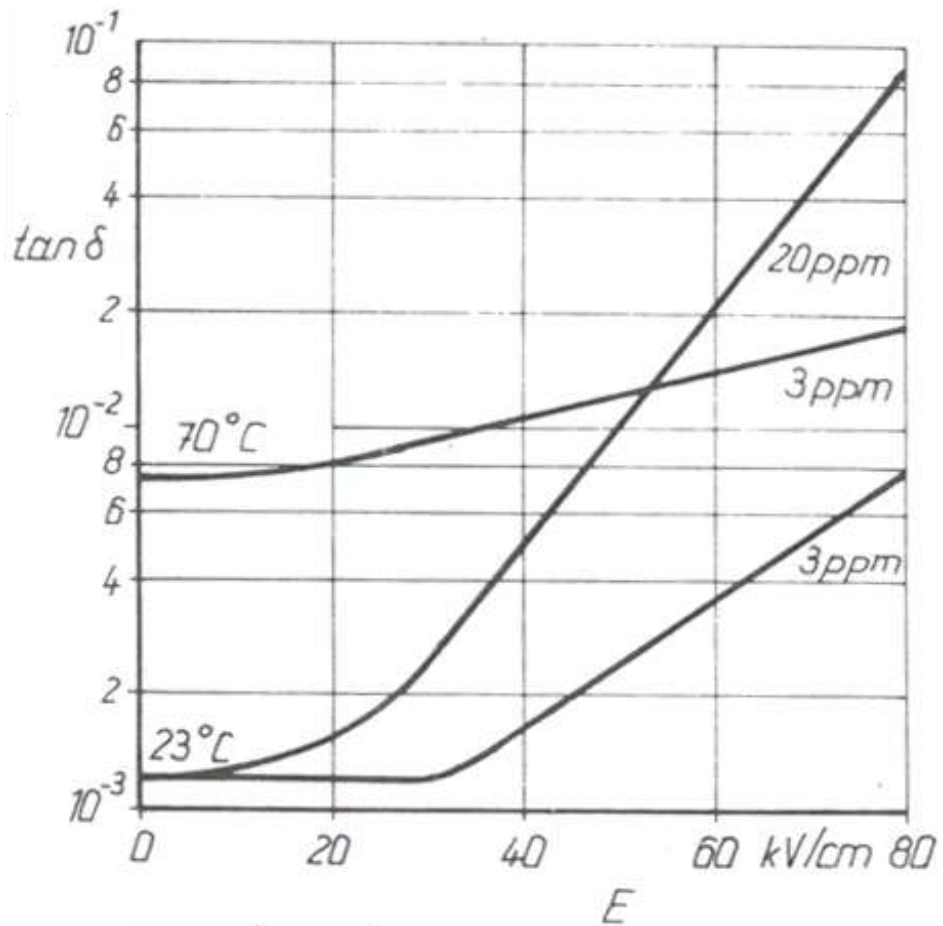


Fig 17. 5 Loss tangent ($\tan \delta$) of a transformer oil measured with increasing voltage/field intensity (50 Hz) at different constant temperatures and for different moisture contents in oil, Bayer et al. [3.6]

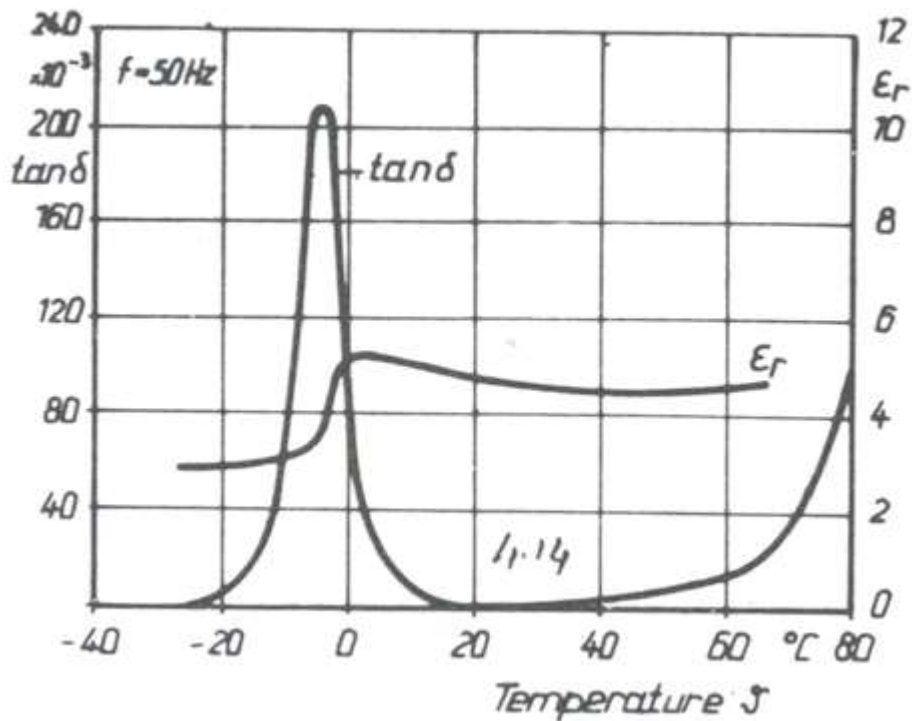


Fig 17.6 Variation of measured values of $\tan \delta$ and ϵ_r with temperature for synthetic insulating liquid Clophen A 50 at 50 Hz constant ac Voltage .

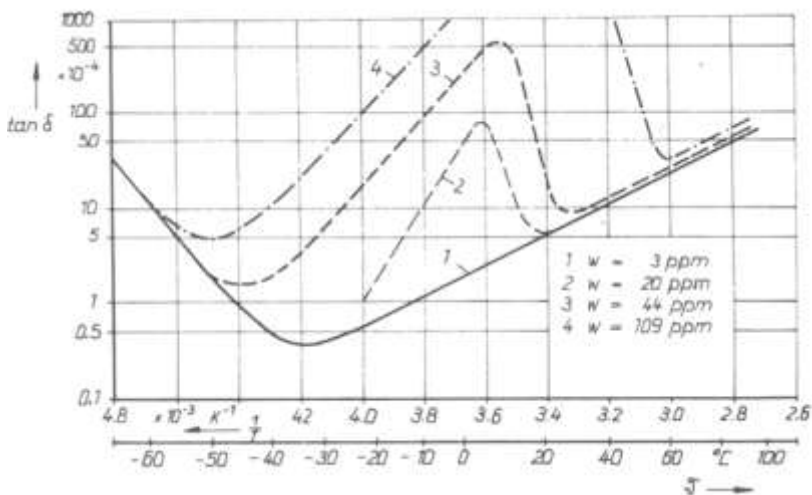


Fig 17.4 Loss tangent ' $\tan \delta$ ' of transformer oil having different ppm moisture contents with varying temperature at 50 Hz constant voltage, Holle [3.2].

The loss tangent is a function of the applied voltage. Increase in $\tan \delta$ of a transformer oil sample, measured at constant temperatures and 50 Hz increasing voltage/field intensity magnitudes is

shown in Fig. 17.5 (Beyer et al. [3.6]). These measurements were made at Schering Institute of HV Engineering, University of Hannover. Extra care was taken to design the measuring arrangement which was developed to be PB free for upto 200 kV. As seen from these curves, the increase in temperature as well as moisture content in oil, both result in a premature increase in $\tan\delta$ values with increasing voltage.

Fig. 17.5 shows the variation of $\tan\delta$ and ϵ_r of synthetic insulating liquid 'Clophen A 50', with respect to temperature measured at 50Hz constant voltage.

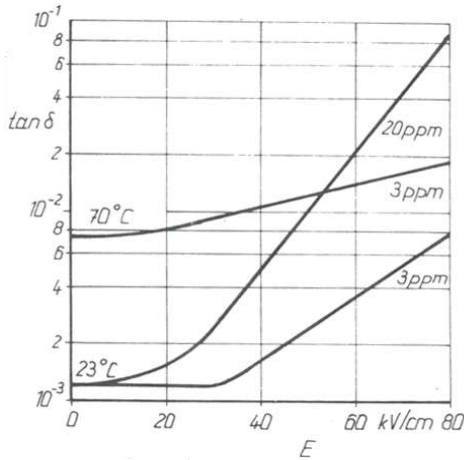


Fig 17. 5 Loss tangent ($\tan \delta$) of a transformer oil measured with increasing voltage/field intensity (50 Hz) at different constant temperatures and for different moisture contents in oil, Bayer et al. [3.6]

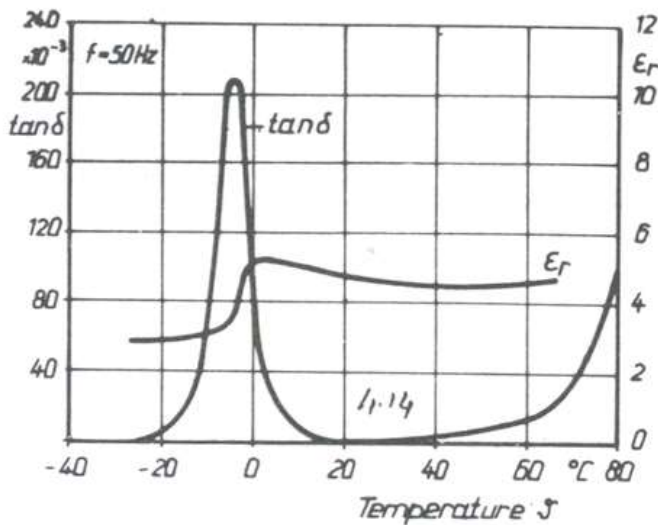


Fig 17.6 Variation of measured values of $\tan \delta$ and ϵ_r with temperature for synthetic insulating liquid Clophen A 50 at 50 Hz constant ac Voltage .

Objectives

In this lecture you will learn the following

Partial Breakdown in Dielectrics

Internal Partial Breakdown in solids and liquids

PARTIAL BREAKDOWN IN DIELECTRICS

Partial Breakdown (PB) are localized electrical breakdown within an insulation system, restricted only to a certain part of the dielectric. In other words, PB are the discharges which do not bridge the electrodes. PB may occur in gaseous, liquid, solid or in any combination of insulation system at extremely nonuniform field locations above a particular field intensity. The field intensity above which the PB may occur depends upon the physical conditions of the dielectric and its properties. The term 'Partial Breakdown' includes a group of local breakdown phenomena; corona breakdown in gaseous dielectrics, internal breakdown at voids or cavities within a liquid or solid dielectrics, and surface discharge also known as 'tracking', which appear on the boundary surface of some solid and liquid dielectrics with air or any other gaseous medium.

Corona or PB in transmission lines in atmospheric air cause power loss which is significant in bad weather (rain) conditions. Besides, it also causes Audible Noise (AN), Electromagnetic Interference (EMI) and generation of ozone. PB in Gas Insulated System (GIS) and liquid dielectrics causes all above effects and also de-generates the enclosed gas or the oil. The damage caused can be said to be reversible to an extent. However, in case of internal breakdown taking place within a solid dielectric, the damage is irreversible. Every breakdown event causes deterioration of the material by the energy impact of high energy electrons or accelerated ions, inflicting electrical and chemical transformations. The actual deterioration is, however, dependent upon the material and the surrounding conditions, but with time it may lead to a permanent damage of the dielectric. Hence, the significance of PB in solid dielectrics is of great importance and will be described in detail in the following lectures.

Internal Partial Breakdown

Partial Breakdown in solid dielectrics may take place at the so called weak points. These weak points may be voids, cavities, cuts, foreign particles or protrusions in the dielectric, as shown in Fig. 18.1. This figure represents a longitudinal cross sectional view of an extruded solid dielectric power cable, provided with extruded semi conductive sheathing on the high voltage conductor as well as on the outer surface of the dielectric. With the development of modern technology, careful handling and maintaining extra cleanliness, the presence of voids and foreign particles in extruded, moulded and cast dielectrics have been minimised, but not ruled out. Voids and cavities, which are the most common type of weak points in solid dielectrics, may vary in size from a few μm to a few mm.

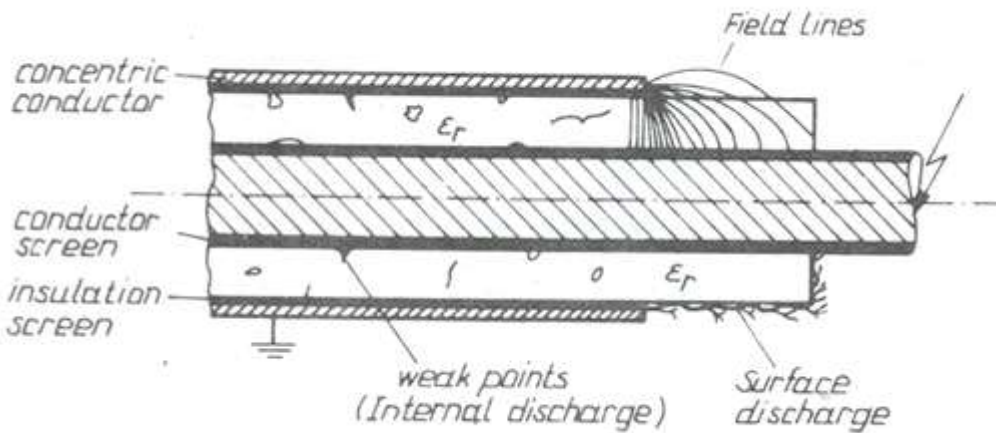
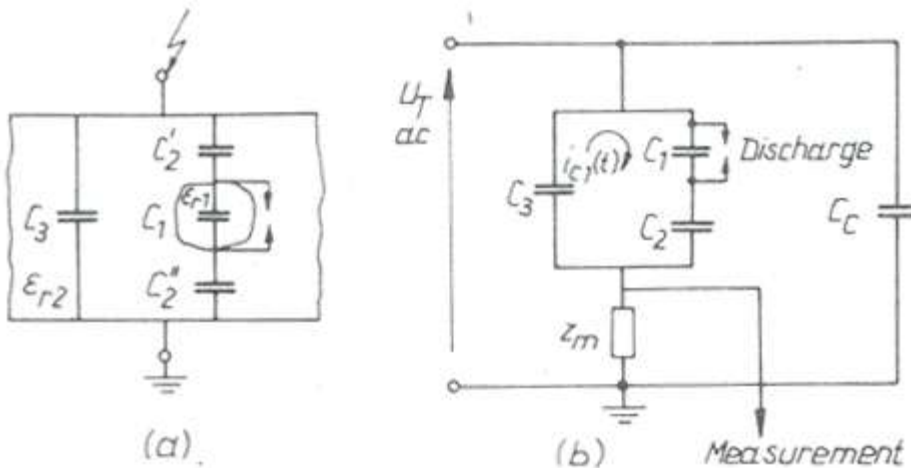


Fig 18.1 A cable cross section showing possibilities of internal and surface discharges. Weak points in general have lower electric strength than the dielectric itself. Still worse is that they acquire higher electric fields. Such weak points can be simulated by a capacitance C_1 within the main dielectric system having capacitance C_3 , as shown in Fig. 18.2(a). If the relative permittivity of a weak point ϵ_{r1} is lower than that of the dielectric ϵ_{r2} the electric stress at the weak point may increase. A protrusion in a dielectric acts as sharp extension of the electrode, causing an extreme distortion in the field locally. Thus, the electric stress within the dielectric increases at the weak points considerably.



C_1 - Capacitance of void
 C_2' and C_2'' - Capacitance between void and electrodes
 C_3 - Capacitance of the test object
 C_c - Coupling capacitor
 C_2 - is equivalent of C_2' and C_2'' in series
 Z_m - measuring impedance

Fig 18.2 Simulation of an internal void Partial Breakdown
 (a) Schematic showing a void forming capacitance
 (b) Equivalent circuit diagram for measurement

It is assumed that a capacitance C_1 is formed due to the void within the main dielectric between two electrodes, as shown in Fig. 18.2(a). Let C_3 be the total capacitance of the electrode system (test object) and ϵ_1 and ϵ_2 the relative permittivities of the void and the main dielectric respectively. The field lines starting and ending at the void form two capacitance C'_2 and C''_2 within the dielectric. C'_2 and C''_2 together in series are combined to form C_2 . The void capacitance C_1 is the origin of PB on applying a voltage to the test object UT, shown in Fig. 18.2(b). Let C_c be the coupling capacitor required in the circuit to suppress the reflections from the open end during the measurement.

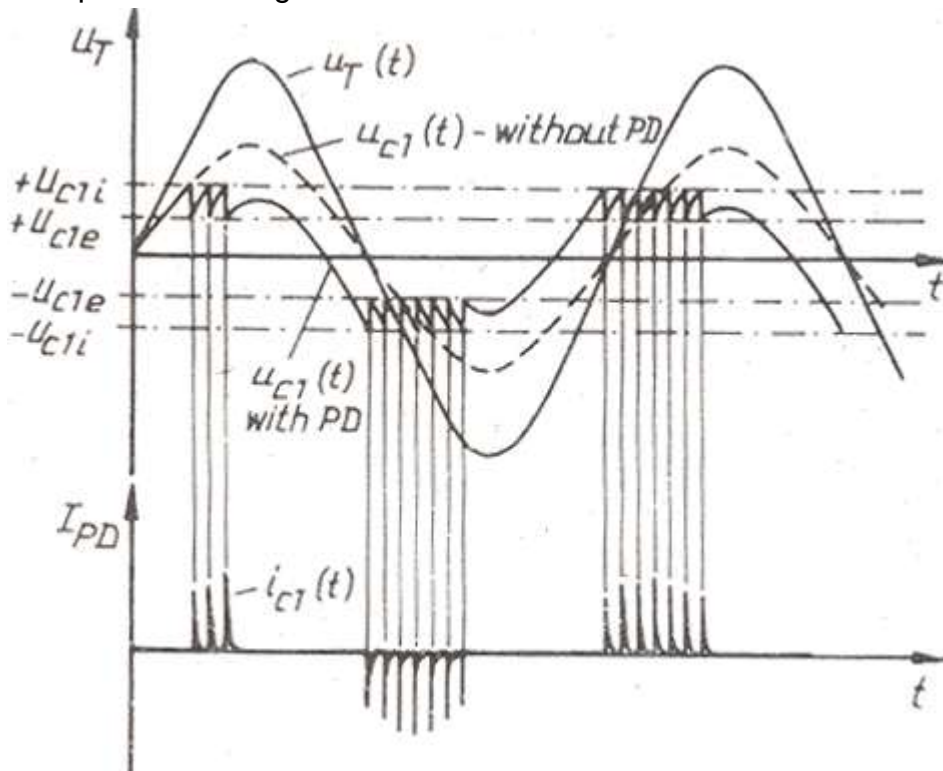


Fig 18.3 PB voltages and pulse currents at a void or cavity in the dielectric. On applying a 50 Hz, ac test voltage U_T , the capacitance C_1 gets charged. C_1 would experience some proportion of the applied voltage U_T , depending upon the magnitudes of different capacitances. The intensity of field at C_1 will depend upon the shape, size and location, etc. of the void, as explained earlier. On raising the applied voltage further, the inception of breakdown across C_1 appears during the rising part of a half cycle, as shown in Fig. 18.3, causing the void capacitance C_1 to discharge. The discharge current $i_{C1}(t)$, which cannot be directly measured, is a very short pulse current of ns range of duration. The opposite polarity charge, produced by this discharge, is displaced towards the electrodes in the field direction, thus neutralizing the original electric field at the void. If the voltage is still rising at the positive or the negative slope of an ac cycle, new field is built up again, repeating the breakdown phenomenon n number of times during each cycle. The PB current pulses thus produced are measured at the external circuit, giving the intensity of PB in Coulombs. On raising the applied voltage on the test object further, the

frequency of occurrence of discharges at C1 and their intensity increases since the rate of repetition of PB increases. In Fig. 18.4, the two oscillograms show the PB inception and intensive PB taking place at higher applied voltage on a test object.

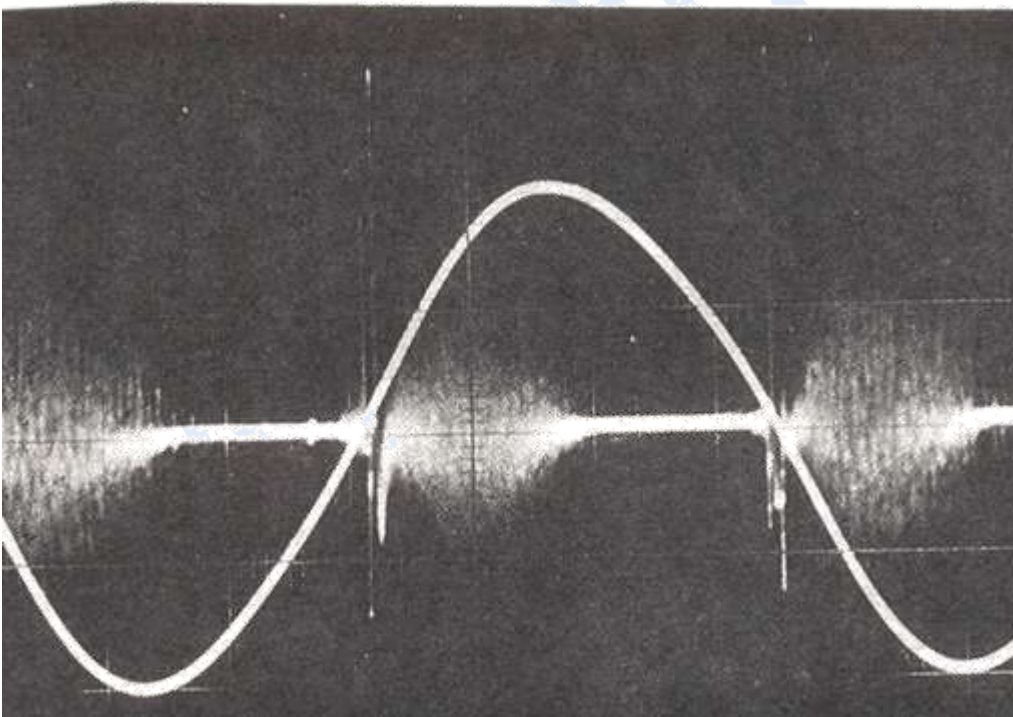
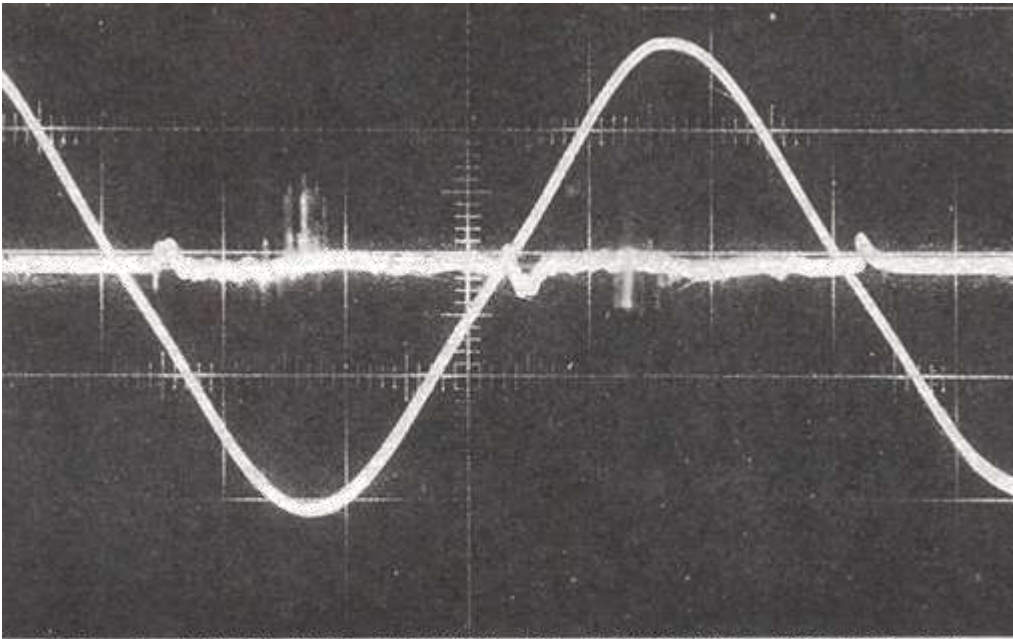


Fig 18.4 Oscillograms of internal PB in solid dielectric.

Assume the magnitude of the voltage at which PD at C1 incept to be U_{c1i} , and the voltage at which PB extinguish U_{c1e} , as shown in Fig. 18.3. The inception voltage U_{c1i} can be given in terms of the applied voltage and capacitances shown in the equivalent circuit diagram as:

$$U_{c1i} = U_T \frac{C_2}{C_1 + C_2}$$

(18.1)

Due to discharge taking place at C1, the voltage drop at C1 may appear to be ΔU_{c1} . Considering no change at C1 initially, ΔU_{c1} is given by,

$$\Delta U_{c1} = U_{c1} \frac{C_2}{C_3 + C_2}$$

If it is assumed that the voltage drop at C1 equals the corresponding drop in applied voltage at the test object ΔU_T , it can be given by,

$$\Delta U_T = U_T \frac{C_2^2}{(C_3 + C_2)(C_1 + C_2)}$$

(18.2)

The actual charge q_{c1} , transposed to the weak point (void) from the circuit in this process is,

$$q_{c1} = \Delta U_{c1} \left[C_1 + \frac{C_2 \cdot C_3}{C_2 + C_3} \right] \quad (18.3)$$

U_{c1i} as well as q_{c1} both are not measurable quantities. However, with the result of potential drop at the test object, a corresponding event takes place at power input terminals. The charge delivered at the power input terminals can be approximated from the equivalent circuit diagram given in Fig. 18.2 (b) as follows:

$$q \approx \Delta U_T \left(C_3 + \frac{C_1 C_2}{C_1 + C_2} + C_i \right)$$

(18.4)

This is a measurable quantity of charge over the measuring impedance Z_m . Since C1 and C2 are unknown, the actual inception voltage at the void U_{c1i} and the charge magnitude q_{c1} transposed to the void are neither measurable nor calculable. This is the reason that the measurable quantity of charge 'q' at the terminals given by Equation 18.4 is described by IEC-270 and also IS-6209 as apparent charge 'qa'. It is defined as follows:

The apparent charge 'qa' of a partial breakdown is that charge which, if injected instantaneously between the terminals of the test object, would momentarily change the voltage between its terminals by the same amount as the partial breakdown itself. The absolute value $|q_a|$ of the

apparent charge is often referred to as the discharge magnitude. The apparent charge is expressed in Coulombs.

The apparent charge q_a defined in this way is not equal to the amount of charge actually transferred across the discharging cavity in the dielectric. It is implied because discharge measuring instruments respond to this quantity. Thus, the magnitude of apparent charge represents the intensity of an individual discharge in a test object. Lemke [3.7] introduced a new concept in this respect in 1975. Since the apparent charge represents the single discharge of maximum intensity taking place in the test object, Lemke called it 'impulse discharge' denoted by ' q_i '. However in a test object, PB may occur at several locations simultaneously. Therefore, the complete phenomenon occurring in the dielectric is not taken into account by q_i . In order to evaluate all the PB taking place in a test object, Lemke introduced a new concept of 'cumulative discharge' ' q_s ' (s - sum total). ' q_s ' takes into consideration all the individual PB occurring in the test object within a certain time period of the applied voltage. Thus, a more comprehensive investigation of PB phenomenon in an object is made possible by measuring q_s . In Fig. 18.5, variation of measured values of q_i and q_s with increasing voltage are illustrated. These curves measured by Lemke [3.7], are for a needle-plane electrode configuration in air, where the PB taken place at the negative half cycle of the 50 Hz ac voltage have been recorded. Similar curves are also measured on test objects with solid dielectrics as insulation.

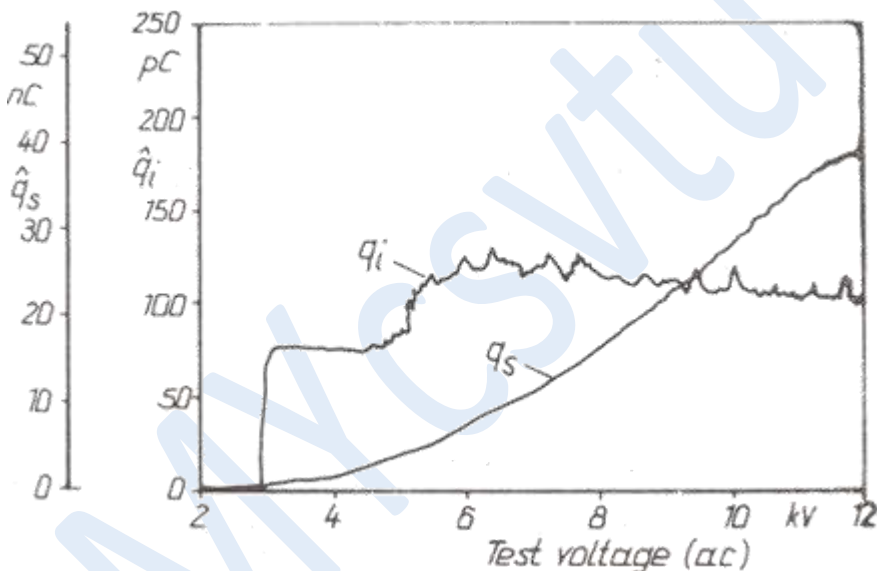


Fig 18.5 Variation of impulse ' q_i ' and cumulative ' q_s ' discharge magnitudes with increasing voltage, Lemke [3.7].

Besides apparent charge, the other important PB quantities for a test object are the PB inception and extinction voltages. These quantities, as defined in IEC-270, are as follows:

PD inception voltage ' U_i '

It is the lowest terminal voltage at which a discharge due to partial breakdown exceeding a specified intensity is observed under specified conditions, when the voltage applied to the test object is gradually increased from a lower value at which no such discharges are observed.

PD extinction voltage ' U_e '

It is the voltage at which PD exceeding a specified intensity cease under specified conditions when the voltage is gradually decreased from a value exceeding the inception voltage. The other quantities related to individual discharge are defined as follows:

Repetition rate 'n'

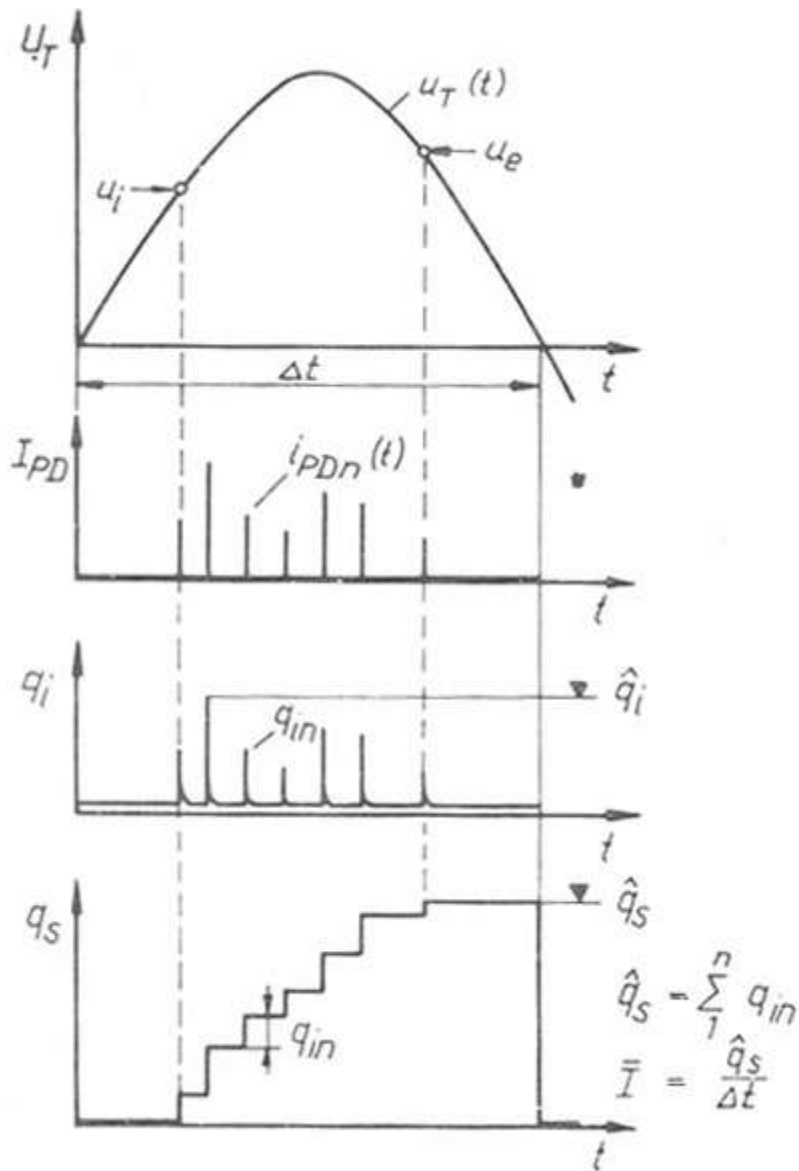
The PB pulse repetition rate 'n' is the average number of pulses per second.

Energy of an individual PB, 'w'

The energy due to PB 'w' is the energy dissipated during one individual discharge. It is expressed in joules. Among integrated quantities, the average discharge current I is defined as the sum of the rectified charge quantities passing through the terminals of a test object due to discharges taking place during a certain time interval Δt , given by,

$$\bar{I} = \frac{1}{\Delta t} [|q_1| + |q_2| + |q_3| + \dots + |q_n|]$$

The measurable PB quantities described above have been explained with the help of a schematic given by Lemke [3.8], as shown in Fig. 18.6. Measurement of these quantities on a test object may be able to provide an evaluation of the quality of finish of the dielectric. Satisfactory performance and the life expectancy of an electrical apparatus depend upon the dangerousness of the weak points in the dielectric. Limiting values of PD quantities are standardised for different products in order to ensure quality of finish of the dielectric on an apparatus.



u_i - PB inception , u_e - PB extinction,
 Δt - time interval of measurement,
 q_i - apparent impulse discharge, q_s - apparent cumulative discharge
 \hat{q}_i - impulse discharge of maximum intensity
 \hat{q}_s - sum total of individual discharge in a time interval of Δt ,
 \bar{I} - average discharge current
 Flg 18.6 Measurable quantities of PB , Lemke [3.8].

Objectives

In this lecture you will learn the following

Surface Discharge (Tracking)

Degradation of Solid Dielectrics caused by PB

Surface Discharge (Tracking)

PB on the surface, also known 'tracking', occur in any gaseous medium and also in vacuum at the interfaces of solid and liquid dielectrics. Surface discharges are caused due to the presence of high tangential component of electric field along a diagonal interface between any solid or liquid and a gaseous medium. Typical examples of the presence of such interfaces in practice are in bushings, insulators, cable terminations and sites in transformers. As shown in Fig. 18.1, when the concentric conductor of a coaxial cable is abruptly terminated, the field intensity at the point of termination becomes very high. An increased tangential component of the field is resulted in the gaseous medium which stresses it with higher field intensity. Surface discharges are caused if an interruption of the creepage current across the surface of the dielectric takes place and the field component at the location exceeds the electric strength of the medium. Surface Discharge or tracking is also a PB phenomenon.

Day in [3.9] describes surface discharge as an untidy process, whose occurrence depends upon the properties of the dielectric but their inception depends upon several other factors too. Day defines tracking as the formation of conducting path on the surface of a dielectric. In most cases, the conduction results from degradation of the dielectric or by deposition of a foreign layer on it. Hence for tracking to occur, the following are essential to be present:

- a conducting film across the surface of the dielectric
- a mechanism by which the creepage current through the conducting film is interrupted when the discharges occur.

The conducting film is usually a form of contamination, such as salt deposition (in coastal areas), carbonaceous dust from fuels and industrial or cellulose fibre deposits along with moisture. Interruption of moisture films is caused when a surface is dried due to the heating effect of the surface current. . As the amount of contamination increases, so does the surface current, until the joule heating in the layer causes it to dry out locally initiating discharges between the receding edges of the wet film. On the surfaces of many dielectrics tracking may not occur under dry and clean conditions. An estimate revealed that tracking is likely only when the creepage currents of the order of 1 mA are able to develop on the surface.

Referring to previous section, the presence of a diagonal interface gives rise to high tangential and normal components of field at the surface. With the result, multiplication of charge carriers takes place right at the surface. On increasing the applied voltage, the same sequence of discharge mechanism is followed on the surface as in case of gaseous and liquid dielectrics, that is, avalanche, streamer and leader surface discharges. Since the charges get trapped over the surface; the more is the discharge magnitude, longer track

lengths with numerous branches are produced depending upon the properties of the material. A typical autograph of surface discharges is shown in Fig. 19.1 taken by Nema [3.10].

The theoretical consideration for a material to have tendency to track is suggested in terms of chemical bond energies of the material by Parr and Scarisbrick [3.11]. Since the primary bonds are important when considering thermal stability of polymers, the tendency to track depends upon the proportion of bond which produces free carbon on pyrolysis, that is, by chemical decomposition of molecules as a consequence of exposure to a high temperature. It can be expressed as follows:

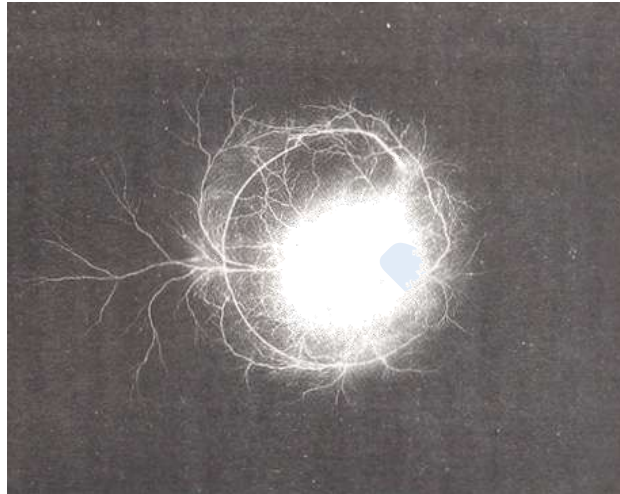


Fig 19.1 A typical autograph of surface discharges showing stable streamer as well as leader corona, Nema [3.10].

$$\frac{T_c}{T_m} = \frac{\text{Dissociation energy of all the bonds which on breaking produce free carbon (kcal/mole)}}{\text{Total bond energy of the molecules (kcal/mole)}}$$

Smaller the fraction T_c/T_m , less is the likely hood of dielectrics to track. Experimental results revealed that if T_c/T_m is smaller than 0.3, the material has no tendency to track. Polymers which do not track are for example, polypropylene, poly-formaldehydes, etc. On the other hand, if this fraction is greater than or equal to about 0.5, the material may track easily. For example, polystyrene, phenol-formaldehydes and polycarbonates are among the polymeric dielectrics which track easily besides the ordinary glass being well known to track.

Since it is the free carbon produced by thermal decomposition which forms the conducting tracks, the degree of resistance to track of a material depends upon its chemical nature and the manner in which it breaks down when subjected to high temperatures. For example, the degradation products of PE are gaseous, therefore the polymer does not track normally except when some conducting contamination is trapped on its surface during erosion. This is the reason that in order to prevent tracking, a creepage distance is often specified to limit surface currents.

For the sake of obtaining a comparative knowledge of tendency to track of materials, IEC-112 and BS-378I have introduced an index, known as 'Comparative Tracking Index' (CTI),

giving standard procedure of its measurements. The CTI can be used as a specification for the measurement of track-resistant quality of a dielectric. The CTI greater than 750 represents the upper stratum of materials in terms of track resistance. However, the use of a material having CTI higher than 750 may not guarantee that tracking will not occur under very bad contamination conditions.

Degradation of Solid Dielectrics Caused by PB

Internal discharges in solid dielectrics cause their degradation and lead to the formation of solid, liquid and gaseous products due to synthesis reactions taking place within the -electrode gap space. Organic compounds containing oxygen are readily synthesized from mixtures of CO_2 , CO and H_2O undergoing discharges. Experimental investigations made by Gamez-Garcia et al. [3.12] on PE and XLPE confirmed their earlier findings that CO_2 , CO, H_2O and acetophenone are the main degradation products. This was revealed by their experimental investigations of products obtained from tests on XLPE degradation due to discharge synthesis reactions, which took place within the electrode gap space. Oxalic acid and other non aromatic compounds result from discharge synthesis reactions involving CO and H_2O . Acetophenone, which evaporates from an XLPE surface after cross-linking, plays an important role in the formation of other degradation products. Benzoic acid, benzamide, toluene and other aromatic compounds result from chemical reactions of this volatile compound during the degradation process taking place in the presence of PB.

If the PB intensity is unusually high, the degradation and erosion mechanism may proceed at sufficiently fast rate. Conductive channels in different shape and size are formed within the solid dielectrics, known as 'Tree' formation. The phenomenon is known as Treeing process. It grows towards the opposite electrode with time. It may lead to complete failure of the insulating properties of the dielectric taking different amount of time which depends upon the material, the field intensity and its shape. The exact conditions determining these mechanisms are yet to be defined through more detailed investigations.



Fig 19.2 Development of Treeing Process in Epoxy Resin

Under one such investigation, treeing process developed in solidified resin is shown in Fig. 19.2. A needle electrode imbedded inside the resin block produces an extremely nonuniform field at the tip of the needle. This gives rise to PB within the solid dielectric on applying a voltage greater than U_i , the PB inception voltage. The PB causes conductive channels due to degradation of the dielectric under heat. These develop in the form of a tree extending towards the opposite electrode, the ground electrode. The development of treeing process in solid dielectrics could be caused at any localised enhancement of electric field intensity. It could be due to a void, foreign particle, metallic protrusion or ingress of water/moisture in the solid dielectric, such a formation of tree is the formation of conductive channels within a healthy material. This process reduces the life of the dielectric drastically.

From the above, it can be concluded that PB in solid dielectrics cause physical changes through chemical synthesis reactions. The nature and extent of these physical changes depend upon the particular local condition and the time factor, which play a very important role.

Module – 4

XX

Objectives

In this lecture you will learn the following

Breakdown in Liquid Dielectrics

Intrinsic and Practical Breakdown Strengths of Liquid Dielectrics

Breakdown in Liquid Dielectrics

A very large number of external factors affect the breakdown strength of liquid dielectrics. For example, electrode configuration, their material, size and surface finish; the type of voltage, its period of application and magnitude, the temperature, pressure, purification of the liquid and its ageing condition. Dissolved water, gas or the presence of any other form of contamination and sludge also affect the breakdown strength considerably. It is, therefore, not possible to describe the breakdown mechanism by a single theoretical analysis which may take into account all known observed factors affecting the breakdown.

The breakdown strength of any dielectric is distinguished into two broad categories known as the 'intrinsic' and the 'practical' breakdown strengths.

Intrinsic Breakdown Strength

The intrinsic breakdown of a dielectric is defined as the highest value of breakdown strength obtained after eliminating all known secondary effects which may influence the breakdown. The concept of intrinsic breakdown is ideal. It is, however, extremely difficult to ascertain whether an observed breakdown was intrinsic or not. Intrinsic strength can be suitably interpreted as the field intensity at which the particles in the material are accelerated without any limit by the direct electrostatic action of the field.

The mean free path of an electron in insulating oils is very short, of the order of 10^{-6} cm. An extremely high field intensity is therefore required to begin the elementary process of

ionization with free electrons having a very short life time. These elementary processes through which energy loss into the liquid takes place, determine the breakdown mechanism. Hence these processes decide the breakdown strength of a dielectric. The elementary processes of ionization are as follows:

- the most likely elementary process in case of hydrocarbon liquids is by excitation or molecular vibration, which is equivalent to thermal vibrations. The vibrational modes of a hydrocarbon are determined by elementary vibrations of the C-C and C-H molecular bonds. The frequencies of such vibrations lie in the infra-red region with corresponding energy quanta of about 0.2 to 0.4 eV ($1 \text{ eV} = 1.6 \times 10^{-19} \text{ J}$). These may lead to local growth of vapour phase of microbubbles.
- the process of dissociation of molecules in neutral, low molecular, gaseous particles due to severe molecular vibrations which requires energy levels in the range 1.5 to 7 eV.
- excitation of metastables which may lead to ionization in a few stages, requiring energy levels of the order of 1.5 to 10 eV.
- ionization process involving scintillation of electrons accompanied with weak luminescence, indicating energy quanta of several eV; which is greater than 10 eV in some liquids.

The elementary processes mentioned above depend upon the molecular structure of a dielectric. These may occur spatially and timely together. However, there is no evidence of ionization by electron collision in liquids as in the case of gases. The electrode process may play its usual role as described.

For a mean free path of electron of the order of 10^{-6} cm and an energy of about 10 eV, the theoretically estimated field intensity required for ionization in insulating liquids is of the order of 10,000 kV/cm. On the contrary, a field intensity of only about 200 to 400 kV/cm may be sufficient to cause ionization by the elementary process of excitation of molecular vibration.

Electric strengths of some highly purified liquids and liquefied gases as given by Lewis in [3.5] are given in Table 20.1. These breakdown strengths appear to have been measured on very thin liquid films and represent nearest comparative values of intrinsic strengths.

Table 20.1 Electric Strength of highly purified liquids and liquefied gases, Lewis in [3.5]

Liquids	Breakdown Strength kV/cm
Good oil	1000-4000
Benzene	1100
Silicone	1000-1200
Hexane	1100-1300
Hydrogen	>1000
Oxygen	2400
Nitrogen	1600-1800

Practical Breakdown Strength of liquid dielectrics

The practical breakdown strength of insulating liquids is measured with help of standard electrodes having weakly nonuniform field between them. The peak value of electrical breakdown strength of commercially available purified insulating oils is about 350 kV/cm. This is highly contradictory to the measured intrinsic strengths of the order of 1000 kV/cm and above. As mentioned above, it is because of the secondary effects which influence the breakdown strength. If the condition of the liquid is very bad (impure, contaminated, etc.) one may measure an electric strength as low as 10 kV/cm only.

In order to compare the electric strengths of different insulating liquids or the same liquid in its different conditions, the methods of measurement of breakdown strength have been standardized by different standards. Simple methods are thus evolved to estimate the quantity of insulating liquids. The methods laid down by TGL-15077, IS-6792, VDE-0370 and IEC-156 are almost identical. According to these, an ac power frequency voltage is applied to 1 - 2.5 mm gap between two identical electrodes, so called 'calottes', of dimensions shown in Fig 20.1. The IS recommends the electrodes to be made of brass having a good surface finish, whereas VDE recommends copper as electrode material. These electrodes are placed in a container of given size and filled with about 300 cc of the sample oil. The measurement is conducted at room temperature (20°C) by increasing the applied sinusoidal waveform alternating voltage at a rate of 2-3 kV/s upto breakdown. The rms value of the breakdown voltage U_b is measured. The Schwaiger factor of uniformity, η for the given gap and electrode configuration is 0.97, that is, the field can be considered to be almost uniform. For each sample of insulating liquid, six measurements of breakdown voltages are recommended to be performed at an interval of 2 min. (VDE), 1-5 min. (IEC) or 10 min. (TGL), stirring the liquid thoroughly after every breakdown. TGL recommends to consider arithmetic mean of the measurement numbers two to six, whereas VDE and IS recommend mean of all the six values to be taken into account. If the mean rms breakdown voltage is U_b in kV, the peak value of electric strength of the liquid is given as follows:

$$\begin{aligned}\hat{E}_b &= \frac{\sqrt{2}U_b}{\eta \cdot d} = \frac{\sqrt{2}U_b}{0.97 \times 0.25} \text{ kV/cm} \\ &\approx 5.8 U_b \text{ kV/cm}\end{aligned}$$

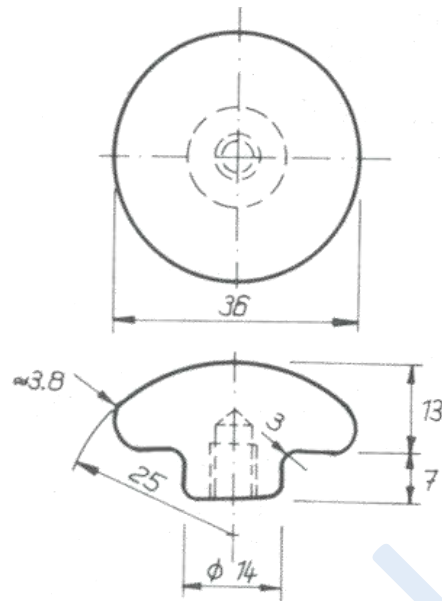


Fig 20.1 Electrode design having $\eta = 0.97$ for the measurement of electric strength of commercial liquid dielectrics according to VDE-0370.

Besides the purity and clean conditions of the sample of oil, the breakdown strength strongly depends upon the moisture content and the temperature of the insulating oils.

Power frequency ac breakdown voltage/ field intensity of transformer oil samples having different moisture content were measured by Holle [3.2] with increasing temperature according to the standard method described above, Fig.20.2

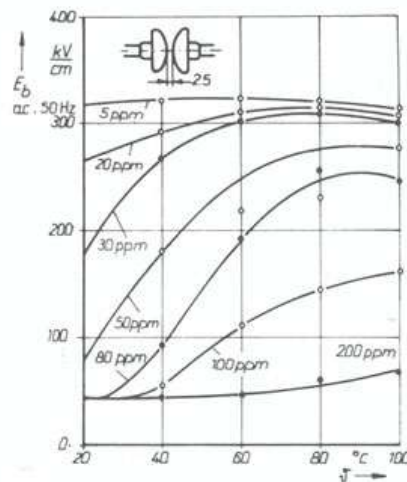


Fig 20.2 ac power frequency breakdown field intensity (rms) with increasing temperature of a transformer oil having different water contents in ppm, Holle [3.2]

These measurement curves illustrate the effect of moisture content in oil samples on their

breakdown strengths. It is interesting to observe that for very low (<20 ppm) and also for very high (>200 ppm) moisture contents the breakdown strength is more or less independent of the temperature. However, between 20 and 100 ppm level of moisture content, the breakdown strength of oil strongly depends upon its temperature.

XXI

Objectives

In this lecture you will learn the following

Breakdown and Prebreakdown phenomena in Solid Dielectrics
Intrinsic Strength of Solid Dielectrics

Breakdown and Prebreakdown phenomena in Solid Dielectrics

The prebreakdown phenomena in solid dielectrics leading to an irreversible rupture of the material (breakdown) is extremely complicated. In this process the local electric field, heat transport, charge injection and accumulation, mechanical stress, chemical and mechanical stability are all strongly and often nonlinearly coupled. Above all, the time factor affecting the breakdown makes the prebreakdown phenomena more complicated.

Intrinsic Strength of Solid Dielectrics

As described in case of liquid dielectrics, the same definition of intrinsic strength holds good also for solid dielectrics. For a homogeneous and isotropic solid dielectric, the intrinsic strength is described as the highest value of electric strength obtainable after all known secondary effects leading to a premature breakdown (below intrinsic strength), seem to have been eliminated.

The concept remains an ideal one and its validity is always dubious, as it is very difficult to know whether an observed breakdown was or was not intrinsic. One may conclude therefore, that the observed results are more likely to be intrinsic, the more they are independent of parameters like temperature, thickness and time. It is also extremely important that the test sample is prevented from self heating and mechanical distortions caused by the field.

In order to measure intrinsic strength, preparation of the test samples is the utmost sensitive part involving a considerable amount of precision techniques. As described by Garton in [5.11], only two methods of measurement are seriously considered, the 'recessed specimen' and the 'McKeown's technique'. Lawson [4.1] measured the intrinsic strength of PE samples with the help of above mentioned specimens at different temperatures described in the following:

' Recessed Specimen '

A spherical depression is either pressed, machined or ground on a ca. 1.5 mm thick plane disc sample of the material. It nearly penetrates the specimen, leaving only a thickness of approximately 50 μm , suitable for breakdown by a reasonable voltage, as shown in Fig. 21.1(a). The radius of the spherical depression should be such that a uniform field is achieved. The surfaces of the recess and of the opposite plane faces are then made conducting by a technique

which provides an extremely good contact with the dielectric, for example, an evaporated film of aluminum, or a graphite coating applied by repeated spraying and polished to a continuous film. Liquid electrodes have also been tried. However, limitations like inadequate cooling of the stressed area and no mechanical support for the thin apex of the specimen remain with such electrodes.

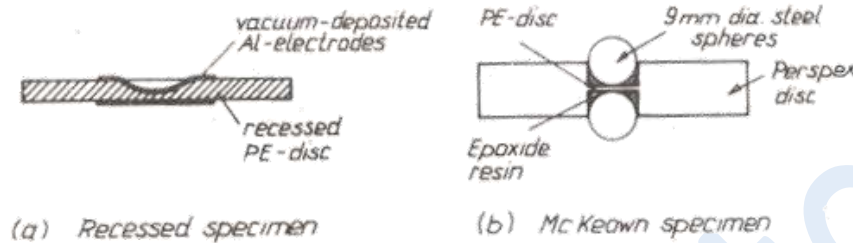


Fig 21.1 Specimens for the measurements of intrinsic strength, Lawson [4.1].

' McKeown Technique '

Two ball bearings used as electrodes in this specimen are located within a cylindrical hole in a disc made of suitable insulating material, such as Perspex. The lower ball is cemented in the position with an epoxyresin, and the hole filled with the same resin in liquid form. Then it is gently heated in partial vacuum until degassed. As shown in Fig. 21.2(b), the polyethylene test sample in the form of a thin film disc is placed in the hole on the top of the ball and the liquid is degassed again. Before encapsulation, the polyethylene film sample were treated chemically by immersion in concentrated chromic acid for five minutes to oxidize their surfaces and make a bond with the epoxide resin. The top ball is then inserted and the whole specimen cured until solid conditions are achieved. The thickness of the test sample assembled can be obtained by measuring the total thickness outside the balls and subtracting twice the diameter of the ball. A proper adhesion of the test sample material with the epoxyresin must be achieved to avoid any partial discharges or tracking on the interfaces. The specimen thus prepared may further require a chemical treatment with a solution of sodium in liquid ammonia in order to prevent corona discharges on the surfaces. As reported by Garton, both these techniques have proved extremely satisfactory at room temperatures for measuring the intrinsic strength of low-loss polymers. However, the results obtained by McKeown specimens have been consistantly higher than those obtained by the 'recessed' specimens.

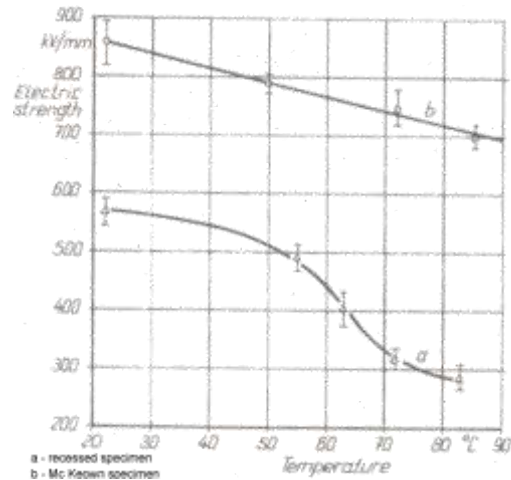


Fig 21.2 Variation of intrinsic electric strength of PE specimens with temperature, Lawson [4.1] .

Lawson [4.1] used McKeown techniques to measure the intrinsic strength of PE with increasing temperature between 20-85°C, as shown in Fig. 21.2. In his experiments, the breakdown tests were carried out under transformer oil to prevent flashover due to surface discharge. The applied voltage raised linearly with time, was obtained from a smoothed half-wave rectifier source. In these experiments, the breakdown occurred in about 15-20 s. In all cases the number of specimens tested were from six to eight, and 95% confidence limit of the mean was considered. Compared to the results obtained from recessed specimens, the fall of intrinsic strength with increasing temperature was greatly reduced by using McKeown specimens. Besides, altogether higher values of electric strength, of the order of 800 kV/mm, were obtained for PE.

The theories developed for intrinsic breakdown aim to arrive at a condition for an irreversible instability of the dielectric which is electronic in nature. These simply assume that in case of intrinsic breakdown the irreversible electronic catastrophe produces conditions in which the lattice is destroyed which is a temperature dependent phenomenon, Lawson [4.1].

The general aim of the measurement of intrinsic electric strength of the dielectrics has been to reveal the extreme complexity of the breakdown mechanism at very high electric fields rather than to find out electric strength. A breakdown in real life always occurs through some secondary mechanism or an external cause. Therefore, to conclude that a breakdown was intrinsic is mostly dubious. In practice, the solid dielectrics are stressed with maximum electric stress not greater than 3% of such high values of intrinsic strengths.

XXII

Objectives

In this lecture you will learn the following

- Thermal Breakdown in solids
- Mechanism of Breakdown in Extremely Non-uniform Fields

'Treeing' a Prebreakdown Phenomenon in Polymeric Dielectrics

Thermal Breakdown

Since it develops very rapidly, the intrinsic breakdown is assumed to have electronic origin. The most simple theoretical approach for intrinsic breakdown has been to derive a theory for an electronic instability in the dielectric subjected to a uniform field, O'Dwyer [4.2]. While measuring the intrinsic strength, if there exists a cause which leads to other than electronic instability, the value of electric strength measured may be anywhere below intrinsic strength. One such cause is 'thermal instability', particularly in the dielectrics having sufficient conductivity. The conductivity is found to increase with electric stress, but the rate of increase may not be linear, Lawson [4.1]. The 'hot electron' theory of breakdown in solid dielectrics developed by Frohlich and Paranjape [4.2] also predicted a stress-enhanced conductivity, which may cause thermal failure before a true instability (intrinsic failure) occurs. This theory involves lattice temperature rise processes and is derived for intrinsic or near intrinsic breakdowns.

The experimental concept of 'thermal breakdown' is different as it is based upon self heating of the dielectric due to power losses. Because of power loss due to conductivity, polarization or other forms of dielectric losses, heat is produced continuously in electrically stressed dielectrics. Depending upon the magnitude of the applied voltage, its period of application and the conduction of heat the dielectric temperature rises. If the heat generated within a dielectric system equals the dissipation of heat to the surroundings by thermal conduction, the temperature rises to an equilibrium value, and a thermally balanced and stable operation of the insulation system takes place. But in practice, the power losses in a dielectric are some function of temperature also. Since the ionic conductivity increases with increasing temperature, the power losses increase with temperature. If the dissipation of heat by cooling processes is not adequate, it is possible that an unstable state may arise in which the temperature increases without limit causing a breakdown.

Mechanism of Breakdown in Extremely Non-uniform Fields

While designing electrode configurations in practice, it is tried to avoid extremely non-uniform fields, especially for solid insulations. Thus, one may say that solid dielectrics are normally not stressed with extremely sharp non-uniform fields in practice. But, the pre breakdown process generally begins at an extreme intensity or distortion of local fields. Under the action of this high local electric field, a solid dielectric may either globally or locally lose its electrical insulating property and mechanical stability, leading to its complete or partial disintegration. A review of the breakdown and pre breakdown phenomena in solid dielectrics made by Zeller [4.3] has brought out certain important conclusions described in the following.

At fields closer to local breakdown i.e. PB inception at the tip of a sharp electrode, massive space charge injection from the electrodes into the dielectric is inevitable. The local electric stress dominated by the space charge may increase considerably. The electromechanical action due to electric force causes dielectric instabilities in solids, giving rise to initiation and growth of electrical trees, a conductive path with the dielectric.

'Treeing' a Prebreakdown Phenomenon in Polymeric Dielectrics

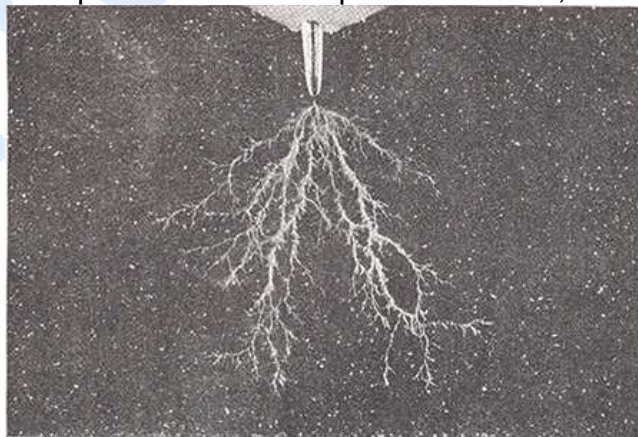
Treeing is an electrical pre-breakdown phenomenon. The name is given to the type of damage caused to the solid dielectrics, which progresses through its certain part under electric stress in extremely non-uniform fields. The path of its growth appears like a miniaturized tree, hence the name given to this phenomenon. Treeing process normally begins at a very sharp, pointed electrode tip due to internal partial breakdown which take place under extremely nonuniform field conditions. Extreme field distortions at protrusions in the dielectrics may also give rise to the development of treeing process.

Treeing may occur and develop slowly due to PB. In the presence of moisture it may develop slowly even without any measurable PB. However, treeing develops rapidly when very high impulse voltage is applied. While treeing is generally associated with ac and impulse voltages, it also takes place under high dc stresses. Evidences are there that the treeing process is aggravated by the presence of moisture, chemical environment, voids and contaminants such as foreign particles. Treeing may or may not be followed by complete electrical breakdown of the part of the dielectric where it occurs. However, in solid polymeric dielectrics it is one of the most common cause of electrical failure. The whole process may or may not take long time for it strongly depends upon the local conditions.

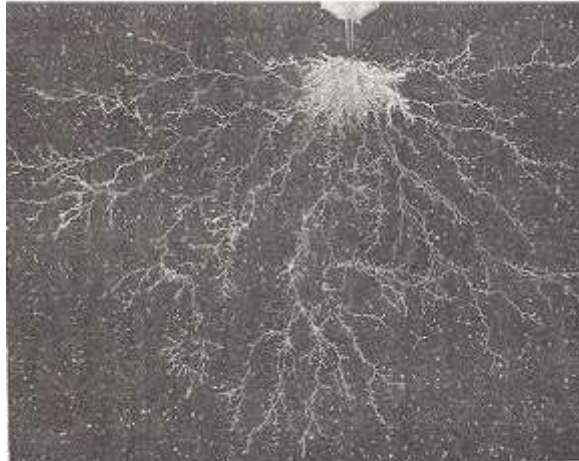
Forms of Treeing Patterns

The great variety of patterns which appear like stems and branches comprising an electrical tree, are described in the literature with large number of corresponding names of the figures such as, dendrite, fan, plume, delta, bush, broccoli, string and bow tie, etc. Eichhorn [4.4]. The reader should therefore not get confused as they all represent the same phenomenon of treeing under different local conditions. In Fig. 22.1 (a), a tree, and in 22.1(b) a bush having tree like branches are shown. These were produced in Piacryl, a transparent solid dielectric, in extremely nonuniform field between needle and plane by Pilling [4.5].

Besides depending upon the in homogeneity of the dielectric material, the pattern of growth of treeing process also depends upon the radius of the tip of needle, diameter of needle, gap length 'd' as well as shape and size of the plane electrode, Loffelmacher [4.6]



(a) A Tree in Piacryl



(b) A bush like tree in Piacryl

Fig 22.1 Treeing in Piacryl, Pilling [4.5].

In figure 22.2 , bow tie type tree is shown, Eichhorn [4.4]. Such a tree developed at a void on the surface of the dielectric and grew up along it on both sides.

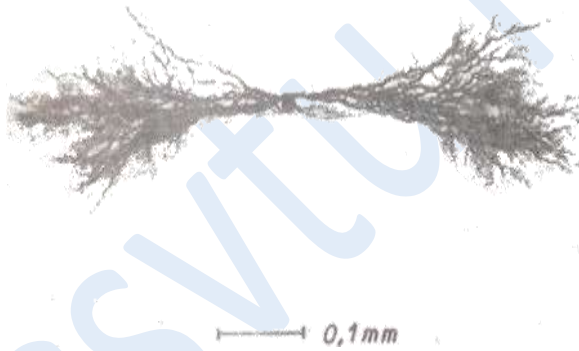


Fig 22.2 A bow tie type tree

XXIII

Objectives

In this lecture you will learn the following

- Development of breakdown in extremely and weakly nonuniform fields
- Time required for breakdown in solids

Requirement of Time for breakdown

Consider a solid dielectric in extremely nonuniform field between needle and plane, as

shown in 23.1(a), applied an alternating field. The field intensity at the tip will be maximum in this electrode configuration if there is no other cause of field distortion present elsewhere in the dielectric. In other words, a local field enhancement will be caused at the tip of the electrode, leading to a favourable condition for the production of free electrons and their acceleration. On increasing the applied voltage when this process acquires certain intensity, the development of a gas filled channel may begin after certain time lag. ut the time required for the first appearance of such a channel be called 'channel appearance' time ' $t_{ch.a}$ '. This is the beginning of the degradation process by treeing in the dielectric. The development of treeing process has been described in the previous section. The time required for the development of a tree upto the opposite electrode ' $t_{ch.d}$ ' may vary considerably in different dielectrics from location to location, depending upon the favourable (or unfavourable for a user) local conditions. As soon as the foremost channel grows upto the opposite electrode, the breakdown takes place. Thus, the time required for breakdown ' t_b ' can be given as the sum of time required for the appearance of the first channel and its development upto the opposite electrode,

$$t_b = t_{ch.a} + t_{ch.d}$$

Practical experience has revealed that in case of extremely nonuniform fields, the time required for the appearance of the first channel ' $t_{ch.a}$ ' is generally very small compared to the time required for the development of a tree upto the opposite electrode ' $t_{ch.d}$ '. In other words, it can be expressed as,

$$t_{ch.d} \gg t_{ch.a} \text{ (in extremely nonuniform fields)}$$

However, in case of weakly nonuniform fields existing between the electrodes, the time-wise development of a breakdown is quite different. As shown in the schematic in Fig.15.1(b), on applying alternating field between sphere and plane in a dielectric, the time required for the appearance of first partial breakdown channel ' $t_{ch.a}$ ' is normally very long compared to the time required for the development of final jump of the breakdown. Almost an abrupt development of breakdown channel takes place in this case, often without any distinct treeing process. Hence,

$$t_{ch.d} \ll t_{ch.a} \text{ (in weakly nonuniform fields)}$$

This phenomenon is explained by the fact that because of higher field intensity which can be generally applied in weakly nonuniform fields, a concentrated treeing process extends itself much faster. Like in gaseous dielectrics, in solids too the complete or global breakdown proceeds with PB leading to treeing process in extremely nonuniform fields. However, in weakly nonuniform field no PB take place, the breakdown channel is formed almost abruptly.

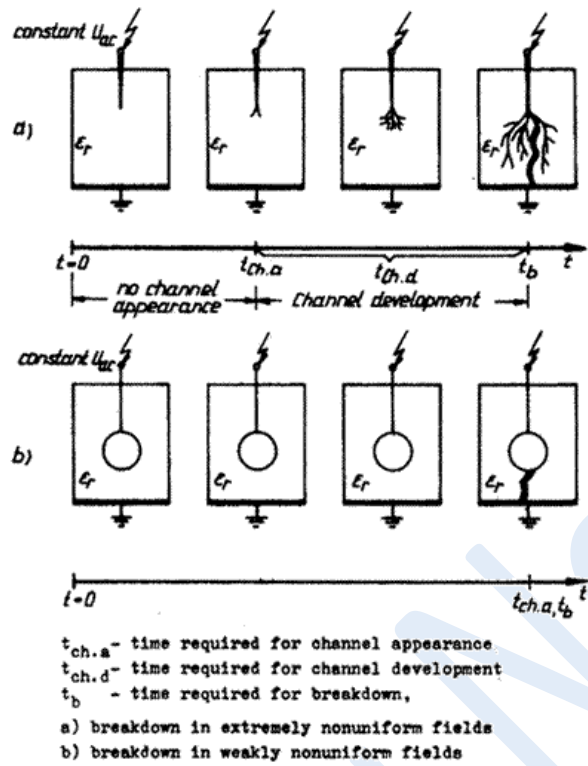


Fig 23.1 Development of breakdown in extremely and weakly nonuniform fields with time.

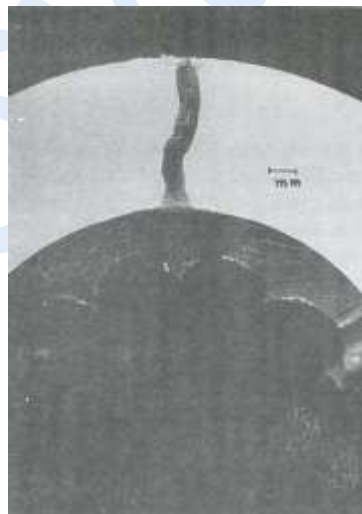


Fig. 23.2 Breakdown channel in coaxial PE cables, Arora [4.7]

Fig 23.2 shows photograph of a breakdown channel in weakly nonuniform field in a 20 kV, coaxial PE cable. A clean breakdown channel appears to have developed abruptly in the

dielectric between the two semiconductive layers without any PB or treeing process.

The time required for breakdown in solid dielectrics strongly depends upon the applied field intensity which in turn depends upon the field configuration. In certain cases, the breakdown process may take even years to develop. This is described as electrical ageing process. On the contrary, it may develop some time abruptly within a very short time.

Module- 5

XXIV

Objectives

In this lecture you will learn the following

- Single Testing Transformer
- Transformers in Cascade
- Advantages and Disadvantage of cascading

Testing Transformers

High Voltage power frequency test transformers are required to produce single phase very high voltages. Their continuous current ratings are very low, usually $\approx 1\text{A}$. Even 1A is a very high current rating. This is because a HV test transformer has to supply only the capacitive charging current to the capacitance formed by the dielectric of the test object. However, since the voltage rating requirements are high, the test transformers are required to be produced with very high insulation level. This increases the size of the test sets tremendously. Hence, single units of test transformers are produced maximum upto 700 kV.

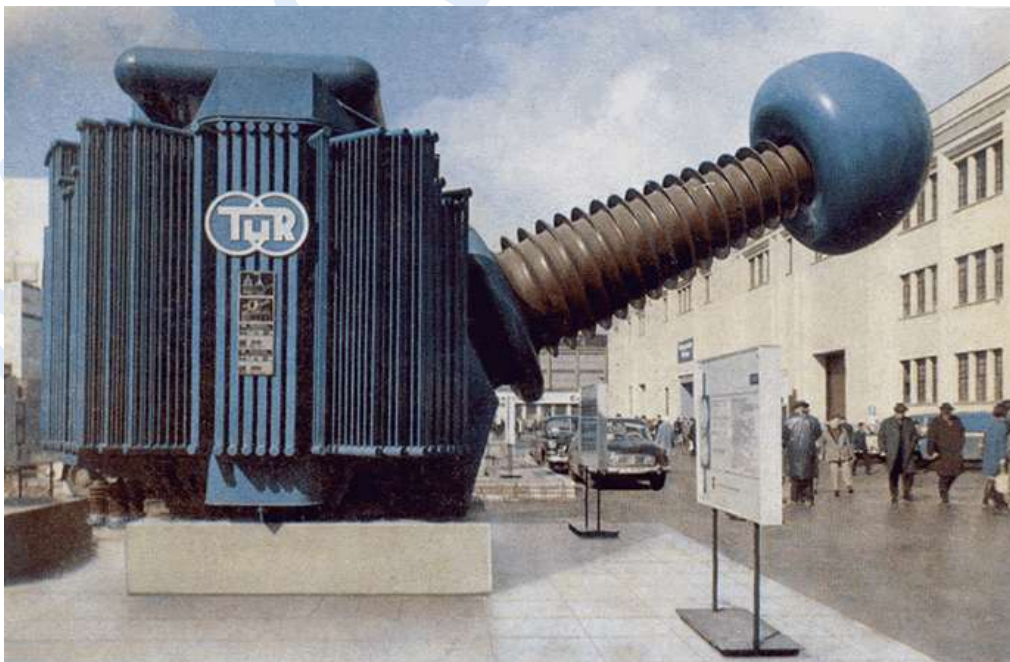


Fig 24.1 A 600 kV, 3.33A Testing Transformer for continuous operation [Courtesy TUR Dresden, Germany]

For the production of higher voltages, a number of identical units are put in cascade to add up their voltages as shown in Fig 24.2.

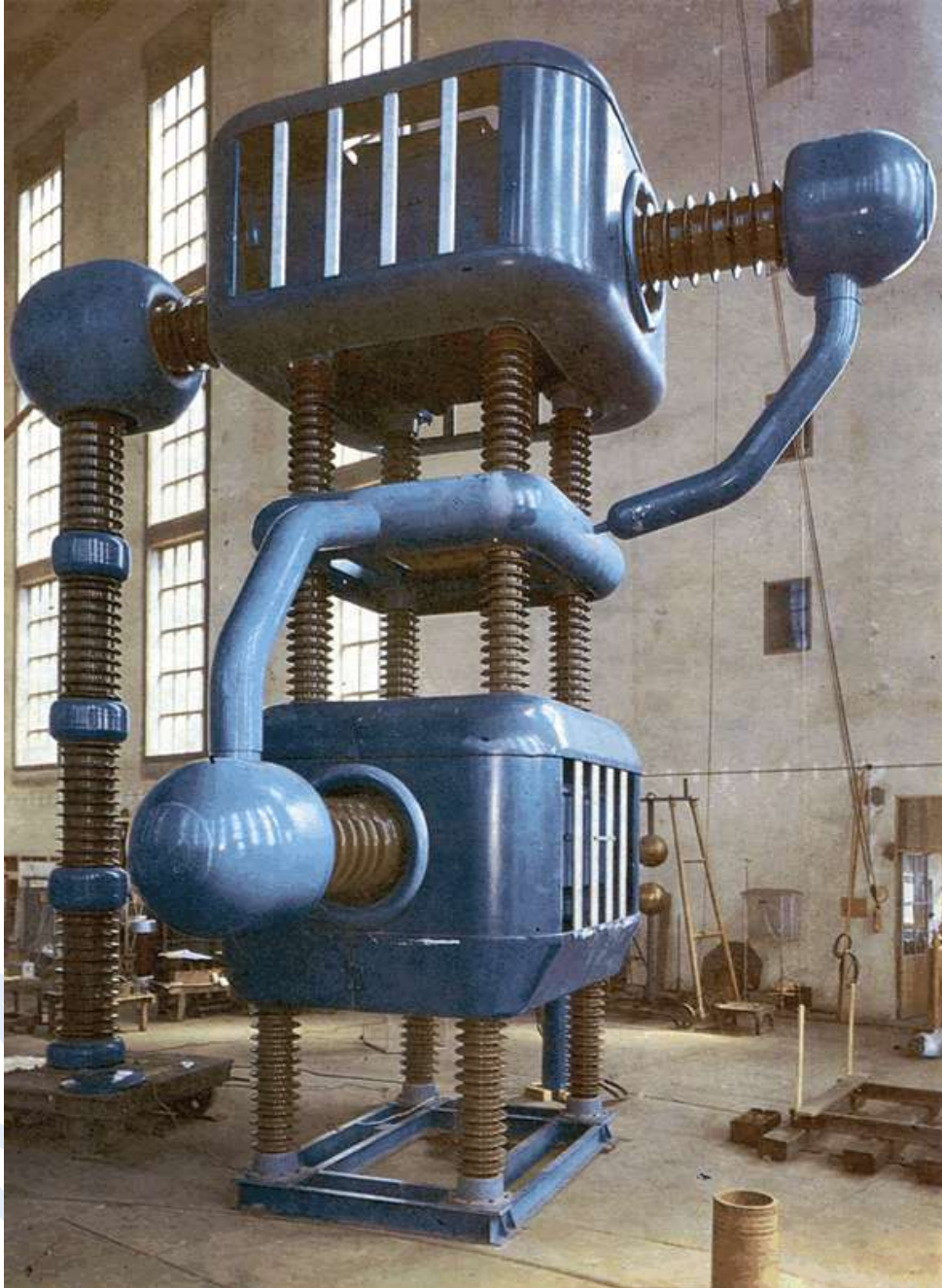


Fig 24.2 A.C. Testing Cascade, 1.2 MV, 1.25 A, short-time operation 4 hours (at an ambient temperature of 35°C). Transformer tanks made of sheet aluminum [TUR Dresden]

Cascaded transformers

- Cascading a number of single identical units makes transportation, production and erection

simpler.

- The cascading principle is illustrated with the basic scheme shown in Fig. 24.3 below in which it can be seen that output of a stage transformer becomes input for the next stage.

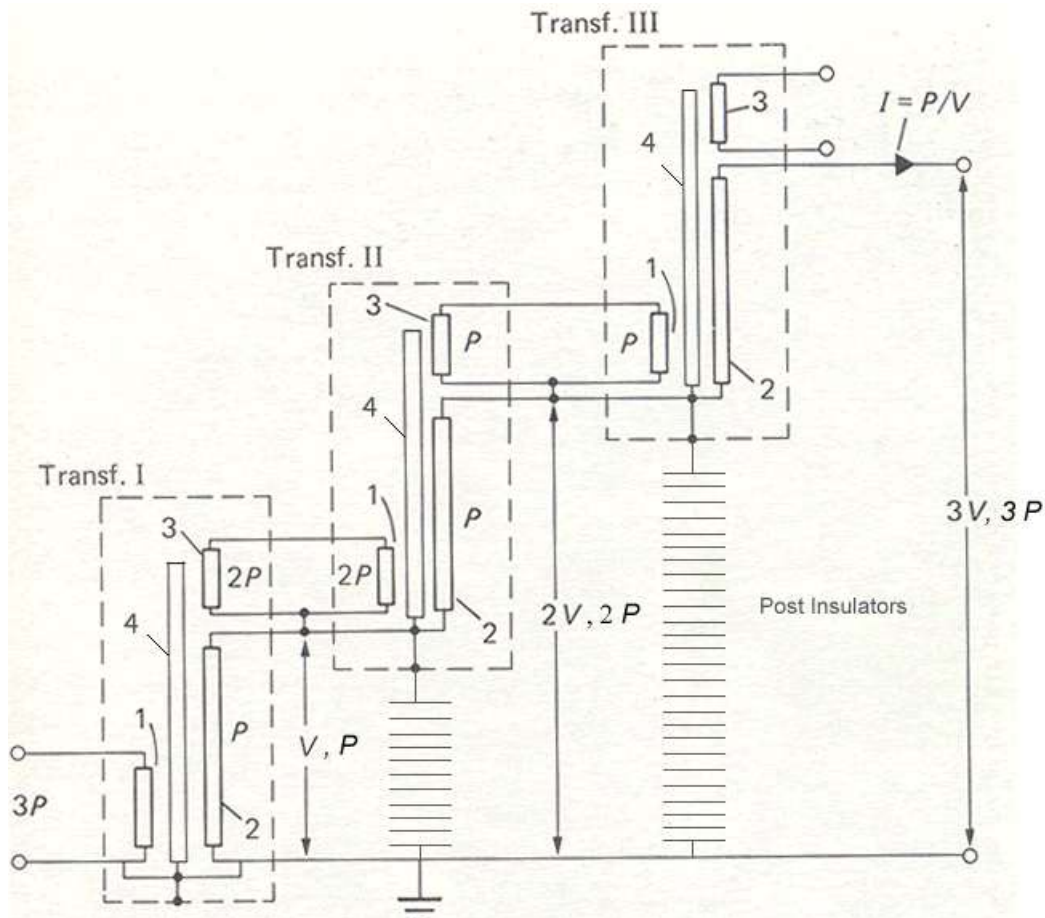


Fig 24.3 Three Transformers in cascade
(1) Primary windings,
(2) Secondary, HV, windings,
(3) Tertiary/ excitation windings (4) Core

- The HV supply is connected to the primary winding "1" of transformer I, designed for a HV output of V . The other two transformers too are connected in the same fashion.
- The excitation winding "3" of Transformer I supplies the primary voltage for the second transformer unit II; both windings are dimensioned for the same low voltage, and the potential gain is fixed to the same value V .
- The HV or secondary windings "2" of both units are connected in series, so that a voltage of $2V$ is produced at the output of 2nd unit. The unit III is added in the same way.
- The tanks or vessels containing the active parts (core and windings) are indicated by dashed lines.
- For a metal tank construction and the HV windings shown in this basic scheme, the core and the tank of each unit would acquire the HV level of the previous unit as indicated. Only

the tank of transformer I is earthed.

- The tanks of transformers II and III are at high potentials, namely V and $2V$ above earth, and must therefore be suitably insulated, hence raised above the ground on solid post insulators.
- Through HV bushings the leads from the excitation windings "3", as well as the tapings of the HV windings "2", are brought to the next transformer.

For voltages higher than about 600 kV, the cascade of such transformers is a big advantage. The weight and the size of the testing set is sub-divided into single units of smaller size and lower weight. The transportation and erection of the test set in cascade becomes simpler. However, there is a disadvantage that the primary windings of the lower stages are more heavily loaded with higher current in such sets.

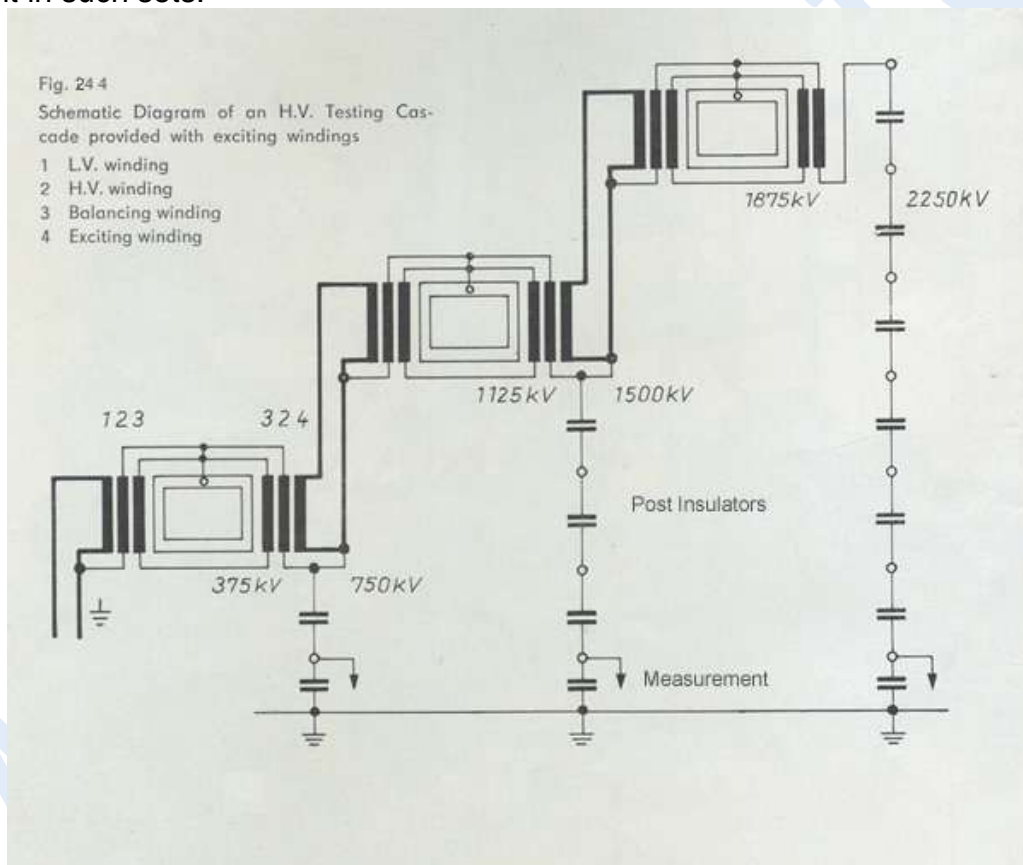


Fig. 24.4 Schematic of an ac test set circuit in cascade

There are several methods of designing the cascade test sets. In Fig. 24.4 schematic diagram of another power frequency test set cascade of $3 \times 750 = 2250$ kV rating is shown. This circuit has a third winding, known as "Balancing Winding". These windings are designed to acquire the intermediate potentials between two stages. In this circuit, the transformers of the upper stages have their excitation windings arranged over the HV windings of the transformers of the lower potential. Fig. 24.5 shows a photograph of this test set installed in open air.

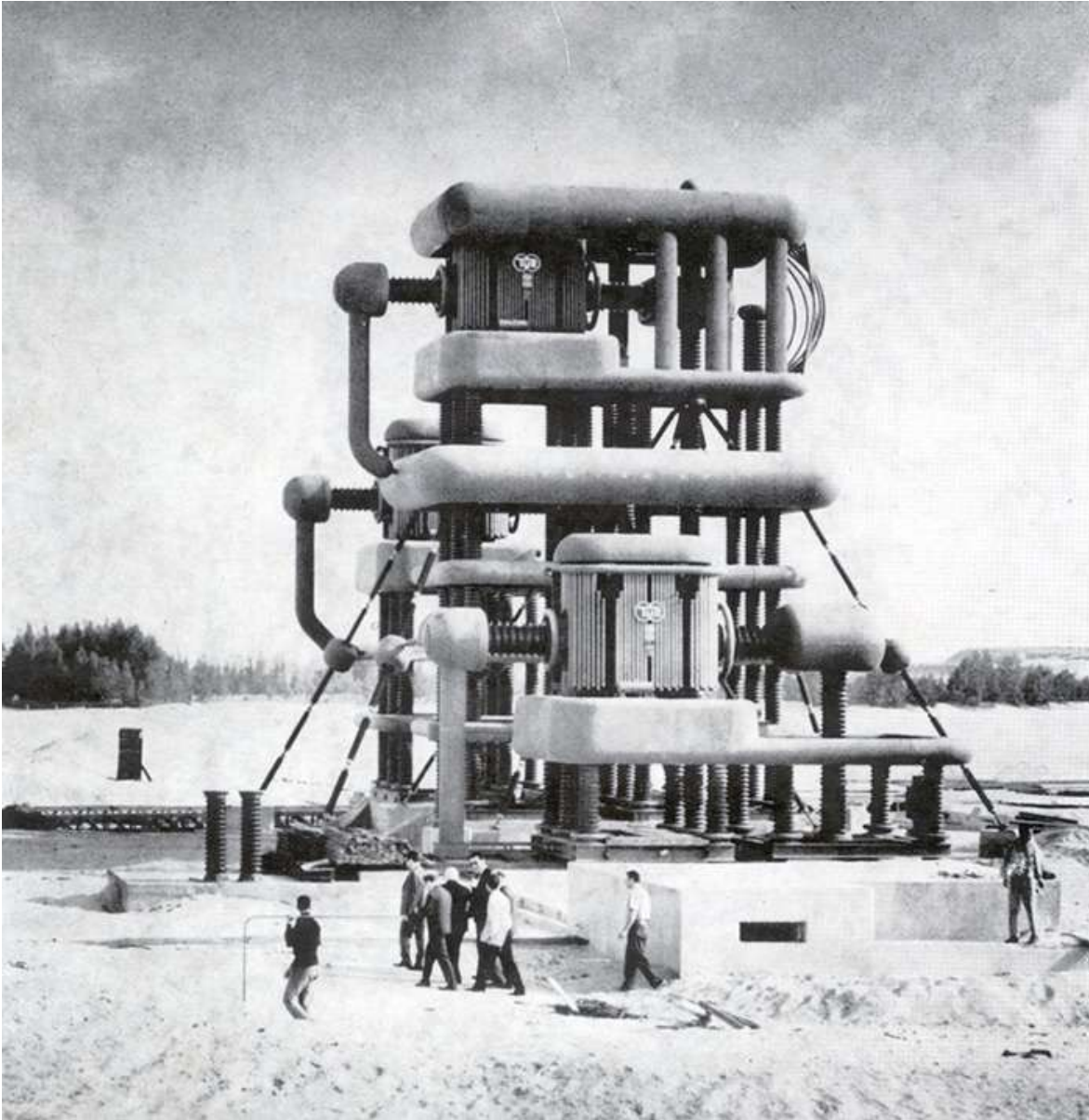


Fig. 24.5 Photograph of an ac test set of 2250 kV, 2250 kVA installed outdoors. People walking on the ground in this photograph gives an idea of the huge size of the test set.

25

Objectives

In this lecture you will learn the following

Tuned Resonant Circuits for HV ac power frequency test equipment

Advantages of the Series Resonant Circuits

Testing of HV equipment having high capacitance, for example, long length of HV power cables, power capacitors, GIS etc. may draw excessive capacitive charging current. Necessity for "Tuned series resonant HV power frequency test equipment" arose in particular by the

cable manufacturing industry when they required to test long lengths of HV cables drawing large capacitive current on the HV side. Fig 25.1 shows such a circuit. The capacitance C_t represents the capacitance of the test object. A variable reactor is connected on the LV (primary) winding of the test transformer. If the inductance of this reactor is tuned to match the impedance of the capacitive load, the capacitive power can be completely compensated. The equivalent circuit diagram for this is a low damped series resonant circuit. The high output voltage can be controlled by a variable ac supply, i.e. a voltage regulator transformer (Feed Transformer) if the circuit was tuned before. The Feed Transformer is rated for the nominal current of the inductor and its voltage rating could be very low.

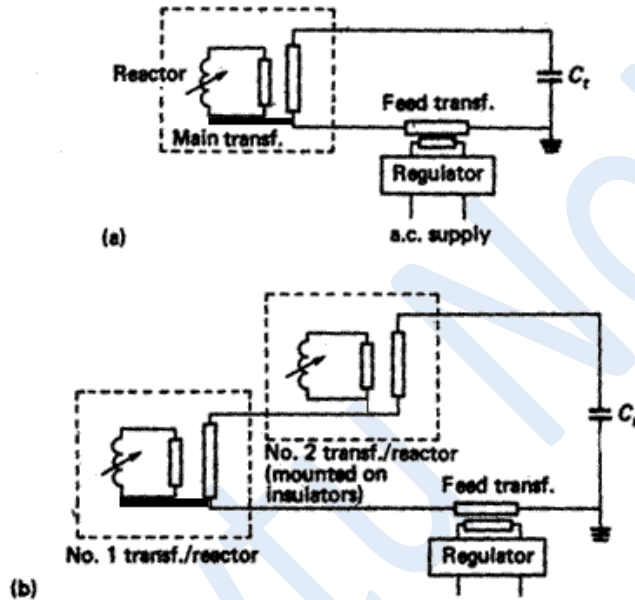


Fig 25.1 Series resonant circuit for transformer/reactor.

- (a) Single transformer/reactor.**
- (b) Two or more units in series.**

For simple high capacitive loads the series resonant circuit, shown in Fig. 25.1 and also in Fig 25.2 (a) are suitable. However, for high capacitance and ohmic loads (loads with high real power losses), the parallel resonant circuit shown in Fig 25.2 (b) is more suitable. Both these series and parallel circuits can be made at the same system by changing the connections of the variable reactor 'L'. Fig 25.3 shows a HV variable reactor which is tuned automatically to the desired value of the capacitive load.

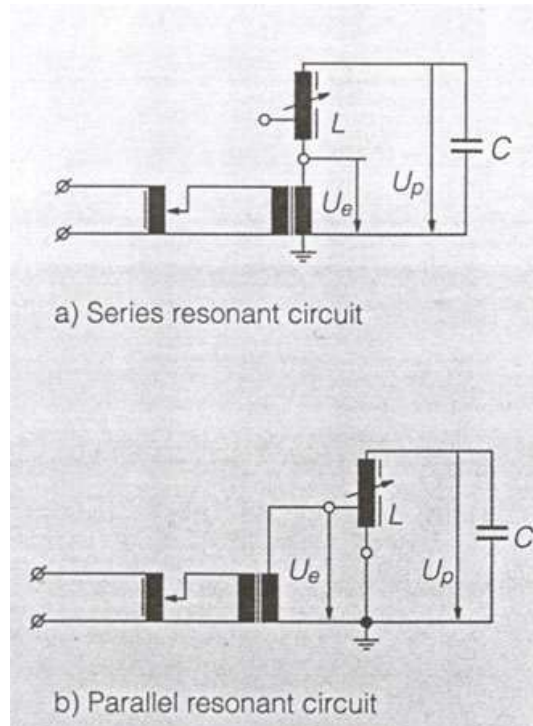


Fig. 25.2 Series and Parallel resonant transformer circuit.

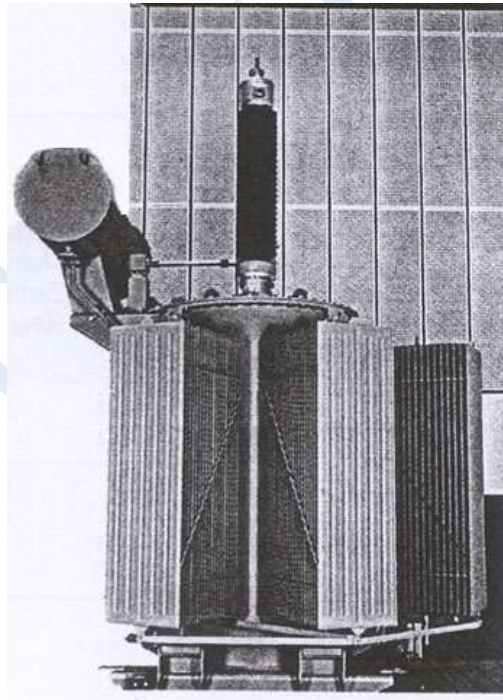


Fig. 25.3 A variable reactor

Advantages of the Series Resonant Circuit

- Dimensions and weight of such test sets are much smaller.
- 100% compensation of capacitive reactive power is possible. Under this condition, the only power drawn from the mains is the active power required.
- The magnitudes of the short circuit currents, in case of insulation failure, are

minimised.

- The voltage wave shape is improved by attenuation of harmonic components already in the power supply. A practical figure for the amplification of the fundamental voltage amplitude at resonance is between 20 and 50 times. Higher harmonic voltages are divided in the series circuit to a decreasing proportion across the capacitive load. Good wave shape helps accurate HV measurement and it is very desirable for Schering Bridge measurements.
- The power required from the supply is lower than the kVA in the main test circuit. It represents only about 5% of the main kVA with a unity power factor.
- If a failure of the test object occurs, no heavy power arc will develop, as only the load capacitance will be discharged under this condition. As the voltage collapses, immediately the load capacitance is short-circuited. This has been of great value to the cable industry where a power arc can sometimes lead to the dangerous explosion of the cable termination. It has also proved invaluable for the development work as the weak part of the test object is not completely destroyed. Additionally, as the arc is self-extinguishing due to this voltage collapse, it is possible to delay the tripping of the supply circuit. This results in a recurring flashover condition with low energy level, making it simpler to observe the path of the flashover in air over the surface of the test object.
- By detuning the resonant circuit, breakdown or disruptive discharge can be achieved.

26

Objectives

In this lecture you will learn the following

High Direct Voltage generation

Basic Halfwave rectifier circuit and Ripple in output voltage

Multistage voltage doubler circuit in cascade

HIGH DIRECT VOLTAGES

- In HV technology direct voltages are mainly used for pure scientific research work and for testing equipment used in HVDC transmission systems. HVDC test sets are also suitable as mobile test units for testing the equipment at site after installation since these are very light weight.
- High dc voltages are even more extensively used in physics (accelerators, electron microscopy, etc.), electromedical equipment (x-rays), industrial applications (precipitation and filtering of exhaust gases in thermal power stations and cement industry; electrostatic painting and powder coating, etc.), or communications electronics (TV; broadcasting stations). Very high static voltages, produced by electrostatic generators, are used in nuclear physics.
- Therefore, the requirements of voltage shape, voltage level, current rating, short - or long-term stability for every HVDC generating system may differ strongly from each other. With the knowledge of fundamental generating principles, it is possible, however, to select proper circuits for any special application.
- The high dc voltages are generally obtained by means of rectifying circuits applied to

ac voltage. Voltage doubler circuits in desired number are then used in cascade for the multiplication of the dc voltage. These are described in the following:

Half Wave rectifier circuit

Shown in the Fig 26.1 is a basic half wave (single phase) rectifier circuit.

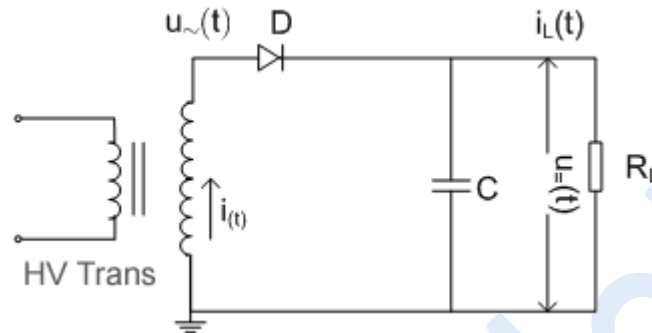


Fig 26.1 Half wave rectifier circuit

where: D - Diode, C - smoothing capacitor, R_L - the resistive load

In Fig 26.2 the voltage output of this circuit is shown

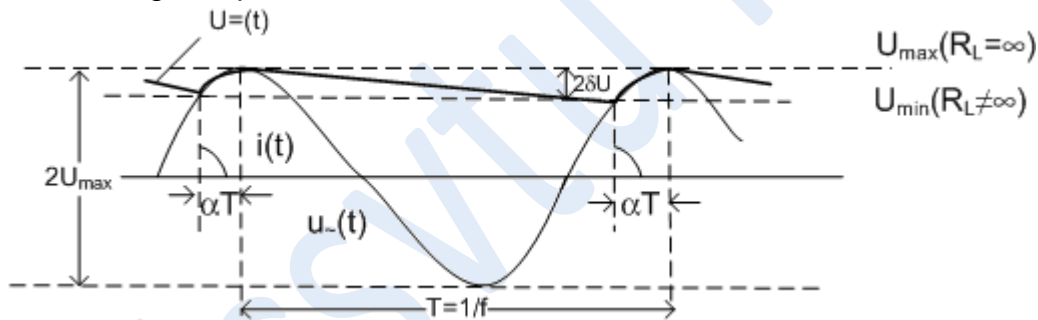


Fig 26.2 Voltages and ripple in the output

As it can be seen, the dc output voltage is not of constant magnitude. The periodic oscillation/deviation from its mean value due to load is known as ripple.

According to IEC 60/1962, the definition of ripple is the periodic deviation from the arithmetic mean value of the dc output voltage of the test set. The magnitude of the ripple is defined as half the difference between the maximum and minimum values of the dc output voltage during one cycle from the generator. The ripple factor is the ratio of the ripple magnitude to the arithmetic value of the dc output voltage.

If \bar{U} is the arithmetic mean value of the dc output, it is given as (defined by IEC and IEEE) following:

$$\bar{U} = \frac{1}{T} \int_0^T u_{dc}(t) dt$$

where T represents the periodic time of oscillation or deviation from the mean value and its

periodic oscillation frequency is given by:

$$T = \frac{1}{f}$$

Let the amplitude of the ripple be δU , then

$$\delta U = 0.5 (U_{\max} - U_{\min})$$

and the ripple factor is given by $\frac{\delta U}{U}$, which should be less than 5% for the dc test voltages.

In the Fig 26.2 above, the time of conduction of the diode t_c is equal to αT . Hence the charge Q transferred to the load R_L is given by:

$$Q = \int_{\alpha T}^T i(t) dt = \int_{\alpha T}^T i_L(t) dt = \frac{1}{R_L} \int_{\alpha T}^T u = (t) dt$$

$$Q = IT = I/f$$

Considering the load current $i_L(t) \approx I$,

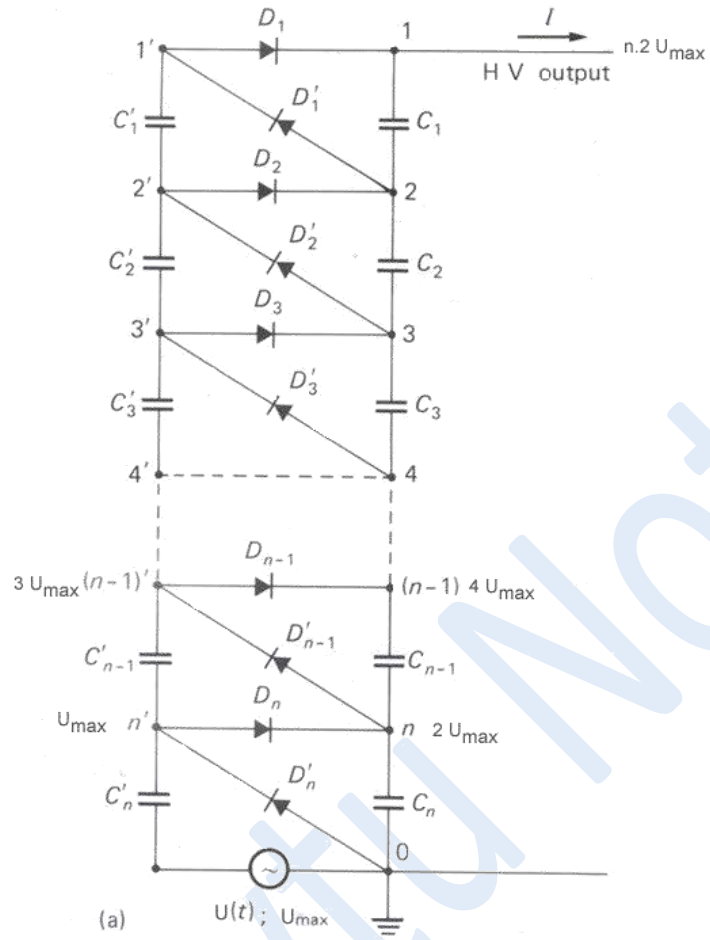
but $Q = 2\delta UC$, therefore $\delta U = \frac{IT}{2C} = \frac{I}{2fC}$

Thus the ripple in the output voltage can be reduced by increasing the frequency of the ac voltage and also by increasing the capacitance of the smoothing capacitor.

$R_L \rightarrow 0$, means failure of the insulation. This condition must be taken in to consideration for the rectifier current while designing the test equipment and smart tripping device should be provided at the transformer input to protect the equipment.

Voltage Doubler Circuit in Cascade

HV dc test sets are produced up to 2.0 MV using halfwave rectifier circuit and voltage multiplier (doubler) circuit in cascade. In 1920 Greinacher proposed such a circuit for the first time which was improved upon by Cockcroft & Walton in 1932. In the Fig. 26.3(a) a n - stage, single phase voltage doubler circuit cascade is shown.



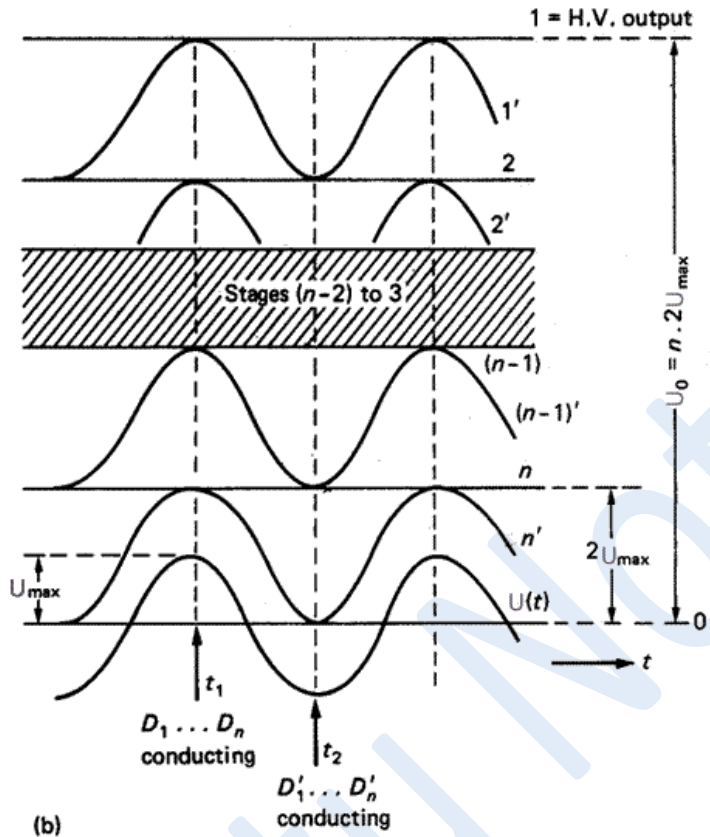


**Fig 26.3 (a) Cascade circuit according to Cockcroft-Walton or Greinacher.
(b) Waveform of potentials at the nodes of cascade circuit, no load.**

Fig 26.3(a) shows a Multi-stage halfwave rectifier voltage doubler circuit in cascade by Cockcroft-Walton.

Considering the load current value to be zero, the steady state potentials at all the nodes of the circuit are shown in Fig 26.3(b). It can be seen that,

- the potentials at the nodes 1', 2'n' oscillate because of the applied ac voltage $U(t)$.
- the potentials at the nodes 1, 2, n remain constant with reference to the ground potential.
- the voltages across all the capacitors are dc, the magnitude of which are $2U_{max}$ except the capacitor C'_n which is stressed with U_{max} only.
- All the rectifier $D_1, D'_1, \dots, D_n, D'_n$ are stressed with $2U_{max}$.
- the HV dc output is of the magnitude $2nU_{max}$

For this multistage cascade, the peak to peak ripple is given by,

$$2\delta U = IT \sum_{i=1}^n \left(\frac{i}{C_i} \right)$$

Since all the diodes D'_1, \dots, D'_n transfer the same charge on the capacitors in the smoothing column the total ripple reduces to

$$\delta U = \frac{I}{2f} \left(\frac{1}{C_1} + \frac{2}{C_2} + \frac{3}{C_3} \dots \frac{n}{C_n} \right)$$

Usually equal capacitance values are provided in each stage as smoothing column hence $C = C_1 = C_2 = \dots C_n$. The above equation can be written as,

$$\delta U = \frac{I}{fC} \cdot \frac{n(n+1)}{4}$$

A photograph of a HVDC Test set of 2000 kV, at 100 mA continuous current rating is shown in Fig 26.4

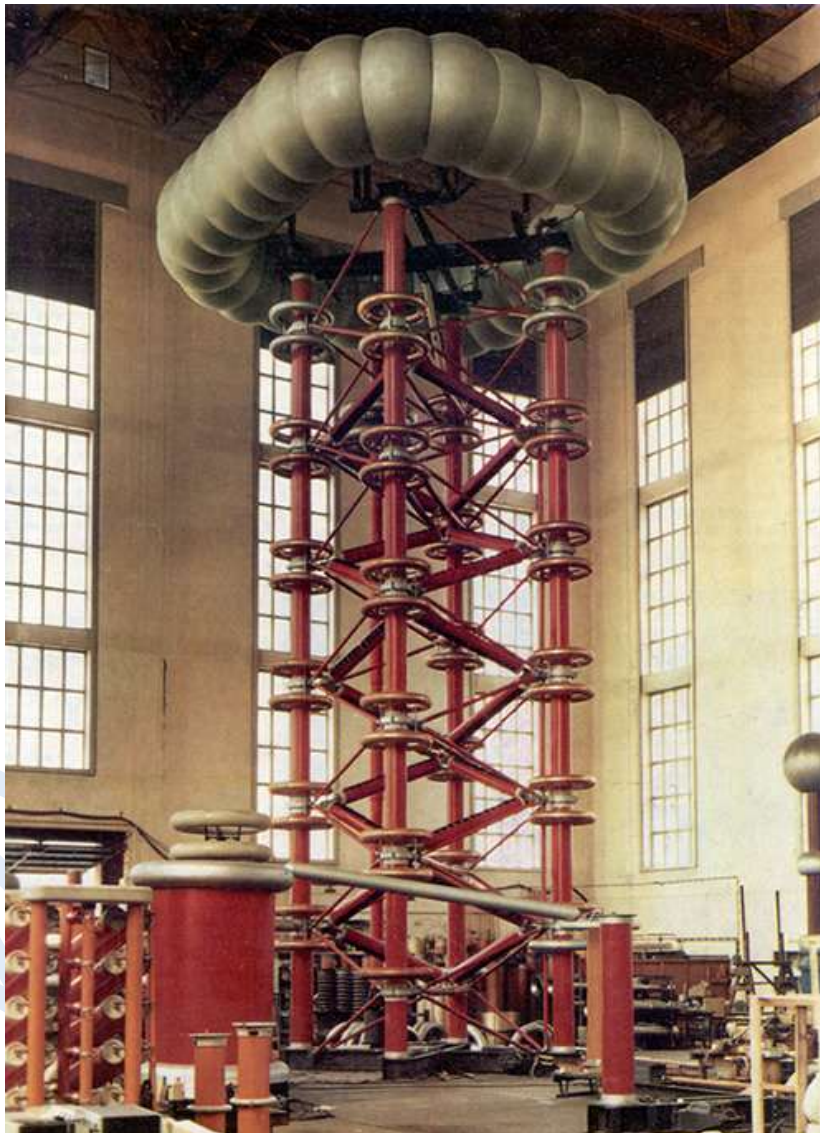


Fig 26.4 2000 kV HVDC Test Set [TUR Dresden]

The dc test set shown in this figure has a ripple factor less than 1% at full load. Such equipment are capable of allowing higher continuous currents at lower voltage output than rated. For instance, the dc generator shown in Fig 26.4 can be used for continuous current

operation of 150 mA at 1900 kV or 200 mA at 1800 kV. These test sets can be operated without external damping resistor as they have a high internal impedance.

27

Objectives

In this lecture you will learn the following

Sources of Transient over voltages in Power System

Standard Lightning and Switching Voltage Wave shapes as specified

Transient over voltages in Power system

Disturbances in electric power transmission and distribution systems are frequently caused by two kinds of transient over voltages. These are two sources of transient over voltage, external and internal, i.e., within the power system. Amplitudes of such transient over voltages may greatly exceed the peak values of the normal ac operating voltage.

External sources of over voltage

The first of this kind of over voltage is lightning over voltage, originated by lightning strokes hitting the phase wires of overhead lines or the bus bars of outdoor substations. The amplitude of lightning (i_l) over voltage depends upon the magnitude of impulse current injected into the power system by the lightning strike and the circuit impedance. If the i_l strikes on a transmission line, the amplitude of the over voltage is equal to $\frac{1}{2} (i_l \text{ current} \times \text{the surge impedance of the line})$ which proceeds as traveling waves in either direction from the point of i_l strike, Fig 27.1.

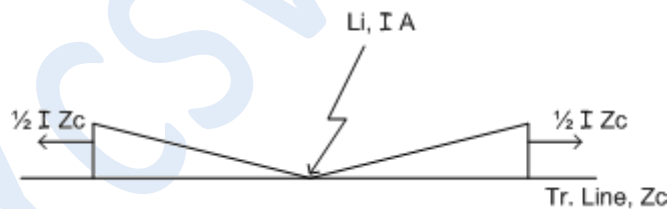


Fig 27.1 Transient over voltage on transmission line

Although the maximum known i_l impulse current injection is of the order of 220 kA, it could be as low as 200 A also. The average value of this current lies between 10 to 15 kA. The surge impedance of transmission lines varies between 250 to 350 Ω . These together determine the magnitude of the transient over voltage due to lightning strike on a transmission line.

The first attenuation of such over voltages is often caused by flash over across the nearest insulator strings on the line. Lightning protection systems, surge arresters and the different kinds of losses in the line damp and distort the traveling wave shapes. Therefore lightning over voltages with very different wave shapes may be present within the transmission

system.

Internal source of over voltage

The second kind of transient over voltage is caused by switching operation in the network, known as 'switching impulse over voltage', si. Normally lagging current flows through a line. When a short circuit occurs, very high magnitude of lagging (inductive) current flows. When a circuit breaker operates (opens) to clear such lagging currents, the voltage impressed across it is greater than the rated voltage of the system. This is because of the energy stored in the inductance of the network which is released when the current stops flowing. The instant energy stored varies with time with the periodic oscillation of the alternating current. Hence, the magnitude of the over voltage impressed across the CB electrodes depends not only upon the value of circuit inductance and the magnitude of current but also upon the instant at which the arc is extinguished. The amplitude of si, also known as switching surge is always related to the operating voltage. Its shape is determined by the impedance of the system as well as by the switching conditions. The rate of rise of switching over voltage transient is usually slower than the li over voltage. However, it is known now that the si wave shape can be very dangerous to insulation systems. With the increasing Basic Insulation Levels (BIL), for 800 kV and above rated voltage level, the lightning overvoltage is not of much significance. However, since the si overvoltage magnitude depends upon the level of the system voltage, these are of much more significant. Fig. 27.2 shows the standard shape of a full lightning impulse voltage as well as a sketch for the same voltage wave chopped at its tail, i.e. interrupted by a disruptive discharge.

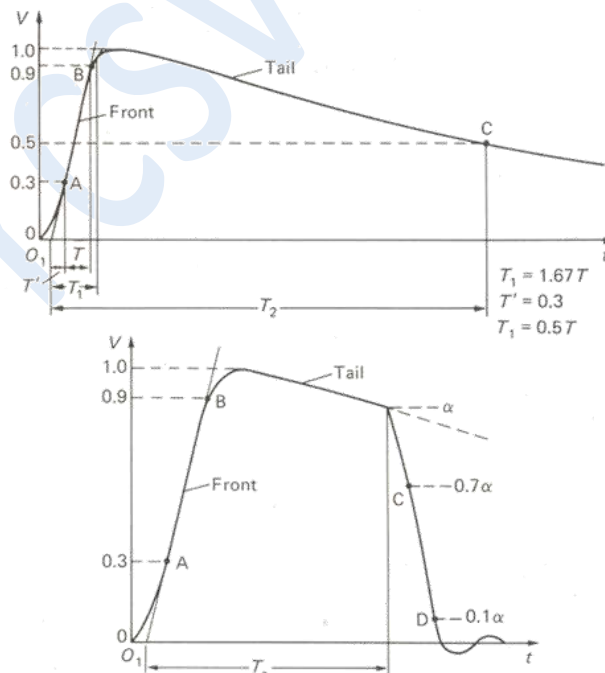


Fig 27.2 General shape and definitions of lightning impulse voltage. (a) Full wave

(b) Wave chopped at its tail.

Although the wave shape is well defined on this diagram, it should be emphasized that the virtual origin O_1 is defined where the line AB cuts the time axis. The specifications permit in general a tolerance upto $\pm 30\%$ for T_1 and $\pm 20\%$ for T_2 . The reason for defining the point A at 30% voltage level is the experience with most of the oscillograms of measured impulse voltages.

The impulse voltage wave shapes are defined by the times T_1 / T_2 . Hence $1/50 \mu s$ is an accepted standard li wave shape. It is quite difficult to obtain a smooth slope within the voltage rise as the measuring systems as well as stray capacitances and inductances may cause oscillations.

Figure 27.3 illustrates the wave shape of one of the standard switching impulse. Impulse wave shapes of $100/2500$, $250/2500$ and $500/2500 \mu s$ are recommended. Permissible tolerance in the case of si for T_{cr} is $\pm 20\%$ and for T_2 it is $\pm 60\%$.

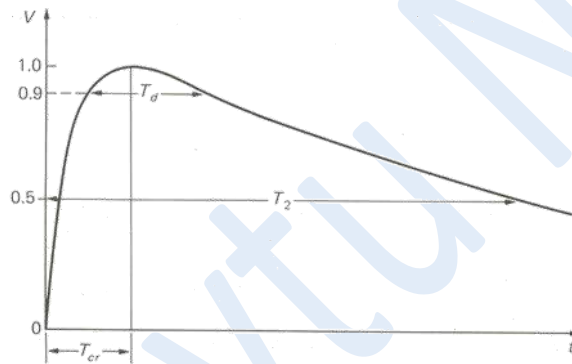


Fig 27.3 General shapes of switching impulse voltages . T_{cr} : Time to crest. T_2 : Virtual time to half value. T_d : Time above 90%.

28

Objectives

In this lecture you will learn the following

- Single-stage Impulse Generator Circuits and their analysis
- Efficiency of these circuits
- Dimensioning of circuit elements for desired wave shapes of the output voltage

Single-stage Generator Circuit

- Two basic circuits for single-stage impulse generator are shown in Fig. 28.1 (a) and (b).

- The capacitor C_1 is charged slowly from a dc source until the spark gap G breakdown and discharges upon C_2 , the load capacitor over the resistors R_1 and R_2 .
- This spark gap acts as a voltage-limiting and voltage sensitive switch.
- An economic limit of the charging voltage U_0 is about 200 to 250 kV. Too large diameter of the identical spheres would otherwise be required to achieve weakly nonuniform field between the spheres for longer gap distances.
- The resistors R_1 , R_2 and the capacitance C_2 form the wave-shaping network. R_1 primarily controls the wave front time T_1 . R_2 over which the capacitor discharges, essentially controls the wavetail time T_2 .
- The capacitance C_2 represents the load, i.e. the object under test as well as all other capacitive elements which are in parallel to the test object (measuring devices; additional load i.e., capacitor to avoid large variations of T_1/T_2 , if the test objects are changed).
- No inductances are assumed so far, and are neglected in the first fundamental analysis, necessary to understand multi-stage generators.
- This approximation is in general permissible, as the inductance of all elements has to be kept as low as possible.
- From the output voltage efficiency point of view, the circuit shown in Fig 20.1(b) is more efficient compared to the circuit in (a). It is because the resistances R_1 and R_2 do not form a voltage dividing system in (b). It is this more efficient circuit which has found wider application. Hence for the analysis, this circuit in Fig 20.1(b) will be considered.

Before starting the analysis, one of the most significant parameter of impulse generators must be described. It is the energy rating of the impulse generator, given by;

$$W = \frac{1}{2} C_1 (U_{0_{\text{max}}})^2 \quad \text{J}$$

(28.1)

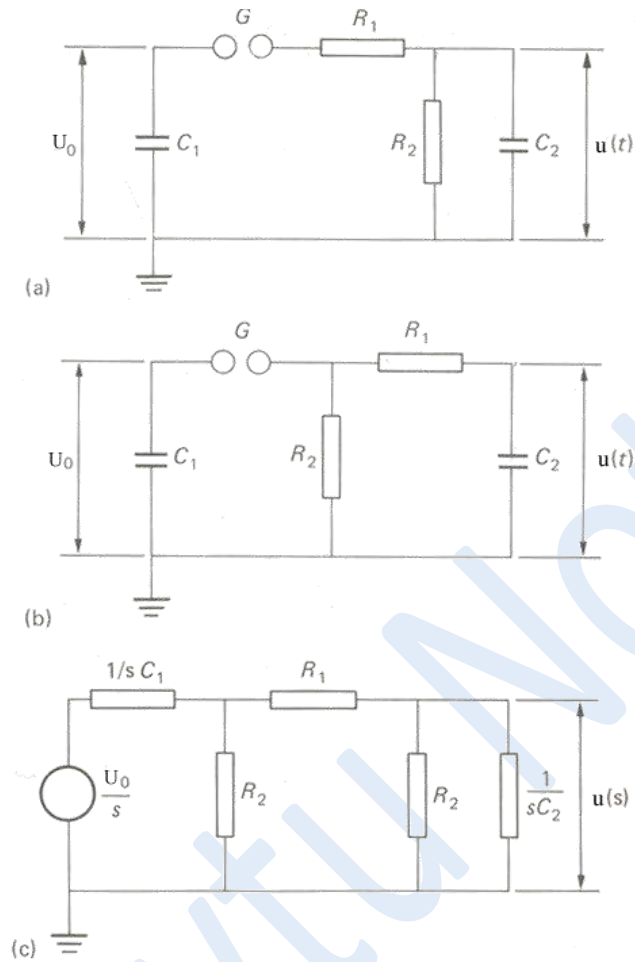


Fig 28.1 Single-stage impulse generator circuits (a) and (b). C_1 : charging capacitor. C_2 : load capacitance. R_1 :Wave front resistance. R_2 : Wave tail resistance. (c) Laplace Transformed circuit.

- C_1 should be always chosen much larger than C_2 , hence it determines the cost of the generator.
- For the analysis we may use the Laplace transform circuit shown in Fig. (28.1(c)) which simulates the boundary condition, that when $t \leq 0$, C_1 is charged to U_0 and for $t > 0$ this capacitor is directly connected to the waveshaping network.
- For the efficient circuit in Fig. 28.1(b), the output voltage is given by,

$$\text{where, } u(s) = \frac{U_0}{s} \frac{Z_2}{Z_1 + Z_2},$$

$$Z_1 = \frac{1}{C_1 s} + R_1;$$

$$Z_2 = \frac{R_2 / C_2 s}{R_2 + 1 / C_2 s}.$$

By substitution we find

$$u(s) = \frac{U_0}{k} \frac{1}{s^2 + as + b}$$

(28.2)

where

$$a = \left(\frac{1}{R_1 C_1} + \frac{1}{R_1 C_2} + \frac{1}{R_2 C_1} \right); \quad (28.3)$$

$$b = \left(\frac{1}{R_1 R_2 C_1 C_2} \right);$$

$$k = R_1 C_2.$$

From the transform tables the following expression in the time domain can be obtained:

$$u(t) = \frac{U_0}{k} \frac{1}{(\alpha_2 - \alpha_1)} [\exp(-\alpha_1 t) - \exp(-\alpha_2 t)]$$

(28.4)

where α_1 and α_2 are the roots of the equation $s^2 + as + b = 0$, or

$$\alpha_1, \alpha_2 = -\frac{a}{2} \mp \sqrt{\left(\frac{a}{2}\right)^2 - b}.$$

(28.5)

- The output voltage $u(t)$ is therefore the superposition of two exponential functions of different signs.
- According to eqn. (28.5), the negative root leads to a larger time constant $1/\alpha_1$ than the positive one, which is $1/\alpha_2$.
- A plot of the expression [eqn. (28.4)] is shown in Fig. 28.2.

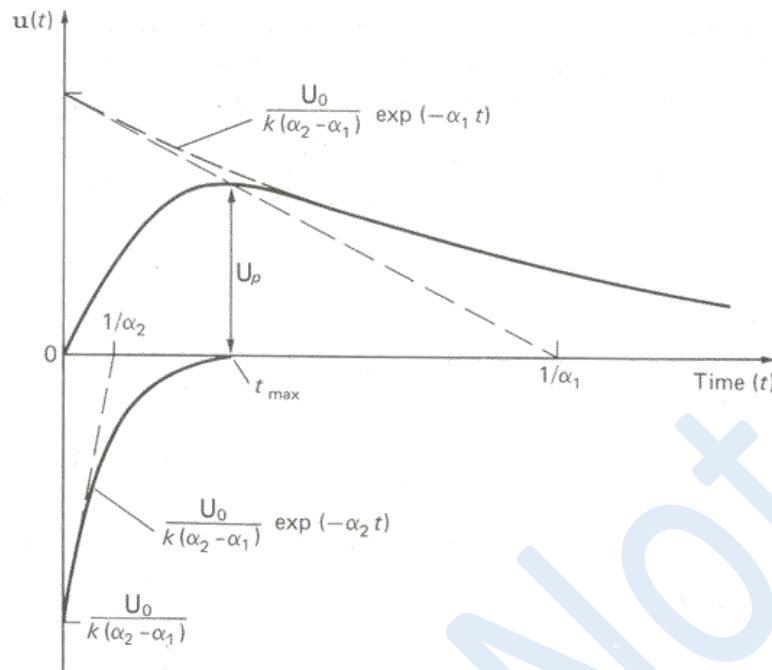


Fig 28.2 The impulse voltage wave components according to the circuit equation

- The voltage efficiency is defined as,

$$\eta = \frac{U_p}{U_0};$$

(28.6)

- U_p , the peak value of the output voltage as indicated in Fig. 28.2. Obviously this value is always smaller than U_0 .
- Time for the voltage $u(t)$ to rise to its peak value can be determined by equating:

$$\frac{d u(t)}{d t} = 0,$$

therefore

$$t_{max} = \frac{\ln(\alpha_2 / \alpha_1)}{(\alpha_2 - \alpha_1)}$$

(28.7)

- Substituting this equation in eqn. (28.4), the efficiency can be found,

$$\eta = \frac{(\alpha_2 / \alpha_1)^{-[\alpha_1 / (\alpha_2 - \alpha_1)]} - (\alpha_2 / \alpha_1)^{-[\alpha_2 / (\alpha_2 - \alpha_1)]}}{k(\alpha_2 - \alpha_1)}$$

(28.8)

- By substitution, the voltage efficiency for the condition $C_2 \ll C_1$ is obtained as;

$$\eta = \frac{C_1}{(C_1 + C_2)} = \frac{1}{1 + (C_1/C_2)} \quad (28.9)$$

- Fig. 28.3 shows the voltage efficiency of the circuit with increasing load capacitance.

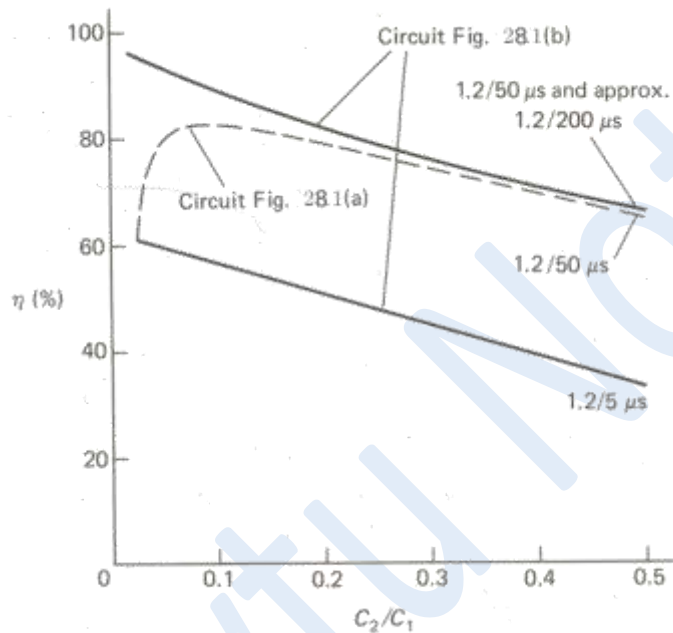


Figure 28.3 Voltage efficiency factor with increasing capacitance ratio C_2/C_1 for lighting impulse.

Dimensioning of the circuit elements:

- It is very important to determine the values of resistors R_1 and R_2 for producing a particular wave shape for known values of C_1 and C_2
- The total load capacitance can easily be measured if it is not known in advance.

For the circuit in Fig. 28.1(b) the values of R_1 and R_2 work out as following,

$$R_1 = \frac{1}{2C_2} \left[\left(\frac{1}{\alpha_1} + \frac{1}{\alpha_2} \right) - \sqrt{\left(\frac{1}{\alpha_1} + \frac{1}{\alpha_2} \right)^2 - \frac{4(C_1 + C_2)}{\alpha_1 \alpha_2 C_1}} \right] \quad (28.10)$$

$$R_2 = \frac{1}{2(C_1 + C_2)} \left[\left(\frac{1}{\alpha_1} + \frac{1}{\alpha_2} \right) + \sqrt{\left(\frac{1}{\alpha_1} + \frac{1}{\alpha_2} \right)^2 - \frac{4(C_1 + C_2)}{\alpha_1 \alpha_2 C_1}} \right] \quad (28.11)$$

- Both these equations contain the time constants $1/\alpha_1$ and $1/\alpha_2$, which depend upon the desired wave shape.
- The values of these time constants are worked out for different shapes, T_1/T_2 , of

the output voltage given by equation 28.4 in the table below.

T_1/T_2 (μsec)	T_{cr}/T_2 (μsec)	$1/\alpha_1$ (μsec)	$1/\alpha_2$ (μsec)
1.2 / 5	-	3.48	0.80
1.2 / 50	-	68.2	0.405
1.2 / 200	-	284	0.381
250/2500	-	2877	104
-	250/2500	3155	62.5

- The nominal values of T_1 and T_2 are difficult to achieve in practice, as even for fixed value of C_1 , the load C_2 may vary for different loads. The exact values for R_1 and R_2 according to eqns. (28.10) and (28.11) are in general not available. These resistors have to be dimensioned for the rated high voltage of the stage.

29

Objectives

In this lecture you will learn the following

- Multistage Impulse Generator Circuit using Efficient circuits
- Methods of Triggering Impulse Generators
- Construction of the triggering device, 'Trigatron'
- Operating characteristics of a Trigatron

Multistage Impulse Generator Circuits

- The difficulties encountered with the requirement of very large size of spheres for the switching of higher voltages, the increase of the physical size of other circuit elements, the problems in obtaining high dc voltage for charging C_1 and, last but not the least, the requirement of corona free structure and leads makes the single stage circuit inconvenient for producing higher voltages.
- In order to overcome these difficulties, in 1923 Marx suggested an arrangement where a number of condensers are charged in parallel over high ohmic resistances and then discharged in series through spark gaps.

A multistage impulse generator, proposed originally by Goodlet, is shown in Fig 29.1. It adopts the efficient circuit discussed earlier.

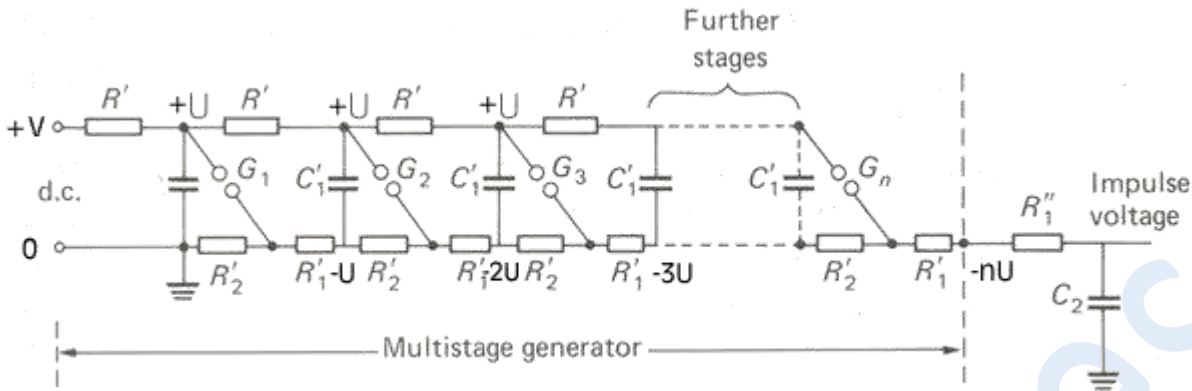


Fig 29.1 Multistage impulse generator with wavetail and front resistors in each stage. R'_2 : stage wavetail resistors, R'_1 : stage wave front resistors, R''_1 : External wave front resistor, R' : Charging resistors

- The charging resistors R' are always large compared with the stage resistors R'_1 and R'_2 , R'_2 is made as small as is necessary for the required wave tail. Adding the external front resistor R''_1 helps to damp oscillations caused by the inductance and capacitance of the connecting leads between the generator and the load, if these leads are long.
- It may be readily seen that this circuit can be reduced to the single-stage impulse generator circuit shown in Fig. 28.1(b). When the generator is fired, or in other words, the stage spark gaps have flash over in sequence, the stage capacitors C'_1 come in series in the complete circuit. Hence the total discharge capacitance C_1 can be determined as:

$$\frac{1}{C_1} = \sum_{i=1}^n \frac{1}{C'_1}; \quad \text{or} \quad C_1 = \frac{1}{n} C'_1$$

and the effective wave front resistance R_1 can be calculated as,

$$R_1 = R'_1 + \sum_{i=1}^n R'_1$$

and the effective wave tail resistance R_2 is given as

$$R_2 = nR'_2 = \sum_{i=1}^n R'_2$$

where n is the number of stages.

- For this circuit, the wave front resistors R'_1 do not contribute to the discharge process of the main capacitors C'_1 . The current through R'_2 does not flow through R'_1 and hence does not reduce the initial generator output voltage, the wave front magnitude of the voltage.

In a multistage impulse generator; it is desired that triggering or flashover takes place first at the stage No. 1 and then in sequence at the higher number stages. Hence, the gap distance setting requirement is such that the gap distance set at stage one is smallest and the gap distances in higher stages are in increasing order by a small

difference.

There are three ways of triggering an impulse generator;

1. Fix the gap distance between the spheres and increase the stage applied dc voltage till the flashover occurs.
2. Set the gap distance between the spheres large enough, apply a desired voltage across them and then reduce the gap distance till flashover takes place.
3. Fix both, the desired stage voltage and corresponding gap distance within prescribed limits (Fig. 29.3). Then apply the trigger pulse to the trigatron on the first stage.

The third method is widely practiced since this is the only method to get impulses of exact desired magnitude repeatedly, Fig. 29.2.

A device, known as "Trigatron", is used to control the flash over at the spark gaps in order to get a desired magnitude of the output voltage repeatedly.

- "Trigatron", consists essentially of three-electrodes.
- The main electrode - indicated as HV and the earthed electrode are equal size spherical electrodes in the first stage of the generator.
- A small hole, drilled in the earthed electrode, holds a metal rod through it inside with the help of a bushing. The annular gap formed between the rod and the surrounding sphere is typically about 1 mm.
- The metal rod, or the trigger electrode forms third electrode, is essentially at the same potential as the sphere since it is connected to it over a high resistance R . The control or trigger pulse is applied between these two electrodes on the rod.
- For this special arrangement, a glass tube is fitted over the rod and it is surrounded by a metal foil connected to the main electrode at the ground potential.
- The function of this glass tube is to produce corona or surface discharges around the rod. The surface discharge or corona causes photoionization in the pilot gap on applying an impulse voltage to the rod. Due to photoionization enough initiatory electrons are made available in the annular gap which breakdown without appreciable time delay consistently at a given voltage across the gap 'd'.

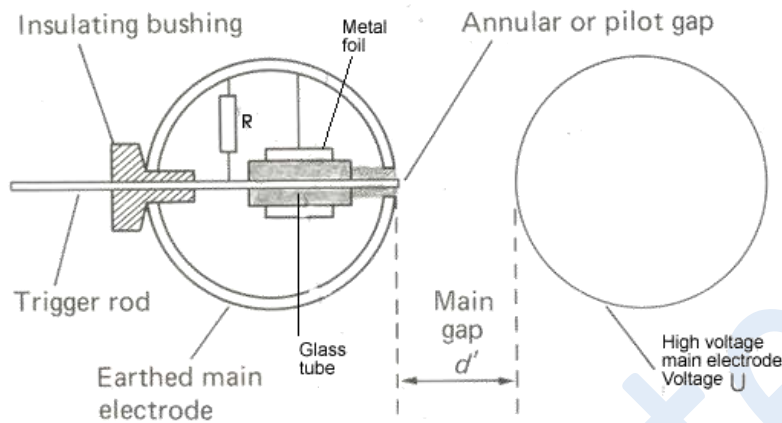


FIG. 29.2 The Trigratron spark gap.

- Thus a surface discharge is caused by the triggering pulse.
- If a voltage U is applied across the main gap, which is not too low but always lower than the peak voltage at which self-firing-i.e. the breakdown in the absence of any trigger pulse-occurs, this main gap will breakdown at a voltage even appreciably lower than the self-firing voltage, if a tripping pulse is applied.
- The Trigratron requires a pulse of some kilovolts, typically ≤ 10 kV, and the tripping pulse should have a steep front with steepness ≈ 0.5 kV/nsec to keep the jitter of the breakdown as small as possible.
- The essential operating characteristic of a Trigratron refers to the voltage operating limits at which a steady operation or triggering is possible. Such characteristics are sketched in Fig. 29.23 where the operating voltage U , the voltage limits across the main gap, are shown for increasing gap distance d .

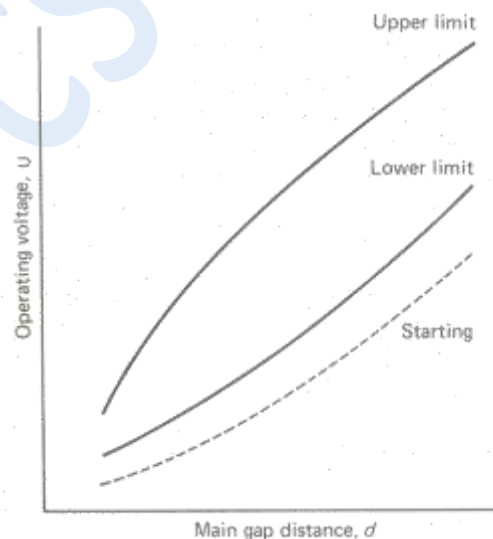


FIG. 29.3 Schematic of functional characteristics of a Trigratron

Objectives

In this lecture you will learn the following

- High voltage measurement techniques
- Chubb-Fortescue Method
- Peak value measurement

High test voltages generated in laboratories require special techniques for their measurement. Each type of high voltage namely; ac (\sim), dc ($=$) and impulse (\wedge) can be suitably measured with more than one different techniques. The choice of the method of measurement in a laboratory is a matter of convenience, cost and the accuracy required for the measurement besides the safety. The complications in measurements increase with the magnitude of the voltage desired to be measured. The problems confine mainly with respect to the large structures of the device and the electric stress control techniques applied to prevent PB and flash overs.

The high voltage measurement techniques in electric power systems are different. These are not discussed in this course.

Different measurement techniques adopted for the three different types of voltages are given in Table 30.1

As it can be seen in this table, the earliest technique of sphere gap and the modern and most accurate technique of potential divider are applicable for the measurement of all the three types of voltages and both their polarities. The sphere gap technique, used widely for over a century, is not used any more. The disadvantages of this method are many. It does not provide a continuous measurement of the voltage and a flashover between the two spheres is essential. This measurement technique is not an accurate one. It may give error upto 3% in the measurement.

The electrostatic voltmeter, suitable for the measurement of ac (rms) and dc voltages, is one of the most accurate instrument. However, due to its size, cost and adjustment problems, it is not used very widely. For the measurement of ac power frequency voltage, the simplest way is to measure the voltage on the primary side or at the low voltage side of the ac test transformer and calibrate the dial of the low voltage voltmeter by multiplication of the turns ratio to get the high output voltage. However, this technique could give rise error in two ways. First, in case of high capacitive loads, the leading current output from the test transformer results in higher actual voltage output than measured with the help of turns ratio at the primary side, the well known Ferranti effect as shown in Fig. 30.1. Secondly, if the output voltage is not perfectly sinusoidal, the peak value is not $\sqrt{2}$ times the rms value. To overcome this problem, measurement of peak value of the output voltage at the high voltage side is recommended.

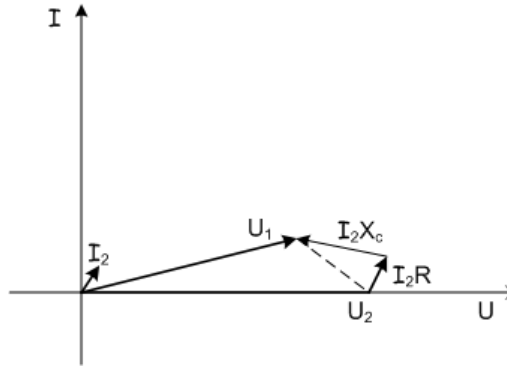


Fig. 30.1 Phaser diagram of the output voltage with leading (capacitive) current

Table 30.1 High Test Voltage Measurement Techniques

Type of Voltage	Method or Technique
ac power frequency	(i) Primary or low voltage measurement (rms)
	(ii) Sphere gap (peak)
	(iii) Electrostatic voltmeter (rms)
	(iv) Series impedance and ammeter
	(v) Potential dividers and oscilloscope (resistive, capacitive or mixed)
	(vi) Peak voltmeters with dividers
dc voltages	(i) Sphere gap, either polarity
	(ii) Series resistance and microammeter
	(iii) Resistive potential divider
Impulse voltages (li & si) either polarity and other high frequency high voltages	(i) Sphere gap
	(ii) potential dividers, oscilloscope (capacitive, resistive & capacitive)
	(iii) Peak voltmeters with series capacitors and potential dividers

Global Breakdown or rupture of insulation properties of dielectrics in general take place at the peak of the voltage applied. The power frequency ac voltage may not always have perfect sinusoidal waveform, the dc output voltage may have ripple and for the impulse voltage the peak is significant. Hence, the measurement of peak magnitude of these voltages is therefore of great importance.

Chubb-Fortescue Method

The most simple yet accurate method for the measurement of peak values of ac power frequency voltage was proposed by Chubb and Fortescue in 1913. The circuit diagram for this method is shown in Fig. 30.2.

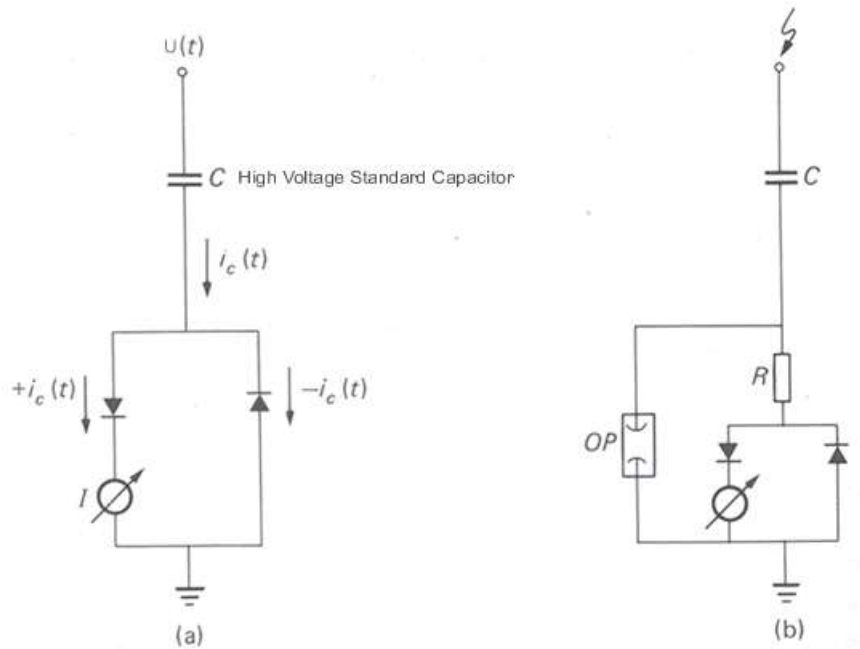


Fig 30.2 ac peak voltage measurement by Chubb and Fortescue. (a) Fundamental circuit. (b) Recommended, actual circuit.

The measuring instrument in this circuit, an ammeter, reads the magnitude of charge per cycle or the mean value of the current

$$i_c(t) = C \frac{dU}{dt}$$

hence,

$$I = \frac{1}{T} \int_{t_1}^{t_2} i_c(t) dt = \frac{C}{T} \int_{t_1}^{t_2} dU = \frac{C}{T} (|U_{+max}| + |U_{-max}|)$$

(30.1)

the limits of integration are shown in Fig. 30.3

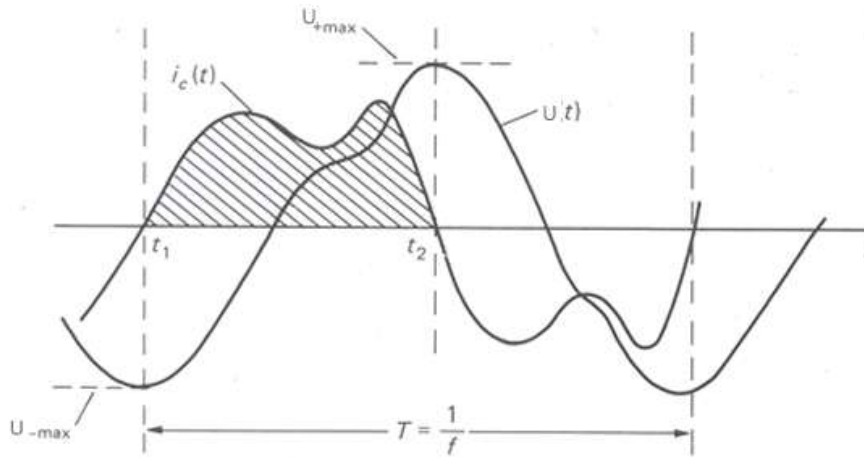


Fig. 30.3 Diagram of voltage $U(t)$ and current $i_c(t)$ from circuit Fig. 30.2(a)

If both, the +ve and -ve, peak values are equal, the expression for the charging current of the HV capacitor can be written as,

$$I = C f U_{p-p} = 2C f V_{max}$$

(30.2)

With knowledge of exact value of f and C , the value of dc current measured gives $2U_{max}$, the actual peak to peak value of the ac voltage.

Peak value measurement

A number of rectifier circuits have been proposed for the measurement of peak value of ac power frequency and impulse voltages to work with capacitive voltage dividers. The first circuit of its kind was proposed by Davis, Bowdler and Stranding in 1930, shown in Fig 30.4

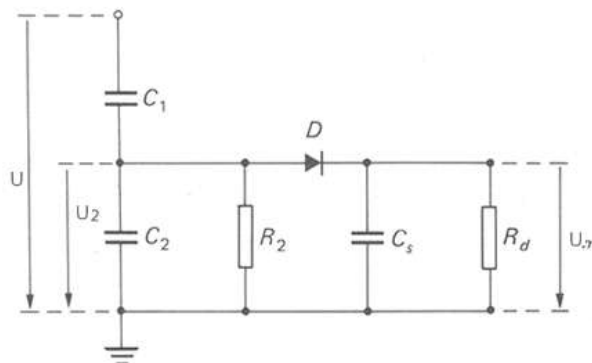


Fig . 30.4 (a) Simple crest voltmeter for ac measurement, according to Davis, Bowdler and Stranding

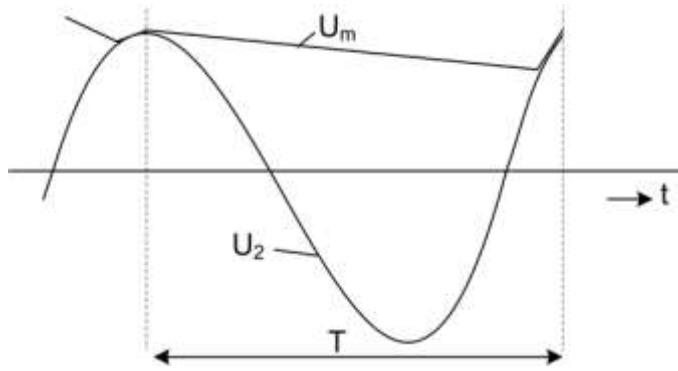


Fig. 30.4 (b)

In this circuit, the measuring capacitors C_m is charged to the peak value \hat{U}_2 , the lower arm voltage of the capacitive voltage divider. If U_2 is decreased, C_m will hold the charge and the voltage across it will not change. Because of the reverse bias current of the diode, there is a danger that U_2 will gain negative dc component over the time. Hence U_m will no longer follow the change in U_2 . Therefore, discharge resistors R_2 and R_d must be included in this circuit. The time constant $R_d C_m$ should be between 0.5 - 1 sec to obtain a good response. When the circuit response conditions are taken care, the peak value of the voltage to be measured is given by the relation

$$\hat{U}_1 = \frac{C_1 + C_2}{C_1} \hat{U}_m$$

31

Objectives

In this lecture you will learn the following

The method of measurement of voltage with the help of Sphere Gap

Construction of Sphere Gap

Effects of earthed objects and atmospheric conditions on the accuracy of measurement

Sphere Gap

This is one of the oldest technique adopted for the measurement of all the types (dc, ac and impulse) high voltages of either polarity. It remained the most widely used method for decades. The field between two identical spheres is a classical example of "weakly nonuniform" field. The breakdown characteristic of such a gap is linear for the gap distances not greater than the radius of the spheres. Measurement voltage is made as a function of minimum distance at which it can flash over or sparkover. The breakdown voltage of the gap does not depend upon the duration of application of voltage and also not upon its variation with time.

Construction of the Sphere Gap

A sphere gap consists of two adjacent metal spheres of equal diameters whose separation gap distance is variable. The ability to respond to peak values of impulse voltages, if the time to peak is not too short ($\approx 1-3 \mu\text{sec}$), is governed by a short statistical time lag or the delay in time required for the availability of an electron to initiate an electron avalanche and hence the breakdown.

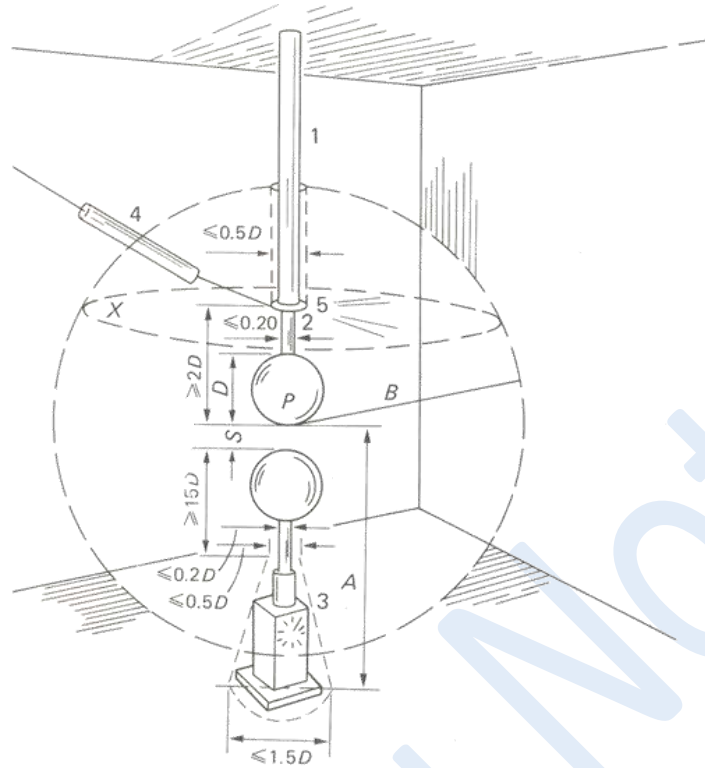


Fig 31.1 Vertical sphere gap. 1. Insulating support. 2. Sphere shank. 3. Opening gear, showing maximum dimensions. 4. High-voltage connection with series resistor. 5. Stress distributor, showing maximum dimensions. P. Sparking point of .v. sphere. A. Height of P above ground plane. B. Radius of space free from external structures. X. Item 4 not to pass throughg this plane within a distance B from P. Note: This figure is drwan to scale for a 100-cm sphere for gap spacing equal to their radius.

- Within the limited gap distance between the spheres, a weakly nonuniform field exists, hence no PB or corona appear before the complete breakdown or flashover.
- For a given dimension of the diameter/radius of the spheres and a gap distance between them, the magnitude of the voltage at which the breakdown occurred is read from the standard calibrated tables available for different types of voltages and for both their polarities.
- The inaccuracy of measurement of voltage by this method is about 3%.



Fig 31.2 Sphere gap in a HV Laboratory

- The accuracy to measurement of voltage with sphere gap is considerably affected by earthed objects around the gap since they form stray capacitance.

Correction Factor

- Since in general the actual air density during measurements differ from the reference conditions, the breakdown voltage of the air gap is given as

$$U_b = k_d U_{b0}$$

where U_{b0} corresponds to the table values and k_d is a correction factor related to air density.

- The actual relative air density (RAD) is given in general terms by

$$\delta = \frac{p}{p_0} \frac{273+t_0}{273+t} = \frac{p}{p_0} \cdot \frac{T_0}{T}$$

where

p_0 = air pressure for standard conditions

p = air pressure at the test conditions

t_0 = 20 °C

t = temperature in °C at the test conditions.

- The correction factor k_d , given in table below for increasing values of RAD are slightly non linearly. However, it can be seen from the table that the correction factor k_d is almost equal to RAD, δ .

Table 31.1 Air density correction factor

Relative air density RAD, δ	Correction factor k_d
------------------------------------	-------------------------

0.70	0.72
0.75	0.77
0.80	0.82
0.85	0.86
0.90	0.91
0.95	0.95
1.00	1.00
1.05	1.05
1.10	1.09
1.15	1.13

Disadvantages:

- For the measurement, breakdown in the gap has to take place.
- Continuous measurement of the voltage is not possible.
- This method is not very accurate.

32

Objectives

In this lecture you will learn the following

Principle of measurement of voltage by Electrostatic Voltmeters
Construction of Electrostatic Voltmetres

Electrostatic Voltmeters

- Electrostatic Voltmeters produced upto 1000 kV rated voltage are suitable for the measurement of ac power frequency and also for higher frequency rms voltages. They can also measure dc voltages.
- For higher voltage range compact voltmeters with SF₆ gas or vacuum insulation gap are also produced.
- These voltmeters were suggested by Kelvin in 1884 for the measurement of rms value of power frequency voltage. They are developed to follow the Coulomb's law which defines the static electric field as a field of force.
- The field produced between two parallel plate electrodes with shaped profile brims, is a uniform field.
- If the voltage applied across these parallel plates having a gap distance 'd' is U, then the uniform field produced in the gap between them will have an intensity E equal to U/d.
- The attracting force F between the plates on area A of the electrodes is equal to the rate of change of stored electrical energy W_{el} per unit distance in the capacitance formed between the plates.

Therefore

$$F = -\frac{\partial W_{el}}{\partial d}$$

or

$$|F| = \frac{dW_{el}}{dd} = \frac{d}{dd} \left(\frac{1}{2} CU^2 \right)$$

$$= \frac{1}{2} U^2 \frac{dC}{dd} = \frac{1}{2} U^2 \epsilon_0 \frac{d}{dd} \left(\frac{A}{d} \right) \quad (\text{since } \epsilon_r = 1)$$

$$= \frac{1}{2} \epsilon_0 U^2 \cdot \frac{A}{d^2}$$

or

$$|F| = \frac{1}{2} \epsilon_0 AE^2$$

(32.1)

Where $\epsilon =$ permittivity of the insulating medium
 $d =$ gap distance between the parallel plate electrodes of area A .

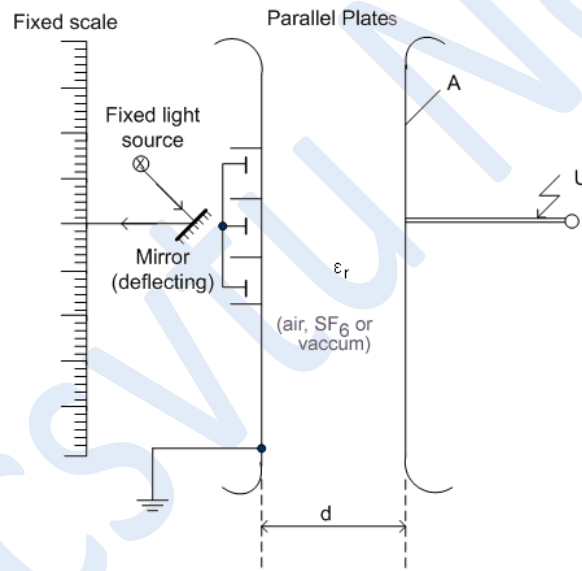


Fig 32.1 Schematic of an Electrostatic Voltmeter

- The attracting force is always positive independent of the polarity of the voltage. If the voltage is not constant, the force is also time (frequency) dependent. Then the mean value of the force is used to measure the rms value of the voltage. Thus

$$\frac{1}{T} \int_0^T F(t) dt = \frac{\epsilon_0 A}{2d^2} \cdot \frac{1}{T} \int_0^T u^2(t) dt = \frac{\epsilon_0 A}{2d^2} (U_{rms})^2$$

(32.2)

where T is a proper integration time.

- Electrostatic voltmeters are arranged such that one of the electrodes or a part of it is allowed to move.

- Thus electrostatic voltmeters are rms indicating instruments if the force integration and its display follows eqn-32.2.
- Various voltmeters developed differ in their use of different methods of restoring forces required to balance the electrostatic attraction. This can be achieved by suspension of the moving electrode on one arm of a balance or its suspension on a spring or the use of a pendulous or torsional suspension.
- The small movement is generally transmitted and amplified by a spot light and mirror system, but many other systems have also been used.
- The electrostatic measuring device can be used for absolute voltage measurements since the calibration can be made in terms of the fundamental quantities of the gap length and forces.
- For a constant electrode separation 'd' the integrated forces increase with $(U_{rms})^2$ and thus the sensitivity of the system for low ranges of the rated voltages of the instrument is small. This disadvantage is overcome, however by varying the gap length in appropriate steps.
- The high pressure gas or even high vacuum between the electrodes provide very high resistivity, therefore the low active power loss.
- The measurement of voltages lower than about 50V is , however not possible as the forces become too small.
- The load inductance and the electrode system capacitance, however, form a series resonant circuit which must be damped, thus limiting the frequency range.
- Sectional view of a 1000 kV standard electrostatic voltmeter using SF₆ gas is shown below in Fig. 32.2

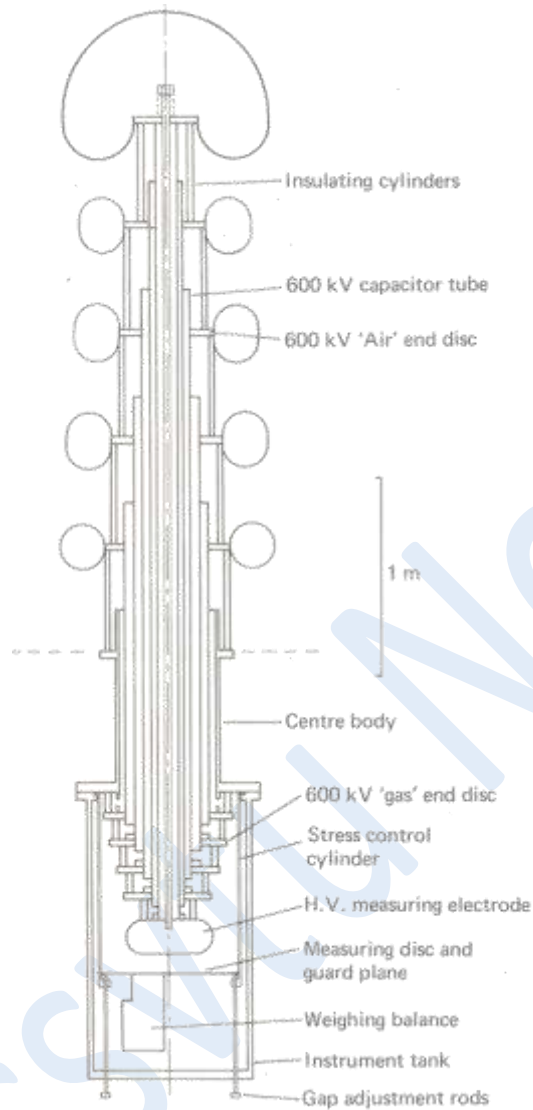


Fig 32.2 Sectional view of 1000-kV electrostatic voltmeter

- A five section capacitor and oil insulated bushing is used to bring the extremely high voltage into the instrument metal tank, filled with pressurized SF_6
- The HV electrode and earthed plane provide uniform electric fields in the region of the 5 cm diameter disc set in a 65 cm diameter guard plane.
- The measurement accuracy of this instrument is of the order of 0.1%.

Objectives

In this lecture you will learn the following

Principle of Potential Dividers

Types of potential dividers

Principle of Potential Dividers

For the measurement of High Voltages of any type, the best technique is by dividing the voltage. The HV potential divider arms could be pure capacitive, pure resistive or a combination of the two. The essential requirement is that the wave shape to be measured is correctly reproduced on the oscillograph with a known voltage reduction ratio. The general potential divider technique is shown in the following Figure 33.1.

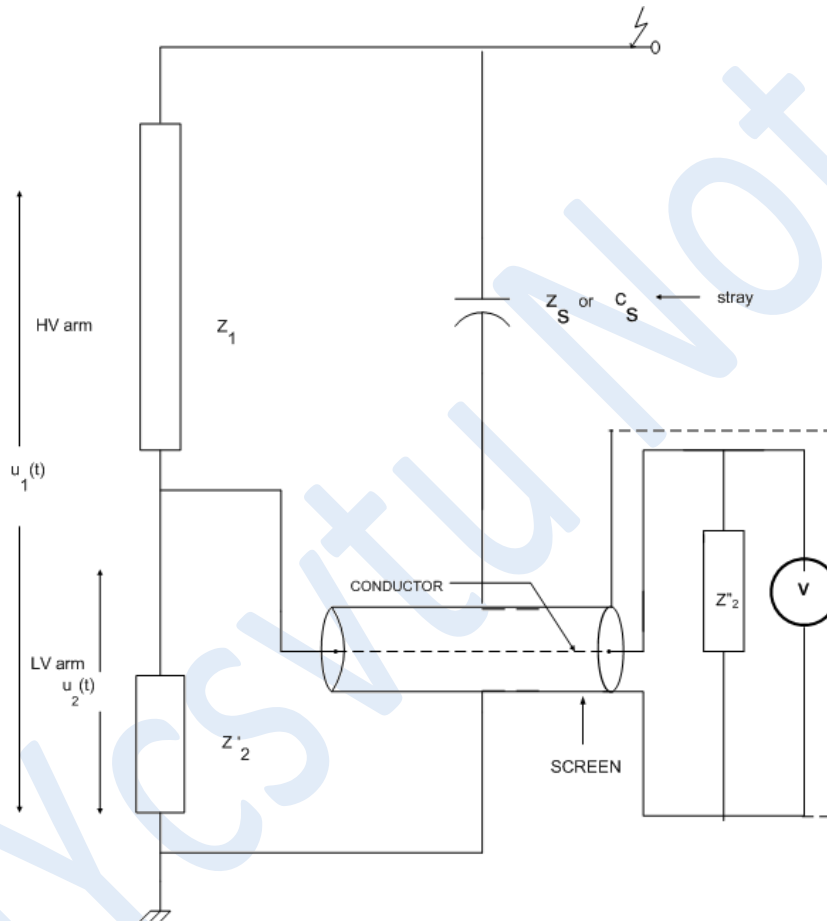


Fig 33.1 Voltage Divider principle

$$\frac{U_1}{U_2} = \frac{Z_1 + Z_2}{Z_2} \approx \frac{Z_1}{Z_2}$$

Z_1 - the high voltage arm of the divider. It could be pure C, pure R or combination of R and C as per requirement.

- Values of Z_1 and Z_2 are chosen such that the potential across Z_2 is around 100 V
- The voltage division ratio can be given as;

$$\frac{Z_1}{Z_2} \gg 1$$

$$Z_2 = \left(\frac{1}{Z_2} + \frac{1}{Z_2''} \right)^{-1}$$

For the circuit in Fig 33.1

where

$Z_2'' =$ terminal impedance of oscilloscope

For the measurement of high test voltages the technique of potential dividers is most accurate. It provides a continuous measurement of all the types of applied high voltages i.e. dc, ac and impulse. However, the suitability of the type of divider depends upon not only the type of voltage but also upon the range of magnitude of the voltage to be measured. The types of potential dividers or basically the construction of the HV arm and their suitability are described in the following:

1. Pure Capacitance Voltage Dividers:

The HV arm of the capacitive voltage dividers, usually having their capacitance in pF range, are compressed gas or vacuum capacitors. The nF range HV capacitors are built in stack or in series a number of capacitors made out of polypropylene or paper filled with oil. In the absence of stray capacitances to earth with such HV capacitors, these provide desired exact value of low capacitance and small dimensions of the HV capacitive arm. The value of low voltage arm of the divider is normally chosen in μF range. Compressed gas (SF_6) filled HV capacitors are built even above 1000 kV (rms) rating. These can also be used as standard capacitors. In Fig 33.2, a photograph and a sketch of such a capacitor are shown. The value of inductance of the long lead (in mts) connecting the low voltage electrode inside such a capacitor causes problems in giving a good response of the divider. Necessary constructional precautions are therefore taken in their design.

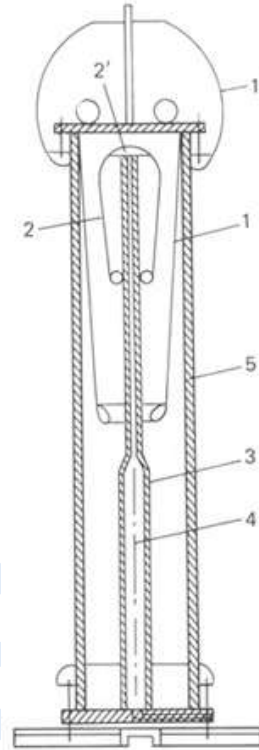


Fig 33.2 (a) Standard (compressed gas) capacitor for 1000 kV rms (Micafil, Switzerland)

(b) Cross-section of a compressed gas capacitor. 1. Internal HV electrode. 1'. External HV electrode. 2. Low-voltage electrode with guarding, 3. Supporting tube. 4. Coaxial connection to I.v. sensing electrode. 5. Insulating cylinder.

Pure capacitance voltage dividers are suitable for the measurement of power frequency and impulse high voltages. However, the cost of the HV capacitors is high and their cost and size increases with their voltage rating.

2. Pure Resistance Potential Dividers

The high potential drop across a resistive arm by simple Ohm's law is used to reduce the voltage to a measurable quantities, circuits for such measurement are shown in Fig 33.3 (a) and (b)

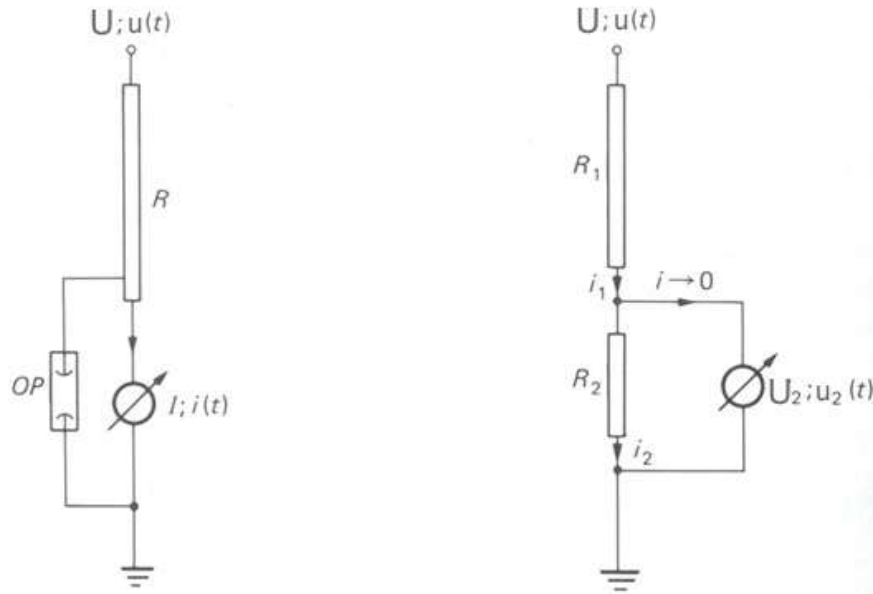


Fig 33.3 Measurement of high dc and ac voltages by means of
(a) ammeter in series with resistor R ;
(b) voltage divider R_1, R_2 and voltmeter of negligible current input. OP , Over-voltages protection.

Such pure resistive arm or divider can be used for the measurement of dc, ac as well as impulse voltages. The wave forms of ac and impulse voltages could also be recorded with the help of an oscilloscope. However, while measuring very high voltages, the resistive arm inductance and stray capacitance cause large error in the accuracy of measurement and hence in response of the measuring device. The wire-wound resistors used earlier were made of constantan, Cu & Ni, manganin, cu, Mn, Ni or Gr and also of nichrome. To overcome the error caused due to inductance of the wire wound resistors, thin film resistors are now used. A conducting element thin film is deposited on the surface of a glass or ceramic rod or tube. The value of the desired resistance is obtained by varying the thickness of the thin film. Such films could be of carbon, metal oxide; stannic and antimony oxides. Nickel-Chromium thin film is obtained by their evaporation in vacuum. Resistive voltage dividers are produced both screened (also known as shielded) and unscreened. Since the effect of stray capacitance is not uniform, it causes a non-uniform potential gradient along its length.

3. Mixed Resistive and Capacitive Dividers

The problem caused by the stray capacitance in resistive voltage divider is over come by

placing actual capacitors in parallel with the resistor units of the HV arm. This gives rise to a mixed resistive and capacitive divider used for highest voltage range of impulse voltage measurement. These are also known as 'damped capacitive divider' or RC divider. These were first introduced by Elsner in 1939, [6.1] . The simplified equivalent circuit of such a divider is shown in Fig 33.4

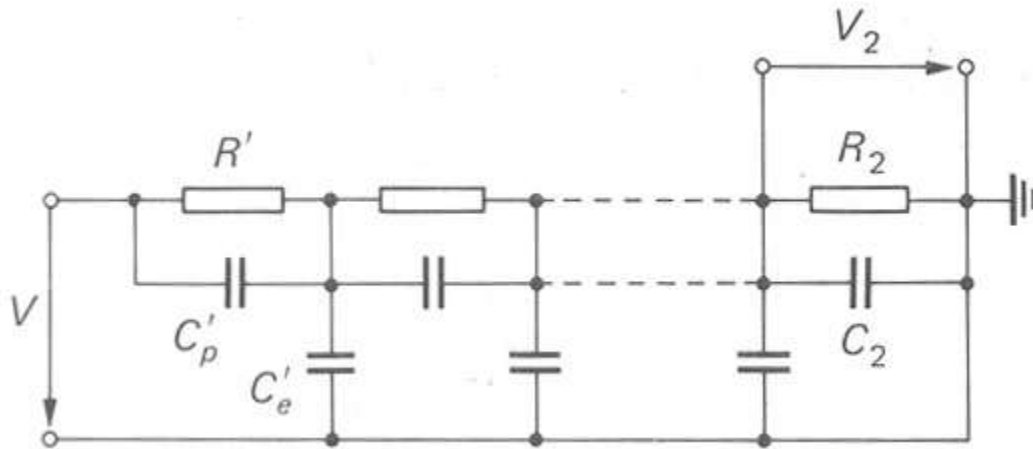


Fig 33.4 Simplified equivalent circuit for parallel-mixed resistor-capacitor dividers.

In this Figure R' represents the resistance of single element of the HV arm where a number of them are in series. C'_p represents the capacitance across each of such element and C'_e , is the stray capacitance to earth of the element. A photograph of such a 4.5 MV voltage divider is shown in Fig 33.5



Fig 33.5 Damped capacitor voltage divider for 4.5-MV impulse voltage, outdoor

Module-7

34

Objectives

In this lecture you will learn the following

- Non destructive testing of Electrical Equipment
- Dielectric Properties of Insulating Materials

Non destructive testing of Electrical Equipment

It implies assessment of the quality of electrical insulation finish provided to the equipment. It is required in order to ensure satisfactory service of the equipment over the stipulated life span. The measurement techniques adopted are mainly electrical.

As it implies, the non-destructive test measurements should not cause any damage to the equipment yet reveal the quality and condition of the dielectric performance.

Introduction:

Any dielectric between two electrodes forms capacitance. The most important electrical parameter of insulating materials is the capacitance offered by them between the given electrode system. The capacitance thus formed is always accompanied with losses determined by the relative permittivity ' ϵ_r ', the specific insulation resistance ' ρ_{ins} ' and the dielectric loss factor ' $\tan \delta$ ' of the material. These represent the insulating properties of the dielectric and depend upon the temperature, frequency and magnitude of the applied voltage, beside the composition of the dielectric itself.

Measurement of Dielectric Properties of Insulating Materials

The properties $\tan \delta$, ϵ_r , R_{dc} and capacitance C_x of a given insulating material are explained in the following:

Permittivity of an insulating material is defined as the product of absolute permittivity of free space (vacuum) ' ϵ_o ' and the relative permittivity ' ϵ_r ' of the material.

$$\epsilon = \epsilon_o \epsilon_r$$

whereas ' ϵ_o ' is a constant and has a value 8.854×10^{-12} F/m, the relative permittivity, ' ϵ_r ' also known as permittivity number, is defined as:

$$\epsilon_r = \frac{C_x}{C_o}$$

Where C_x is the capacitance of a condenser constituting the given material as dielectric and C_o is the capacitance of the same condenser constituting vacuum in place of the dielectric.

ϵ_r is a function of temperature of the dielectric. It also varies with the frequency and magnitude of the applied voltage. Hence ϵ is not a constant.

Insulation Resistance ' R_{dc} ' of a dielectric is represented by the dc resistance offered by the material. It is generally described as 'specific insulating resistance ' ρ_{ins} ' which is reciprocal of the dc conductivity κ_{dc} .

$$\rho_{ins} = \frac{1}{\kappa_{dc}} \quad \Omega \cdot m$$

Considering a block of an insulating material in uniform field between two plates of area A at a distance d apart and applied a dc voltage U shown below.

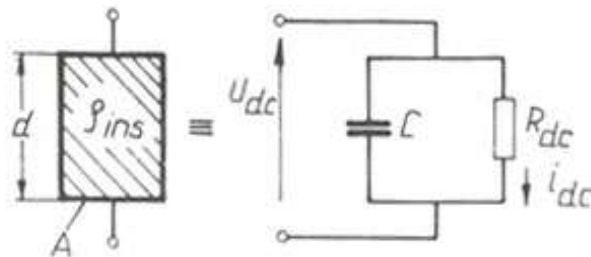


Figure 34.1 An insulating material and its equivalent circuit diagram

The insulation resistance offered by this block of dielectric can be written as:

$$R_{dc} = \rho_{ins} \frac{d}{A}$$

$$I_{dc} = \frac{U}{R_{dc}} = \frac{U.A}{\rho_{ins}.d} = \frac{E.A}{\rho_{ins}} = k_{dc}.A.E$$

(Since $E = U/d$ for uniform field)

The dc conductivity of a dielectric is a function of temperature and time for which the voltage is applied. It initially depends upon the orientation of dipoles in the material. Then by the movement of free charge carriers and ultimately by the development of space charge in front of the electrodes. R_{dc} can be directly measured with the help of a Megaohm meter.

A schematic illustration of the variation of k_{dc} with respect to the time of application of direct voltage for an insulating oil is shown below;

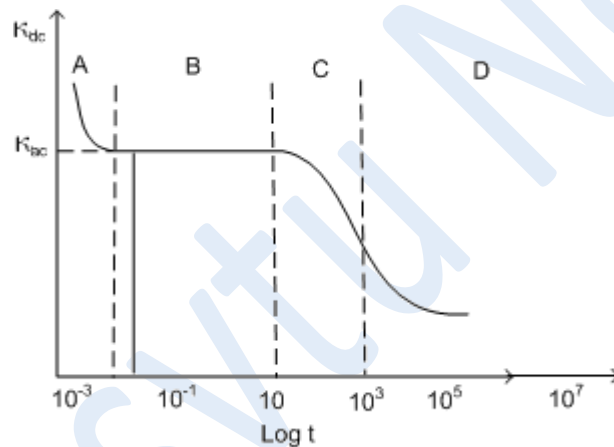


Figure 34.2 A Schematic of dc conductivity of an insulating oil with respect to the time of applied voltage

In every dielectric matter, including those which have a low concentration of free charge carriers, a conductive current through the dielectric is always present on applying a voltage across the volume of the dielectric.

Besides, a small surface current determining the surface resistivity also may flow.

Accordingly two different conductivities, volume and the surface conductivities of a dielectric, are distinguished

Reciprocal of these conductivities give volume and surface resistivities respectively.

- Specific insulation resistance ρ_{ins} , represents the specific volume resistance ' ρ_v ' or the volume resistivity of the dielectric. It has a unit of $\Omega.m$.
- Specific surface resistance ' ρ_s ' or the surface resistivity has accordingly a unit

of Ω only.

When an alternating voltage is applied to dielectrics, they undergo active as well as reactive power losses in the capacitance formed by the dielectric. The dielectric losses vary not only with the magnitude of the applied voltage but also with the frequency of the voltage and the temperature of the dielectric. The magnitude of the losses are best assessed with the knowledge of "Dielectric Loss Tangent, $\tan\delta$ ". Like the relative permittivity or the permittivity number, ϵ_r , $\tan\delta$ is also a function of

$$\tan\delta = f(v, f, \nu)$$

Dielectric loss tangent

' $\tan\delta$ ' is defined as the quotient of active to reactive power loss in a dielectric when an alternating voltage is applied.

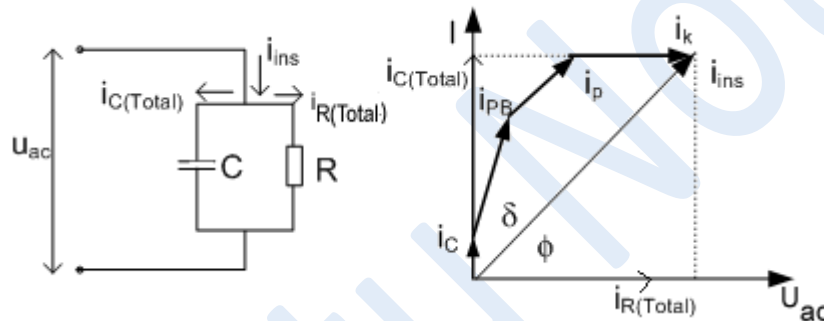


Figure 34.3 Conductive mechanisms in insulating materials with alternating voltages where

- i_c = capacitive charging current
- i_{pB} = partial discharge impulse currents
- i_p = polarization currents
- i_k = conductive currents

$$\tan\delta = \frac{\text{Active Power}}{\text{Reactive Power}} = \frac{u \cdot i_{ins} \cdot \cos\phi}{u \cdot i_{ins} \cdot \sin\phi} = \frac{i_{R(Total)}}{i_{C(Total)}}$$

The active part of total insulation current through the capacitor is $\omega C U \tan\delta$. Hence the active power loss ' P_{ac} ' is given by.

$$P_{ac} = \omega C U^2 \cdot \tan\delta$$

Where C is total effective capacitance of the test object: $\tan\delta$ is a function of temperature, frequency and magnitude of the applied voltage U.

Objectives

In this lecture you will learn the following

- Measuring circuit and equipment involved for the measurement of $\tan\delta$
- Measurement of Insulation Resistance and Specific Insulation Resistance
- Measurement of ϵ_r , Permittivity Numbers of dielectrics

Measuring circuit and equipment involved for the measurement of $\tan\delta$ with Schering Bridge

For the measurement of active power loss in the dielectric on applying ac voltage, this bridge circuit was developed by H. Schering in 1919. Since then it is used widely for HV measurements and non-destructive testing for quality assessment of the factory finish and working state of dielectrics in different equipment.

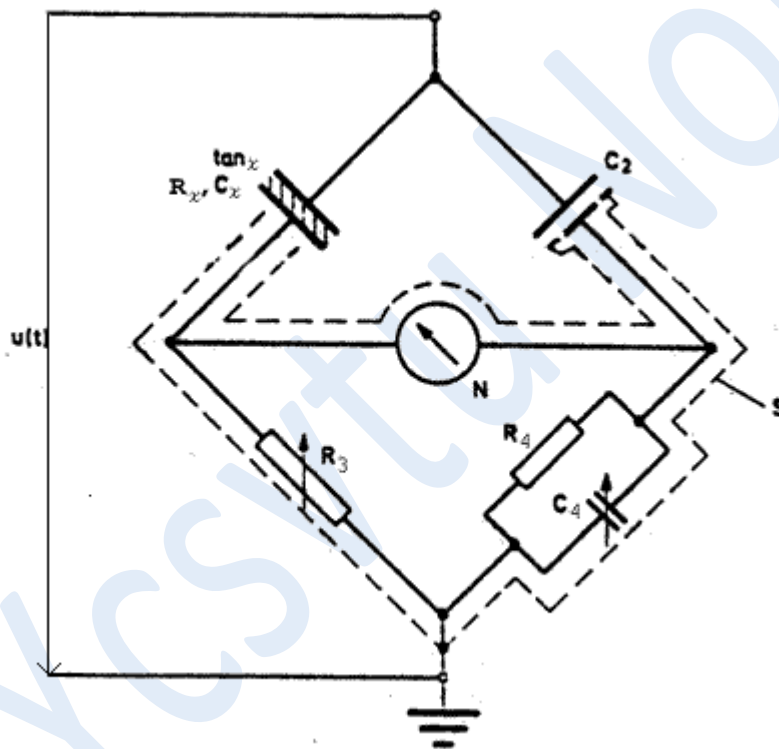


Fig 35.1 Circuit of the Schering bridge

- C_x Test object
- C_2 Standard capacitor, loss free
- R_3, C_4 Balancing elements
- R_4 Fixed resistor
- N Null indicator
- S Screening

The portions of the circuit shown under screening are all at low voltage. Only the test object C_x and the standard capacitor C_2 are at high voltage. C_2 must be an active power loss free ($R_2 = \infty$) capacitor. The bridge is equipped with over voltage protective devices. By adjusting resistor R_3 and the capacitor C_4 the bridge can be balanced. When the bridge is balanced, the following relation holds good, considering R_x and C_x to be in parallel.

$$\tilde{Y}_4 \tilde{Y}_x = \tilde{Y}_2 \tilde{Y}_3$$

or

$$\left(\frac{1}{R_4} + j\omega C_4 \right) \left(\frac{1}{R_x} + j\omega C_x \right) = \frac{j\omega C_2}{R_3}$$

On comparing the real and imaginary parts of the equation, we obtain:

$$\tan \delta_x = \frac{1}{\omega R_x C_x} = \omega R_4 C_4$$

The other required quantities are given as;

$$C_x = C_2 \frac{R_4 / R_3}{1 + \tan^2 \delta_x} = C_2 \frac{R_4}{R_3}$$

$$\epsilon_r = \frac{C_x}{C_o} \text{ and } R_x = \frac{1}{\omega C_x \tan \delta_x}$$

For 50 Hz, if R_4 is chosen to be equal to $1000/\pi$ and since $\omega = 100\pi$, $\tan \delta = C_4 \cdot 10^5$ It is directly measured by varying C_4 and putting its value in Farads.

Guard-ring capacitor

This is a measuring cell especially designed according to VDE specifications (German) for measuring dielectric properties of liquid dielectrics. The provision of guard-ring eliminates the effect of stray capacitances. The details of the Guardring capacitor are as follows.

A. Principal data

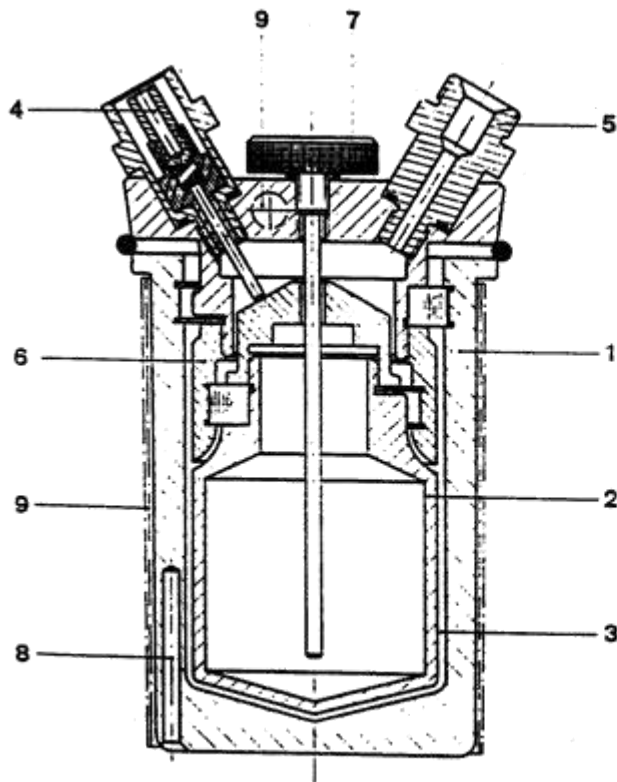
Cylindrical capacitor conforming to VDE 0370 with guard-ring, used as cell for the measurement on liquid insulating materials.

Spacing between electrodes	2 mm
No-load capacitance C_o , with air/vacuum	about 60 pF
Max. measuring voltage	2000 V = 10,000 V/cm (field)
Necessary amount of liquid required	about 40 cm ³

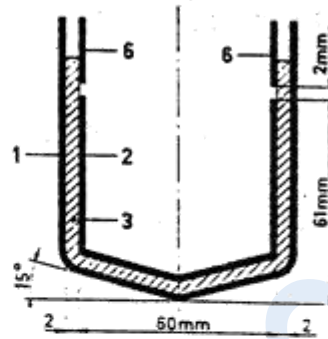
The measuring cell may be heated up to 150 °C and can be evacuated for carrying out measurements in an inert gas.

Material: (high-tension and measuring electrodes, guard-ring)
Stainless steel.

Dimensions 240 mm dia. x 220 mm high
Total net weight about 10 kg.



Basic circuit diagram



Key

- 1. High-tension electrode
- 2. Measuring electrode
- 3. Oil under test
- 4. Measuring electrode connection
- 5. Vacuum connection
- 6. Guard-ring
- 7. Temperature sensor with indicating instrument
- 8. Platinum temperature sensor
- 9. Heater

Figure 35.2

Direct measurement of insulation Resistance at room temperature by a Megaohm meter

The Insulation Resistance $R_{dc} (R_x)$ can be measured directly with the help of a measuring instrument known as MΩ meter and the specific insulation resistance of the oil sample is calculated as follows,

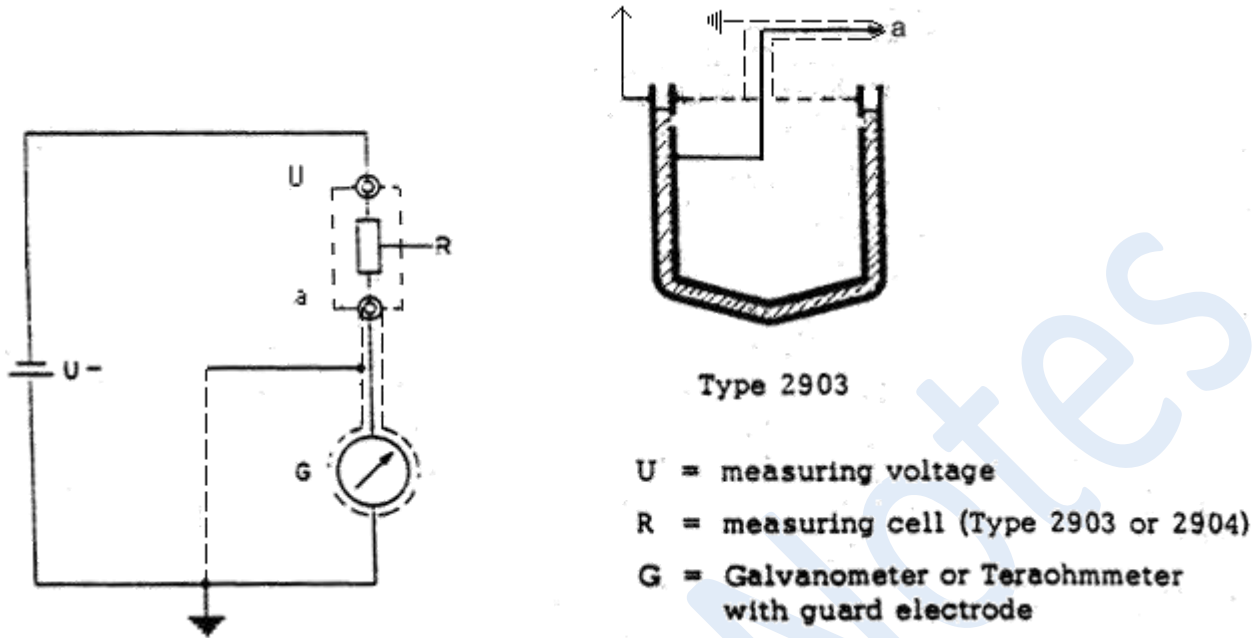


Figure 35.3

$$\rho_{ins} = \frac{R_{ins} \cdot C_0}{\epsilon_0} \Omega \cdot m = \frac{R_{ins} \cdot 60 \times 10^{-12}}{8.854 \times 10^{-12}} = \frac{R_{ins} \times 60}{8854} \Omega \cdot m$$

- R_{ins} - resistance in Ω
- C_0 - capacitance in pF of the Guardring capacitor with air/vacuum.
- ϵ_0 - absolute permittivity in vacuum = 8.854×10^{-12} F/m.

36

Objectives

In this lecture you will learn the following

Measurement of Partial Breakdown in equipment

Measurement of Partial Breakdown (PB) in Dielectrics

PB in solid dielectrics are most damaging. These may reduce the life of the equipment drastically. The damage not only depends upon the intensity of PB but also upon the location and the time required for the formation of conducting path (treeing process). The phenomenon of PB and its measurable quantities are described in Lecture 18 and 19 in detail. A Partial Breakdown Detector is required along with a PB free experimental set up at the required voltage as shown in figure 36.7. The measurement of quantities e.g. PB inception, PB extinction voltages and the level of permissible discharge at a given voltage are specified in BIS6209 and IEC-270. Besides, location of PB in any electrical equipment e.g. cables, transformers, electrical machines or GIS requires special

techniques.

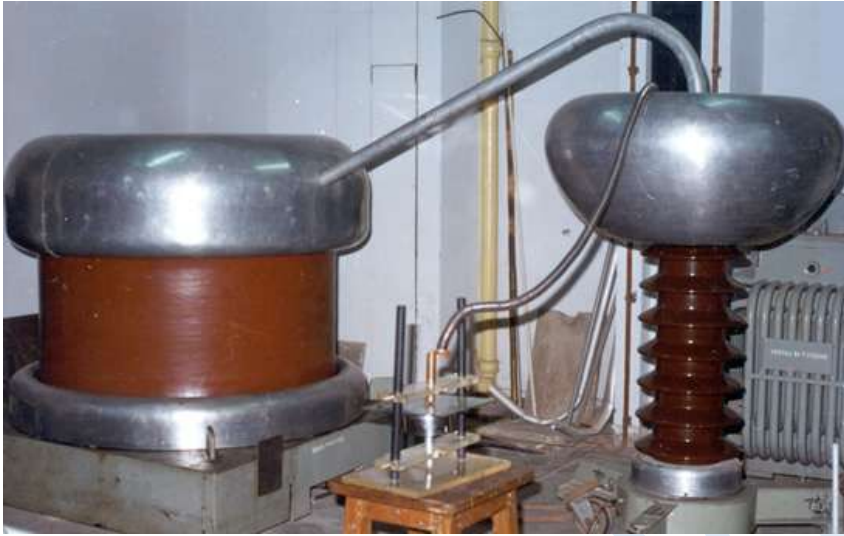
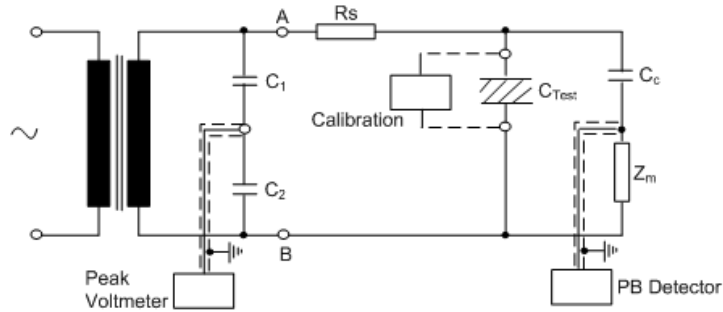


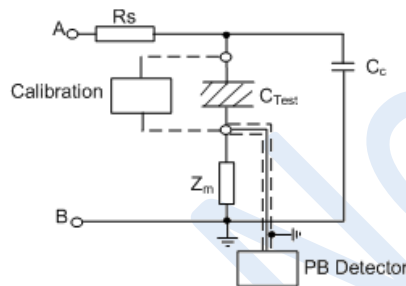
Figure 36.1 A PB free 100 kV Transformer and 1.1 nF Coupling Capacitor setup in HV Laboratory at IIT Kanpur

There are three basic circuits which can be employed for the measurement of PB measurable quantities suitable to convenience or specific requirement. These circuit are shown in Fig. 36.2 (a), (b), (c). As it can be seen in this figure, the coupling capacitor C_c , Measuring impedance Z_m are essential part of the circuit in all the three methods. C_1 and C_2 comprise of capacitive voltage divider for the measurement of the test voltage applied on the test object C_{Test} .

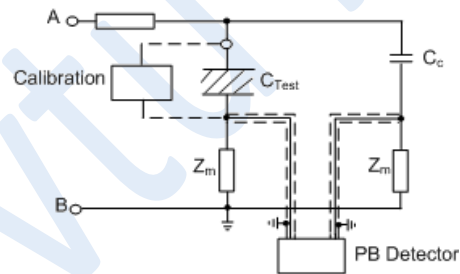
If a global breakdown or complete rupture of dielectric is expected to take place during the PB measurements, it is advisable to choose the circuit shown in Fig. 36.2 (a) in order to protect the measuring impedance Z_m and the voltage measuring unit from over-voltages developed at breakdown.



(a) Measurement at coupling capacitor



(b) Measurement at the Test Object



(c) A bridged circuit for measurement

C_1, C_2 – Capacitive voltage divider
 R_s – series resistance
 Z_m – measuring impedance
 C_{Test} – The test object
 C_c – Coupling capacitor

Fig 36.2 Partial Breakdown Measurement Circuits

If the capacitance of the coupling capacitor C_c is smaller than the capacitance of the test object, the sensitivity of the measurement with circuit in Fig. 36.2 (b) is higher than with the circuit in (a) .

The bridge circuit, shown in Fig. 36.2 (c), is more suitable for the measurement at sites having high electromagnetic interference (EMI). Some times it is difficult to make distinction between the PB pulse generated within the test object and the external interference. However, incorporation of suitable filters in modern PB detection facilitate the measurement even under external EMI.

Calibration of the measuring circuit is required to be done with "standard calibrating charge generator". The measurable quantity of the apparent charge and the sensitivity of the measurement depend largely upon the calibration.

Objectives

In this lecture you will learn the following

Electrical insulation level design and surge performance of high voltage installations
BIL for design of apparatus

Insulation Coordination and Over Voltages in Power Systems

The subject of electrical insulation level design and surge performance of high voltage equipment, transmission lines and sub stations is customarily referred as 'insulation co-ordination'. The insulation provided to electrical installations in the power system is subjected not only to the normal operating voltage which varies within quite narrow limits, but it has to withstand a variety of over voltages having their shapes, magnitudes and durations in a wide range. Thus one can distinguish between steady state and transient over-voltages with which the power system is stressed some times.

The steady-state over voltages, also known as temporary over voltages, are generated within the system due to the connection or disconnection of circuit elements or the initiation or interruption of faults. By circuit elements is meant here the bulk loads connected over lines.

The transient over voltages have external as well as internal sources in the power system. The lightning strike (an external source) on the power system gives rise to lightning over voltages. The circuit breaker operation within the system gives rise to "switching over voltages". It is nothing but the restriking voltage impressed across the circuit breaker electrodes as it opens.

Both these types of transient over voltages proceed in the form of 'traveling waves' from the point they are generated and stress the insulation above the system voltage as they travel . In the process, they attenuate and ultimately they end up at the loads.

The intensity of lightning over voltage depends upon the magnitude of lightning impulse current injected into the system by the lightning strike which in turn depends upon the nature. The magnitude of current injected into the line, multiplied by its surge impedance determines the over voltage magnitude. The lightning over-voltage wave shape is standardized as $\approx 1/50 \mu\text{s}$ duration to be generated in the laboratory by the Impulse Generator for insulation testing. The magnitude of lightning current could be as high as 200 kA recorded by researchers. The probability of higher order of current is very low. However, the average magnitude of impulse current accompanied with li

strike is estimated to be between 10-15 kA. After the lightning strike, the injected charge (the current) always tries to find the least resistance path to the ground. Only when it does not get passage to the ground, it can create havoc.

The magnitudes of switching over voltages, their waveforms (much slower than the lightning) depends upon the factors such as the speed of switching operation of the circuit breakers, their arc quenching characteristics/properties, the instant at which the arc across the electrodes is extinguished and the energy stored in that part of the power system inductance. The modern SF₆ gas and vacuum circuit breakers give rise to "Very Fast Transient Over Voltages", (VFTO). These re-strike on the system repeatedly very fast before, the arc is extinguished, hence pose a big problem. The magnitude of switching over voltages could rise to even 3.0 p.u. Every time it occurs, it has a different shape/waveform. Hence it is difficult to standardize the switching waveshape for its production in the HV laboratory. A popular standard waveshape is 250/2500 μ s. As compared to lightning, it is a much slower waveshape. It is because of this, the breakdown strength of dielectrics is highest for lightning impulse voltage and it is minimum for a particular shape of switching impulse. Further, the magnitude of switching impulse voltage keeps rising as the rated voltage of operation of the system is raised over the time.

The insulation level provided to various installations in the power system by design must withstand the expected maximum voltage of lightning and also switching it is going to face as transient over voltages in its life. The Basic Insulation Level (BIL) provided for lightning and switching are defined separately in the following:

BIL for design of apparatus

BIL for lightning impulse insulation level is the electrical withstand voltage of insulation expressed in terms of the crest value of the 'standard lightning impulse', as per IEC-71. In case of switching transients, it is defined as the switching impulse withstand voltage of specified magnitude and the shape depending upon the rated system voltage.

The BIL level is actually determined by the transient over voltage protection techniques provided by the horn gaps and surge diverters or the lightning arrestors (LA). ZnO₂ gapless surge diverters are used at the sub-stations and in particular for the transformers being the costliest equipment. It is the residual transient voltage across the LA which is impressed upon the transformer. The transformer must be designed, developed and tested to withstand the residual voltage of the specified LA in the network.

Reference

- [1] Diesendorf, W., "Insulation Co-ordination in High Voltage Electric Power System", Butterworth, London (1974)
- [2] Hileman, Andrew R., "Insulation Co-ordination for Power System", Marcel Dekker, Inc. New York, (1999)